New Jersey Institute of Technology
Digital Commons @ NJIT

Theses | Theses and Dissertations

Fall 1996

Removal of volatile organic compounds from contaminated groundwater by pervaporation

Sukla Chandra
New Jersey Institute of Technology

Follow this and additional works at: https://digitalcommons.njit.edu/theses

 Part of the Chemical Engineering Commons

Recommended Citation
Chandra, Sukla, "Removal of volatile organic compounds from contaminated groundwater by pervaporation" (1996). *Theses*. 1057.
https://digitalcommons.njit.edu/theses/1057

This Thesis is brought to you for free and open access by the Theses and Dissertations at Digital Commons @ NJIT. It has been accepted for inclusion in Theses by an authorized administrator of Digital Commons @ NJIT. For more information, please contact digitalcommons@njit.edu.

Copyright Warning & Restrictions

The copyright law of the United States (Title 17, United States Code) governs the making of photocopies or other reproductions of copyrighted material.

Under certain conditions specified in the law, libraries and archives are authorized to furnish a photocopy or other reproduction. One of these specified conditions is that the photocopy or reproduction is not to be "used for any purpose other than private study, scholarship, or research." If a, user makes a request for, or later uses, a photocopy or reproduction for purposes in excess of "fair use" that user may be liable for copyright infringement,

This institution reserves the right to refuse to accept a copying order if, in its judgment, fulfillment of the order would involve violation of copyright law.

Please Note: The author retains the copyright while the New Jersey Institute of Technology reserves the right to distribute this thesis or dissertation

Printing note: If you do not wish to print this page, then select "Pages from: first page # to: last page #" on the print dialog screen

NJIT New Jersey's Science & Technology University

The Van Houten library has removed some of the personal information and all signatures from the approval page and biographical sketches of theses and dissertations in order to protect the identity of NJIT graduates and faculty.

ABSTRACT

REMOVAL OF VOLATILE ORGANIC COMPOUNDS FROM CONTAMINATED GROUNDWATER BY PERVAPORATION

by
Sukla Chandra

Effective removal of non-aqueous phase liquid pools in groundwater and volatile organic compounds (VOCs) from contaminated soils can be achieved by surfactant flushing. This surfactant-rich ground water contains VOCs like trichloroethylene (TCE), dichloroethylene (DCE), etc. Membrane pervaporation technique is employed here to remove TCE from these micellar systems where a very high percentage of the VOC is trapped inside the micellar core. The micellar solution flows through the bore of microporous hydrophobic hollow fibers wherein the micelles break down and release the surfactants and the TCE. The TCE is then removed through the pores and a nonporous thin silicone skin on the outside surface of the fiber, the other side of which is subjected to vacuum to allow pervaporation-based removal of the VOC. This research has characterized such a process for removal of TCE with or without surfactant. It was established that the presence of surfactant adversely affected the removal of TCE. The flux of TCE was found to be an increasing function of feed flow rate and Reynolds number. This research has also briefly explored the permeation of nonvolatile hydrocarbons such as dodecane from water flowing through the fiber bore by using a similar hollow fiber membrane.

REMOVAL OF VOLATILE ORGANIC COMPOUNDS FROM CONTAMINATED GROUNDWATER BY PERVAPORATION

by
Sukla Chandra

A Thesis
Submitted to the Faculty of
New Jersey Institute of Technology
in Partial Fulfillment of the Requirements for the Degree of
Masters of Science in Chemical Engineering

Department of Chemical Engineering,
Chemistry, and Environmental Science

October 1996

APPROVAL PAGE

REMOVAL OF
VOLATILE ORGANIC COMPOUNDS FROM
CONTAMINATED GROUNDWATER BY PERVAPORATION

Sukla Chandra

Dr. Kamalesh K. Sirkar, Thesis Advisor — Date
Professor of Chemical Engineering and Environmental Science, NJIT

Dr. Angelo Perna, Committee Member — Date
Professor of Chemical Engineering and Environmental Science, NJIT

Dr. Robert G. Luo, Committee Member — Date
Assistant Professor of Chemical Engineering and Environmental Science, NJIT

BIOGRAPHICAL SKETCH

Author: Sukla Chandra

Degree: Masters of Science

Date: October 1996

Undergraduate and Graduate Education:

- Masters of Science in Chemical Engineering,
  New Jersey Institute of Technology, Newark, NJ, 1996
- Bachelor of Science in Chemical Engineering,
  Jadavpur University, Calcutta, India, 1989

Major: Chemical Engineering

To my parents

ACKNOWLEDGEMENT

I would like to express my sincere thanks to my advisor, Professor Kamalesh K. Sirkar, for his valuable advice and constant support and guidance throughout this research. I would also like to thank Dr. Angelo Perna and Dr. Robert Luo for participating in my thesis committee.

I also want to thank all the members of the Membrane Separation and Biotechnology group for their constant support and timely suggestions, all of which helped to overcome the difficult phases of this research. In particular, I would like to acknowledge the help received from my colleagues Sarma, Shankar and Uttam as well as Drs. Majumdar and Abou Nemeh. Sincere thanks are also due to Ashish for his help with the experiments during the last stages of the thesis. In addition, I thank Judy for her care in smoothening out the administrative kinks associated with my graduate studies at NJIT.

I would like to thank my family and in-laws for their encouragement and moral support. Finally I want to thank my husband, Nilanjan, for his love and patience, without which I could not have finished this research.

TABLE OF CONTENTS

Chapter	Page
1 INTRODUCTION	1
1.1 The Problem	1
1.2 Conventional Treatments	2
1.3 Surfactant Flushing	3
1.4 Removal Techniques of VOC from Aqueous Solution	4
1.5 Proposed Removal Technology	5
1.6 Objective of the Research	10
1.7 Research Approach	10
2 THEORY	12
2.1 Theory of Pervaporation	12
2.1.1 Process	12
2.1.2 Transport of Solute	14
2.1.3 Concentration Polarization	15
2.2 Theory of Surfactants	17
2.2.1 Characteristics of Surfactant	17
2.2.2 Surfactant Classification	18
2.2.3 Micelle Formation by Surfactants	19
2.2.4 Critical Micelle Concentration	19
2.2.5 Solubilization by Using Surfactants	21
2.3 Postulations	25
3 MATERIALS AND METHODS	29
3.1 Chemicals and Gases Used	29
3.2 Hollow Fiber Modules and Module Fabrication Procedure	29
3.3 Experimental Setup	32

TABLE OF CONTENTS
(Continued)

Chapter	Page
3.3.1 Pervaporation Setup	32
3.3.2 Oil Permeation Setup	34
3.4 Analytical Procedure	36
3.4.1 High Pressure Liquid Chromatography	36
3.4.2 Gas Chromatography	37
3.5 Experimental Procedure	41
3.5.1 Preparation of Feed	41
3.5.2 Sampling	44
3.5.3 Experiment	45
3.5.4 Reproducibility of Experiments	49
4 RESULTS AND DISCUSSION	52
4.1 Phase One	52
4.2 Phase Two	64
4.3 Phase Three	76
4.4 Phase Four	82
4.4.1 Oil Permeation Experiments	88
5 CONCLUSIONS	97
APPENDIX A	99
A.1 Calculation of Flux	99
A.1.1 Calculation of TCE Flux	99
A.1.2 Calculation of Water Flux	100
A.2 Calculation of Mass Transfer Coefficient	101
A.2.1 Boundary Layer Mass Transfer Coefficient	101
A.2.2 Overall Mass Transfer Coefficient	102
REFERENCES	105

LIST OF TABLES

Table		Page
3.1	Characteristics of the modules used	30
3.2	Experimental parameters for TCE pervaporation	49
3.3	Experimental parameters for dodecane permeation	49
3.4	Properties of surfactants used	50
3.5	Physical and chemical properties of TCE	51
4.1	Experimental data for TCE removal in module #1 for 5% and 3% SDS	60
4.2	Experimental data for the fluoropolymer module	60
4.3	Effect of feed concentration on TCE removal for 1% SDS	67
4.4	Effect of feed flow rate on TCE removal for 1% SDS	67
4.5	Effect of feed flow rate on TCE removal for 0.3% SDS in a Twins module	74
4.6	Effect of feed temperature on TCE removal for 0.3% SDS in a Twins module	74
4.7	Effect of feed flow rate for 0.3% SDS and the Trio module arrangement	74
4.8	Effect of feed concentration on TCE removal in a surfactant-free system	84
4.9	Effect of feed flow rate on TCE removal in a surfactant-free system	84
4.10	Comparison of TCE flux and mass transfer coefficient with or without a surfactant	88
4.11	Experimental data for dodecane permeation	92
4.12	Experimental data for flow and pressure effect on dodecane permeation	95
A.1	Mass transfer area of pervaporation modules	100

LIST OF TABLES
(Continued)

A.2 Regression data for k_m for 1% SDS system 104

A.3 Regression data for k_m for 0.3% SDS system . . . 104

A.4 Regression data for k_m for surfactant-free system 104

LIST OF FIGURES

Figures		Page
1.1	Micellar feed of surfactant and VOC into the fiber	7
2.1	Schematic diagram of pervaporation process	13
2.2	Phenomenon of concentration polarization	16
2.3	Changes in some physical properties of an aqueous solution of sodium dodecyl sulfate in the neighborhood of critical micelle concentration	20
2.4	Micellar structure of surfactant and TCE	24
2.5	Micellar feed of surfactant and VOC into the hollow fiber with dry pores filled with vapor	27
3.1	Pervaporation experimental unit	33
3.2	Experimental setup for oil permeation	35
3.3	Calibration curve of TCE	38
3.4	Effect of equilibration time on TCE output	40
3.5	Equilibration time of Dodecane in headspace	42
3.6	Calibration of the FID response for n-dodecane	43
3.7	Modules in series with feed in tube	48
4.1	TCE removal with 5% SDS	54
4.2	TCE removal with 1% SDS	56
4.3	Effect of feed concentration on TCE removal with 1% SDS	58
4.4	TCE removal with 0.3% SDS	59
4.5	Effect of SDS concentration	62
4.6	TCE removal in fluoropolymer module	63
4.7	Effect of TCE concentration in feed with twins module	65
4.8	Effect of feed flow rate with 1% SDS	68
4.9	Mass transfer coefficients in 1% SDS system	69

LIST OF FIGURES
(Continued)

4.10 Effect of feed flow rate with 0.3% SDS 72

4.11 Mass transfer coefficients in 0.3% SDS system . . 75

4.12 TCE removal by pervaporation; effect of temperature 77

4.13 Effect of feed flow rate in trio module 78

4.14 Comparison of system performance using different surfactants 80

4.15 Effect of xanthan gum 81

4.16 Effect of feed concentration in surfactant-free system 83

4.17 Effect of flow rate in surfactant-free system . . 85

4.18 Mass transfer coefficients in surfactant-free system 87

4.19 Comparison of mass transfer coefficients for different systems 89

4.20 Permeation of dodecane 90

4.21 Flux drop in dodecane permeation; tube-side feed . 93

4.22 Comparison of dodecane flux with or without surfactant 96

CHAPTER 1

INTRODUCTION

1.1 The Problem

Volatile organic compounds (VOCs) such as trichloroethylene (TCE), benzene, toluene, carbon tetrachloride, trichloroethane, etc. are frequently found in contaminated ground water and soil from various industrial and military facilities. Some of these VOCs are potential carcinogens and a threat to any living being. Due to their volatile nature, VOCs can threaten the environment through different pathways. Chlorinated hydrocarbons (TCE, perchloroethylene (PCE) and 1,2 dichloroethylene (1,2-DCE)) are ubiquitous groundwater contaminants due to their widespread use as cleaners/ degreasers. Approximately 50% of the U.S. Environmental Protection Agency's (EPA's) list of priority pollutants is composed of VOCs - compounds known to be toxic, or carcinogen, or both (EPA/540/SR-94/512). These organic solvents are frequently released to the environment as a separate organic phase or nonaqueous phase liquid (NAPL).

When a NAPL migrates through the subsurface, capillary forces act to retain a portion of the organic liquid as discrete ganglia within the pores (Abriola et al., 1995). These immobile ganglia may occupy between 5 and 40% of the pore volume at residual saturation (Wilson et al., 1984). They frequently represent a long-term source of groundwater

contamination due to very low aqueous solubility of most NAPLs. There are some sites which have dense NAPLs commonly known as DNAPLs. DNAPLs, due to their large densities and low viscosities, are not typically confined to the unsaturated zone. These dense liquids tend to migrate vertically under gravitational forces and may spread deep within the aquifer formation (Abriola et al., 1995).

1.2 Conventional Treatments

Pump-and-treat remediation was initially prescribed as the method to cleanup subsurface organic contaminations. More recently, the limitations of this approach have been recognized. This is due to the fact that there are three zones where subsurface contaminations exist; the source area (the original contaminated soil that continue to discharge into the ground water plume), the concentration zone (center of mass of the ground water plume), and the dilute ground water plume (Sabatini et al., 1995). It is generally recognized that conventional pump-and-treat remediation methods are ineffective and costly when NAPLs are present. The failure of this approach is due to the very low aqueous solubility of the NAPLs and their slow rate of dissolution.

Another conventional technology for soils contaminated with VOC is Soil Vapor Extraction (Ball and Wolf, 1990). It can be applied in situ to subsurface soils, or above ground to excavated soil piles. Soil vapor extraction is performed by applying a vacuum to the soils to induce volatilization of

soil contaminants. The extracted air is usually treated for VOC removal prior to discharge to ambient air. However, the subsurface airflow and contaminant transport processes are complex and are generally not understood.

1.3 Surfactant Flushing

Over the past few years considerable interest has focused on surfactant flushing as an alternative method for recovering residual NAPLs and DNAPLs from contaminated groundwater (Fountain et al., 1991; West and Harwell, 1992). A common goal of subsurface remediation is extraction of subsurface contaminants ("pump") with above ground treatment for waste processing and management ("and treat") (Sabatini et al., 1995). This technique is based on the ability of surfactants to increase the aqueous solubility of NAPLs via micellar solubilization and to mobilize and entrap the NAPLs through surface tension reduction at organic-water interface.

Surfactant washing has been used to remove sorbed or deposited polychlorinated biphenyls (PCBs) and polycyclic aromatic hydrocarbons (PAHs) from soil (Pennell et al., 1993). Abriola et al. (1995) developed a model to describe the three most important phenomena in surfactant enhanced subsurface remediation of DNAPLs: rate-limited micellar solubilization, extent of NAPL mobilization, and the effect of physical heterogeneities. Fountain et al. (1995) successfully demonstrated two field studies involving surfactant enhanced remediation of DNAPLs at two different sites. They concluded

that the surfactant enhanced remediation could remove a portion of the DNAPL mass rapidly and the ultimate remediation level is governed by the hydrology of the site. Shiau et al. (1995) presented the solubilization studies of chlorinated organics (TCE, PCE, and 1,2-DCE) using food grade surfactants. This work provided a guidance for selecting the most effective surfactant for optimum surfactant-enhanced subsurface remediation.

1.4 Removal Techniques of VOC from Aqueous Solution

The huge volume of wastewater generated in surfactant enhanced subsurface remediation is rich in surfactant and VOC. This has to be treated to remove VOC before it can be discharged or reused. Activated carbon bed can be used effectively at very low concentration of VOC, but becomes very costly at higher concentrations as the spent carbon has to be regenerated or disposed of (Lipski and Cote´, 1990) in an environmentally acceptable manner approved by EPA. Carbon adsorption is also not very effective when the aqueous solution is surfactant rich as the organic compounds compete for adsorption sites with the surfactants and therefore removal efficiency decreases as these sites become saturated.

Air stripping is an alternative method for removal of VOC from any aqueous phase. But this process is limited to compounds that significantly partition to air over water (high Henry's law constant). Furthermore, groundwater often promotes fouling due to iron oxidation and/or carbonate precipitation,

reducing process efficiency and resulting in increasing maintenance cost. The most difficult problem is foaming due to surfactants. This requires addition of antifoaming agents which prevent recirculation of the surfactant flushing solution. Also the efficiency of stripping is low since the micelles hold the VOCs.

1.5 Proposed Removal Technology

An alternative method, the membrane pervaporation (PV) technique, which is a single step continuous process, is proposed in this research to remove VOC from the waste generated from surfactant-enhanced subsurface remediation. In the pervaporation process, the contaminated water to be used in pump-and-treat process flows on one side and vacuum is pulled from the other side of the membrane. The membrane is highly selective to the VOC over water. The VOCs dissolve in the membrane, diffuse through it and are evaporated on the other side of the membrane. This vapor which is highly enriched in VOCs is condensed and the condensate separates into two layers of organic and aqueous phases. By this process of pervaporation a very high reduction of volume of waste is obtained as the contaminant is collected almost in pure form. The small water layer in the condensate can be recycled back to the feed. Such a process can reduce the VOC concentration to the level of low ppms.

The feed from the surfactant flushed water is in the micellar range and a newer PV technique is needed to treat

this feed. Oil-in-water emulsions have been broken up and the oil collected through the pores of hydrophobic microporous hollow fibers, if emulsion flows under a mild pressure on either side of such fibers without a nonporous skin (Magdich and Semmens, 1988; Tirmizi et al. 1995). In the proposed technology the feed will flow through the bore of a hydrophobic microporous hollow fiber with a nonporous hydrophobic coating on the outer diameter. During the process the pores will get filled up with VOC and surfactant and the mixture will get pressed onto the nonporous coating. As a vacuum is maintained on the other side of the skinned hollow fiber the VOC will be removed continuously and selectively from the micellar feed. A schematic diagram of the hollow fiber is given in Figure 1.1. As silicone is highly selective for VOC over water, a coating of polydimethylsiloxane (PDMS) will be used on the polypropylene substrate of the hollow fibers. Pervaporation effectiveness will be judged by VOC and water fluxes, VOC-water selectivity and level of VOC removal. The coating in this membrane is applied by plasma polymerization; therefore it can withstand the application of a vacuum. Normally applied coatings will be stripped off.

In membrane processes it is recognized that mass transport is a function of the membrane itself and of the mass transfer resistances that may develop on either side of the membrane. In pervaporation when the preferentially permeating compound is present in trace amounts in the bulk of the feed, and its flux is high, concentration polarization may develop

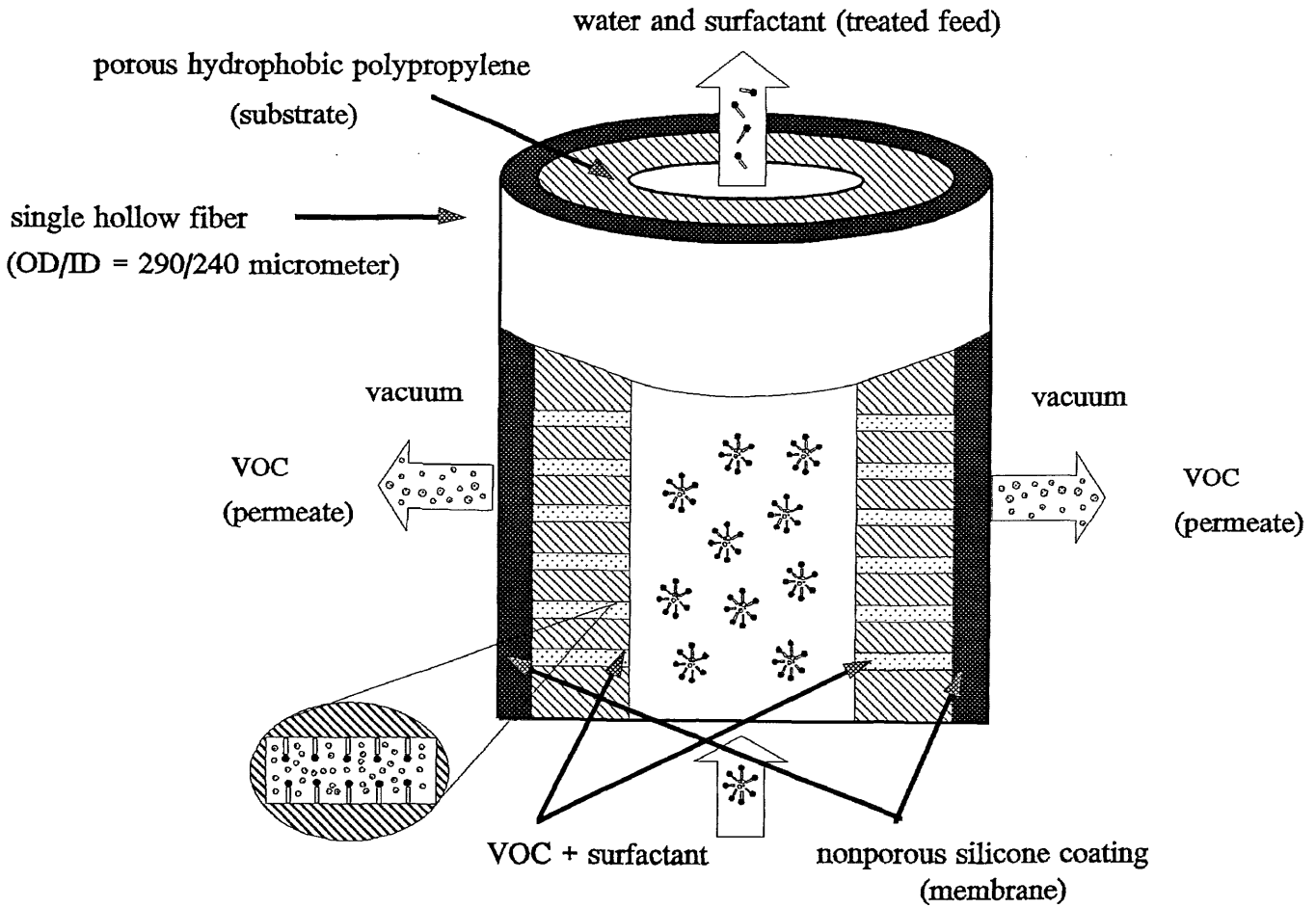

Figure 1.1 Micellar feed of surfactant and VOC into the hollow fiber

at the liquid/membrane interface (Lipski and Cote´, 1990). This phenomenon was observed by Psaume et al. (1988) in the separation of TCE from water using silicone rubber capillaries. The experimental results for axial Reynolds numbers ranging from 10 to 60 showed that the flux was limited by concentration polarization. Their data were described using a liquid film mass transfer correlation, neglecting any resistance of the membrane itself to mass transfer.

Membrane resistance cannot always be neglected. Lipski and Cote' (1990) demonstrated a resistance-in-series model in pervaporation of TCE for calculating the mass transfer coefficient and also developed a model for cost analysis of such processes. The separation factor obtained ranged from 357 to 1110. Liu et al. (1996) and Wijmans et al. (1990) also demonstrated the performance of VOC removal by pervaporation based on a resistance-in-series model. Wijmans et al. (1990) obtained 100-200 fold enrichment of 1,1,2-trichloroethane by pervaporation. Yang et al. (1995) studied the removal of TCE and toluene from an aqueous solution at low concentration range (upto 500 ppm) using conventional silicone rubber capillary-based pervaporation system and a hollow fiber contained liquid membrane (HFCLM). The solute recovery ranged from 83-95% depending on the feed composition and flow rate. A very high separation factor ranging from 10000-11500 was obtained using the HFCLM module.

Lipe et al. (1994) studied the ultrafiltration of TCE and naphthalene in micellar solution using two anionic

surfactants, such as Dowfax. It was observed by them that the surfactant with higher micellar partitioning coefficient for each contaminant gave higher separation efficiency.

Often the surfactant-flushed water has nonvolatile organic compounds. Pervaporation process is not suitable for their removal because of their low vapor pressures. Tirmizi et al. (1996) studied the demulsification of water/oil emulsions using hollow fiber membranes. They carried out experiments with porous polypropylene membranes even at oil concentrations as low as 1% and obtained a purified stream containing 25 ppm oil content. Magdich and Semmens (1988) and Tirmizi et al. (1995) employed porous hydrophobic hollow fibers to remove the oil phase from an oil-in-water or water-in oil emulsion by preferential pore wetting and pressure driven flow through the pore. They observed a typical phenomenon of water breakthrough after only a few hours or minutes of starting the experiments (page 81, Magdich and Semmens, 1988).

If a similar feed of oil-in-water emulsion is brought to the substrate side of a silicone coated hydrophobic fiber, then the difficulty of water permeation could be avoided since the hydrophobic silicone coating will not allow the breakthrough of water. In this thesis, this phenomenon was explored very briefly with dodecane and water mixture as an oil-water emulsion with or without a surfactant. The oil-water emulsion flowed under pressure through the fiber bore. The shell side was kept at atmospheric pressure. Dodecane was chosen in this research to be the model oil. Magdich and

Semmens (1988) also studied oil removal from an oil-in-water emulsion by using porous hydrophobic hollow fibers having a nonporous silicone coating on the outside surface; in their case the emulsion flowed at a higher pressure on the shell /side and over the nonporous coating. Thus the porous hydrophobic surface was not properly utilized.

1.6 Objective of the Research

The overall research objectives of this thesis are:

A) Develop a hollow fiber membrane-based pervaporation process to remove and recover volatile organic compounds (VOCs) from surfactant-flushed groundwater contaminated with nonaqueous phase liquid pools (NAPLs) via bench-scale investigation.

B) Demonstrate the efficiency and utility of such a process using prototype membrane modules. This research will focus primarily on the removal of the VOC trichloroethylene (TCE). TCE is one of the priority pollutants declared by EPA. TCE is designated as a chronic waste ("U" waste; NO.U228) in EPA 40 CFR 261.33.

C) Explore the possibility of removing dodecane from an oil-in-water emulsion by permeation through the substrate-side of the silicone-coated hollow fiber.

1.7 Research Approach

The approach adopted consists of the following steps:

1) Procure hollow fibers of the appropriate type and fabricate hollow fiber modules.

2) Study the removal of TCE from synthetic surfactant-containing water by pervaporation using hollow fiber membrane modules.

3) Compare the tube-side and shell-side performances of the modules made of thin silicone coated hollow fibers.

4) Study the effect of the feed matrix, e.g surfactant type, surfactant concentration on the percent removal of TCE and the fluxes of TCE and water.

5) Study the effect of feed temperature on TCE removal and the fluxes of TCE and water.

6) Study the hydrodynamic effects on TCE removal and the fluxes of TCE and water.

7) Study long-term performance of the modules keeping the surfactant concentration above the critical micelle concentration (CMC) level.

8) Focus on membrane performance using sodium dodecyl sulfate (SDS) as a model surfactant and broaden the scope of research using other surfactants such as Dowfax 8390.

9) Study the performance of two or three similar hollow fiber membrane modules in series.

10) Develop preliminary conclusions on the relative roles of various resistances to the pervaporative transfer of TCE via mass transfer resistance calculations.

11) Study the feasibility of removing dodecane from an oil-in-water emulsion flowing under pressure with or without SDS on the tube-side of the silicone-coated hollow fiber module.

CHAPTER 2

THEORY

2.1 Theory of Pervaporation

2.1.1 Process

Pervaporation is a membrane process which is a combination of permeation and evaporation. A permselective membrane is used to separate a mixture of volatile solvents. This process is termed "pervaporation" as the unique phenomenon of phase change occurs as the liquid solutes diffuse across the membrane. A liquid mixture contacts one side of the membrane and is removed as a vapor from the other side, which is maintained generally under vacuum. Transport through the membrane is induced by maintaining the vapor partial pressure on the permeate side lower than the vapor partial pressure of the liquid feed. A schematic diagram of a pervaporation process is shown in Figure 2.1. The permeate vapor is normally cooled and collected in a condenser where the permeate separates into two distinct aqueous and organic phases. The aqueous phase can be recycled back to the feed tank and the organic phase is disposed off. Since different species permeate at different rates, an organic solute present in water in trace amount is highly enriched in the permeate. This reduces the volume of waste generated which is a very attractive feature for industrial applications.

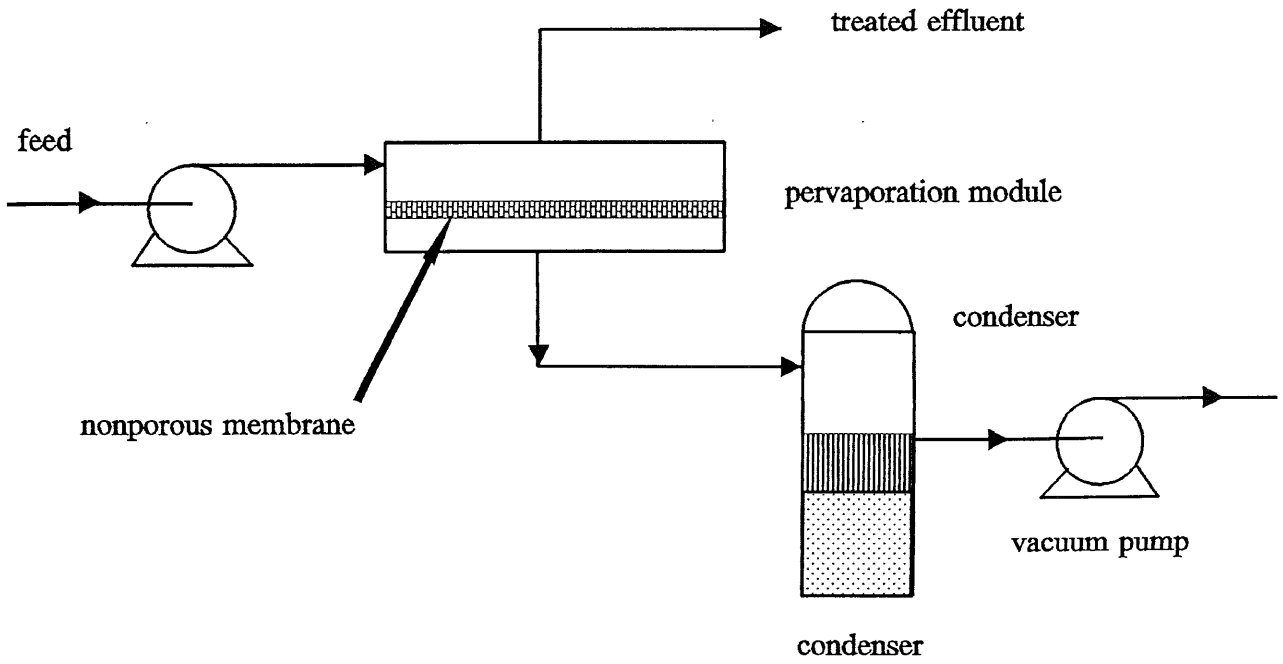

Figure 2.1 Schematic diagram of pervaporation process

2.1.2 Transport of Solute

Pervaporation differs from other membrane processes in that the membrane constitutes a barrier between the feed in the liquid phase and the permeate in the gas phase. Transport across the nonporous membrane generally follows the well-known solution-diffusion model (Binning et al., 1961). The first step of this process is the sorption of the liquid on the membrane at the feed side. The next two steps are: diffusion of the volatile organic compound (VOC) and water through the membrane and desorption on the permeate side. Sorption and diffusion are the more important steps whereas the desorption step is not normally considered as the rate controlling step (Fleming and Slater, 1992). The driving force across the membrane is the chemical potential gradient between the liquid and the vapor. The chemical potential of component i can be expressed as

$$\mu_i = \mu_i^0 + RT \ln a_i \tag{2.1}$$

where μ_i° is the chemical potential at standard state, a_i is the activity of the permeating component, R is the universal gas constant, and T is the absolute temperature. The activity of the component i is defined as

$$a_i = \frac{p_i}{p_i^0}. \tag{2.2}$$

In this definition, the quantities p_i° and p_i are the saturation vapor pressure and the partial pressure of

component i respectively. For multicomponent mixtures the component activity is represented by

$$a_i = \gamma_i x_i \tag{2.3}$$

where γ_i is the activity coefficient and x_i is the mole fraction.

The performance of a pervaporation module is characterized by a separation factor, α_{pervap}, defined as

$$\alpha_{pervap} = \frac{(C''_i / C''_j)}{(C'_i / C'_j)} \tag{2.4}$$

where C'_i, C'_j and C''_i, C''_j are the concentrations of components i and j in the feed solution and in the condensed permeate stream respectively.

2.1.3 Concentration Polarization

When a fluid is passing through the bore of a hollow fiber, the velocity of a fluid is not constant throughout the radial distance. It decreases with increase in the radial distance from the center of the bore. To facilitate mass transfer analysis through the membrane, the velocity gradient is replaced by a stagnant boundary layer adjacent to the membrane (Wijmans et al., 1996). When a feed solution containing a low concentration of VOC passes through the bore of the membrane all permeating species, mainly the VOC, have to pass through the boundary layer which is shown in Figure 2.2. This boundary layer which acts as a resistance to mass transfer can significantly affect the performance of the membrane process.

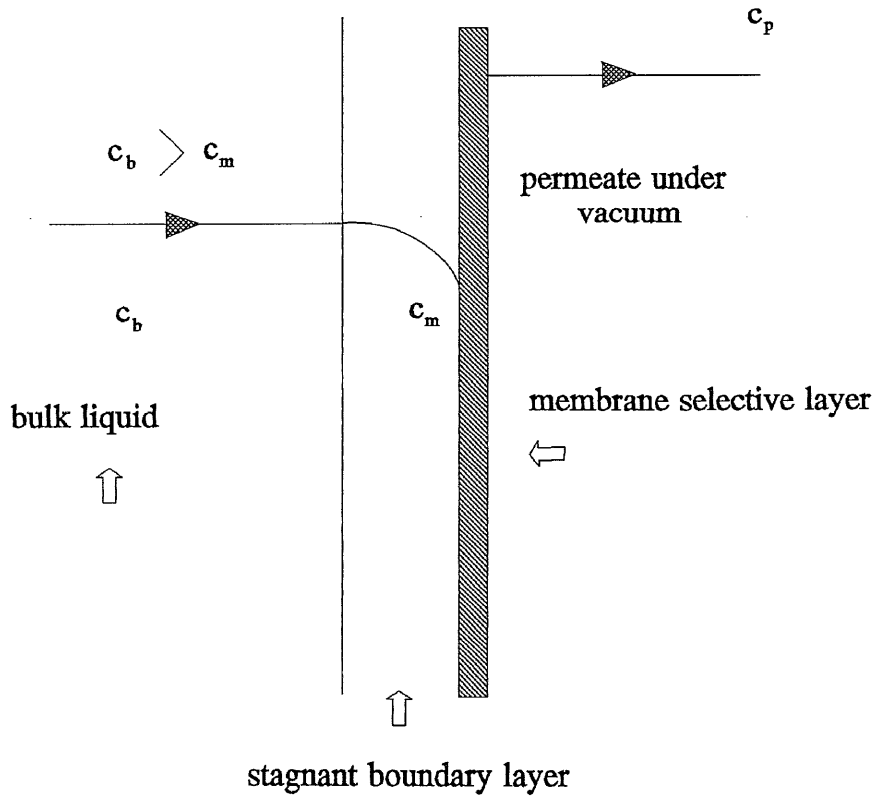

Figure 2.2 Phenomenon of concentration polarization

The VOC selectively passes through the membrane if any separation is achieved. In that case the concentration of VOC in the condensed permeate, C_p, is higher than the bulk concentration of the VOC in the feed, C_b. As VOC gets depleted at the surface of the membrane a concentration gradient develops in the stagnant boundary layer. This phenomenon is called concentration polarization. If the resistance of the membrane to mass transfer is neglected, then the resistance to mass transfer in the boundary layer controls the process and transport of VOC in boundary layer becomes the rate limiting step. The membrane resistance cannot be neglected under certain conditions. If the Reynolds number is increased the boundary layer resistance will be reduced and eventually in the turbulent regime the membrane resistance may become rate controlling.

2.2 Theory of Surfactants

2.2.1 Characteristics of Surfactant

A surfactant (a contraction of the term surface-active agent) is a substance that when present at a low concentration in a system, has the property of adsorbing onto the surfaces or interfaces of the system and of altering the interfacial free energies of those surfaces considerably (Rosen, 1989).

Surface-active agents have a characteristic molecular structure consisting of two groups. The group with very little attraction for the solvent is called the lyophobic group and the group with strong attraction to the solvent is called

lyophilic group. This is known as amphipathic structure (Rosen, 1989). When a surfactant is added to a solvent, the lyophobic group in the interior of the solvent may cause distortion of solvent liquid structure increasing the free energy of the system. In an aqueous solution of a surfactant the distortion by the lyophobic (hydrophobic) group results in an increase of free energy and the work required to bring the surfactant molecule to the surface is much less. So the concentration of the surfactant is high at the surface. On the other hand, the lyophilic (hydrophilic) group prevents the surfactant from forming a separate phase. The ampipathic structure thus increases the concentration of the surfactant at the surface and reduces the surface tension, and also orients the surfactant molecule at the surface with the hydrophilic group towards the aqueous phase.

2.2.2 Surfactant Classification

Surfactants can be classified into four groups depending on the structure of the hydrophilic group.

a) Anionic- The surface-active portion contains a negative charge, e.g. SDS;

b) Cationic- The surface-active portion contains a positive charge, e.g. tertiary ammonium chloride;

c) Nonionic- The surface-active portion contains no charge, e.g. SPAN 80;

d) Zwitterionic- The surface-active portion may contain negative or positive charge, e.g long-chain amino acid.

2.2.3 Micelle Formation by Surfactants

At higher concentrations, the property of surfactants to form colloidal-sized clusters in a solution results in micelle formation. Micelle formation or micellization is an important property because of its effect on detergency and solubilization.

2.2.4 Critical Micelle Concentration

The bulk properties of a surfactant solution are always found to be unusual indicating the presence of colloidal particles in the solution. When the equivalent conductivity of an anionic surfactant in water is plotted against the square root of the normality of the solution, the curve shows a sharp drop in conductivity at a certain point indicating a sharp increase in the mass per unit charge of the material in the solution. The concentration at which this phenomenon occurs is called the critical micelle concentration (CMC). Changes in some physical properties in the neighborhood of the CMC of SDS is shown in Figure 2.3 (Preston, 1948). The determination of the value of the CMC can be done by using any of these physical properties, but most commonly the breaks in the electrical conductivity, surface tension or light scattering or refractive index concentration curves have been used for that purpose (Rosen, 1989).

The shape and size of the micelle produced in the aqueous media is of paramount importance in determining the properties of the surfactant solution, such as its viscosity and its

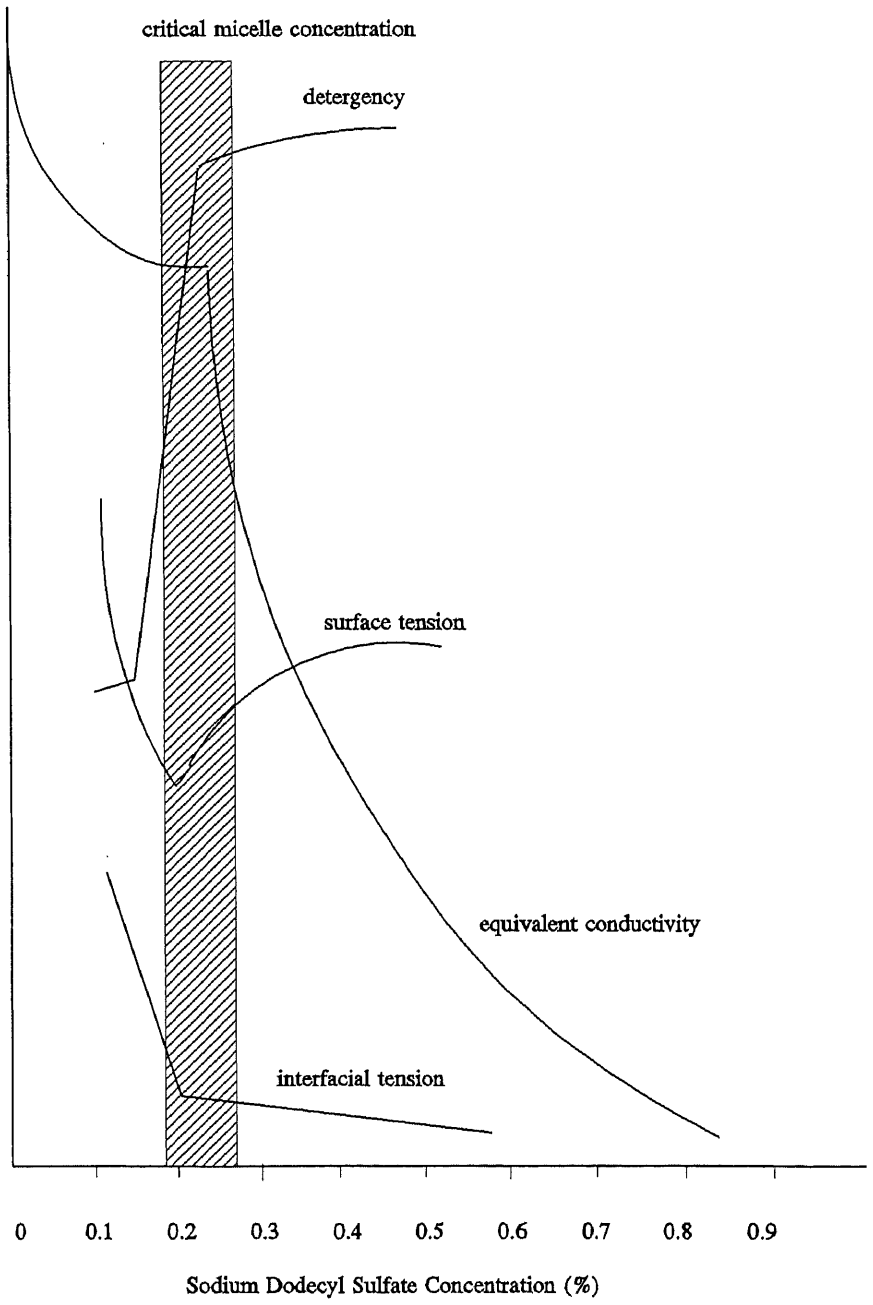

Source: W. C. Preston, J. Phys. Colloid Chem., 1948

Figure 2.3 Changes in some physical properties of an aqueous solution of sodium dodecyl sulfate in the neighborhood of critical micelle concentration.

capacity to solubilize in water hydrophobic substances. The factors known to affect the CMC in aqueous solution are:

a) the structure of the surfactant;

b) the presence of added electrolyte;

c) the presence of second liquid phase, and

d) the temperature of the solution.

2.2.5 Solubilization by Using Surfactants

One of the most important properties of surfactants directly related to the micelle formation is solubilization. Solubilization may be defined as the spontaneous dissolving of a substance by reversible interaction with micelles of a surfactant in a solvent to form thermodynamically stable isotropic solution with reduced thermodynamic activity of the solubilized material (Rosen, 1989). As explained before, micelles can be seen as spheres or cylinders, etc. having a polar exterior which is the hydrophilic portion of the surfactant, and a nonpolar hydrophobic interior. Due to the polar nature of the exterior the micelles are highly soluble in water and the interior acts like a pseudo-oil-phase into which the organic compounds partition (Shiau et.al, 1994). As a result of this organic compounds partitioning into the micelle, the aqueous solubility of the compounds increases. The apparent solubility of organic compounds increases with increase in the number of micelles (Rosen, 1989). The micellar partitioning coefficient, K_m, is used to determine the partitioning of the organic compound between the micellar

phase (X_m) and the bulk aqueous phase(X_{aq}). K_m is defined by the following relation:

$$K_m = \frac{X_m}{X_{aq}} \tag{2.5}$$

where,

$$X_m = \frac{C_m}{(C_m + S_m)} \tag{2.6}$$

$$X_{aq} = \frac{C_{aq}}{C_0} \tag{2.7}$$

In the above equation X_m is the intramicellar mole fraction of organic compound, that is, the ratio of the molar concentration of solubilized organic compound, C_m, to the total molar concentration of the surfactant, S_m, and organic solute, C_m.

At lower level of surfactant concentrations, a normally solvent-insoluble material shows very little solubility until a certain concentration of surfactant is reached, after which solubility increases almost linearly with increase in surfactant concentration. This critical concentration is the CMC of the surfactant which was discussed in section 2.2.4.

A theory of micellar structure, based upon the geometry of different micellar shape and space occupied by the hydrophilic and hydrophobic groups of the surfactant molecule, has been developed by Israelachvili, Mitchell and Ninham and Mitchell and Ninham (Rosen, 1989). The shape of the micelle is dependent on the parameter $V_H/l_c a_o$, where V_H is the

volume occupied by the hydrophobic groups in the micellar core, l_c is the length of the hydrophobic group in the core, and a_o is the cross-sectional area occupied by the hydrophilic group at the micelle-solution interface. The volume V_H, is calculated from the following relation

$$V_H = (27.4 + 26.9n)\ \text{Å}^3 \qquad (2.8)$$

where n is the number of carbon atoms of the chain embedded in the micellar core (Tanford, 1980). The length of the hydrophobic end, l_c can be calculated from the relation

$$l_c \leq (1.5 + 1.265n)\ \text{Å} \qquad (2.9)$$

For SDS, the value of the parameter, $V_H/l_c a_o$ is calculated from the above relations to be 0.48. A micelle is likely to be cylindrical in aqueous media if the value of the above parameter falls between 0.33-0.5 (Rosen, 1989). However, Van'ons optical techniques revealed the shape of micelles of SDS solutions at low concentration to be rather spherical and monodispersed (Ogino and Abe, 1993).

When amphiphilic molecules are dissolved in water, they can achieve segregation of their hydrophobic portions from the solvent by self-aggregation, which are known as micelles (Tanford,1980). In aqueous media, the surfactant molecules are oriented in all the structures with their polar heads toward the aqueous phase and their hydrophobic ends away from it. Figure 2.4 shows the solubilization of TCE in the micelle of SDS. The hydrocarbon chains in the micelle are generally

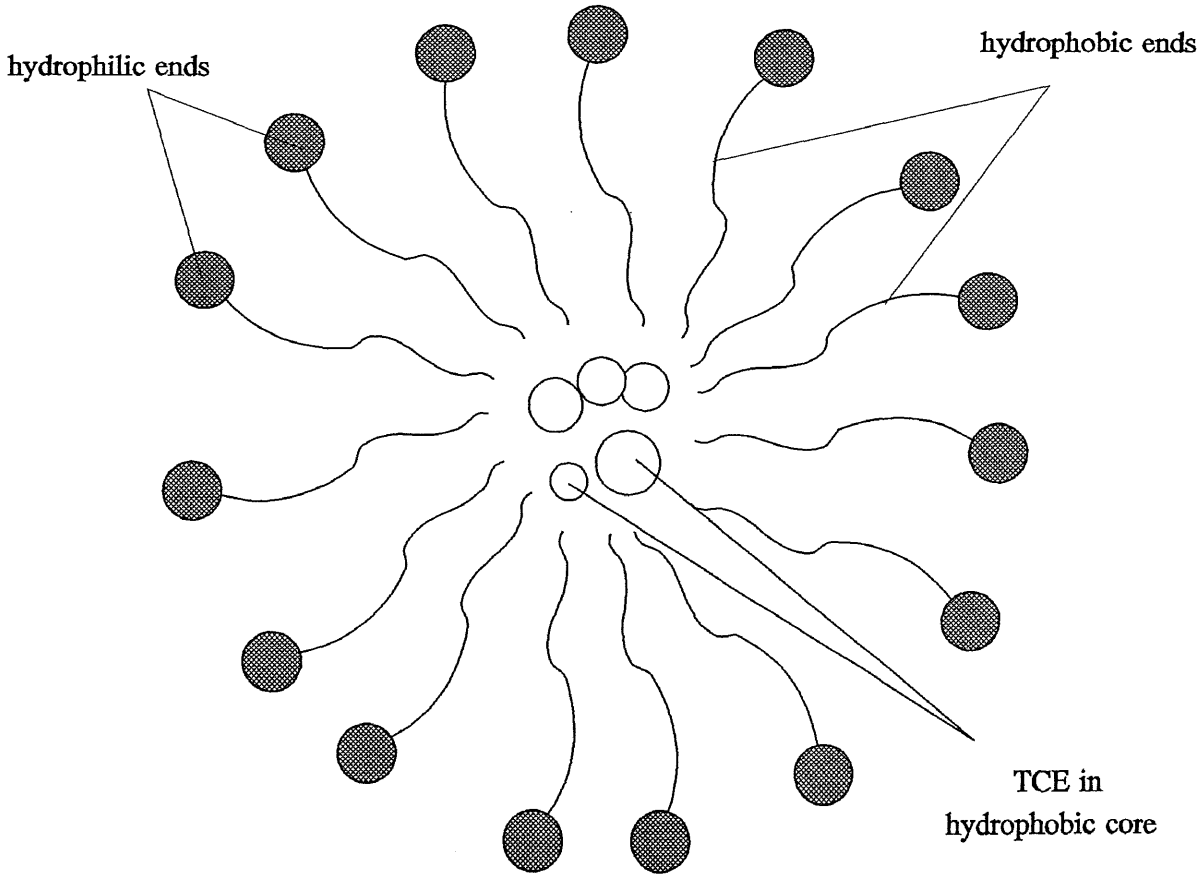

Figure 2.4 Micellar structure of surfactant and TCE

disordered , so that the hydrophobic core is regarded as a small volume of hydrocarbon where TCE can get solubilized. Micelles formed by simple amphiphiles are quite small, with aggregation number varying between 40 to 100 with a dodecyl hydrocarbon chain as in SDS (Tanford 1980).

The self-association of amphiphiles in aqueous solution into micellar aggregates is predicted by the hydrophobic effect, but the tendency to form relatively smaller micelles with an aggregation number of 100 or less is due to the existence of a repulsive force which prevents the formation of bigger micelles. So the existence of the upper limit of the micelle size is due to the repulsive force of the head groups which increases with increase in the aggregation number.

If the CMC exceeds the solubility of a surfactant at a particular temperature, then the minimum surface tension will be achieved at solubility rather than CMC. The temperature at which the solubility of an anionic surfactant is equal to the CMC is called the Krafft point (Rosen, 1989). At this temperature the surfactant molecules tend to form micelles rather than ions. Therefore, the surfactants show a higher interfacial effectiveness, if used above their Krafft point.

2.3 Postulations

This section will postulate about the mechanisms of transport of TCE in a surfactant-containing solution to the pores of the hydrophobic membrane having a nonporous silicone coating. The surfactant concentration may vary; it may be above or below

the CMC. When the surfactant concentration level exceeds the CMC limit, TCE is solubilized in the hydrophobic core of the micelle and a very low concentration of free TCE exists in the bulk solution. In such cases the most probable phenomenon will be the following.

If the surfactant solution does not wet the hydrophobic membrane pores, the micelles collide with the membrane wall, thereby breaking the core and releasing the TCE on the hydrophobic substrate surface or the pore mouth. TCE will be vaporized in the gas-filled pores and permeate through the silicone skin as in vapor permeation. Figure 2.5 shows a such a hollow fiber with silicone coating, where the pores are filled with TCE. Higher surfactant loading, lower Reynolds number, etc. will reduce the frequency of collision of the micelles with the membrane wall, the amount of TCE solubilized per molecule of surfactant and therefore reduce the flux. As the flux of TCE is dependent on the free TCE available for transport through the membrane, the presence of surfactant should adversely effect the performance of the membrane module. Such a situation will occur at the lower range of SDS concentrations, since there is no effective pressure gradient driving the liquid feed into the pore: all the pressure difference effectively appears across the nonporous silicone skin. As the surfactant concentration increases the number of micelles is increased and all of the TCE will be trapped in the core of the micelles. Further such a solution may spontaneously wet the pores and allow micellar solution to

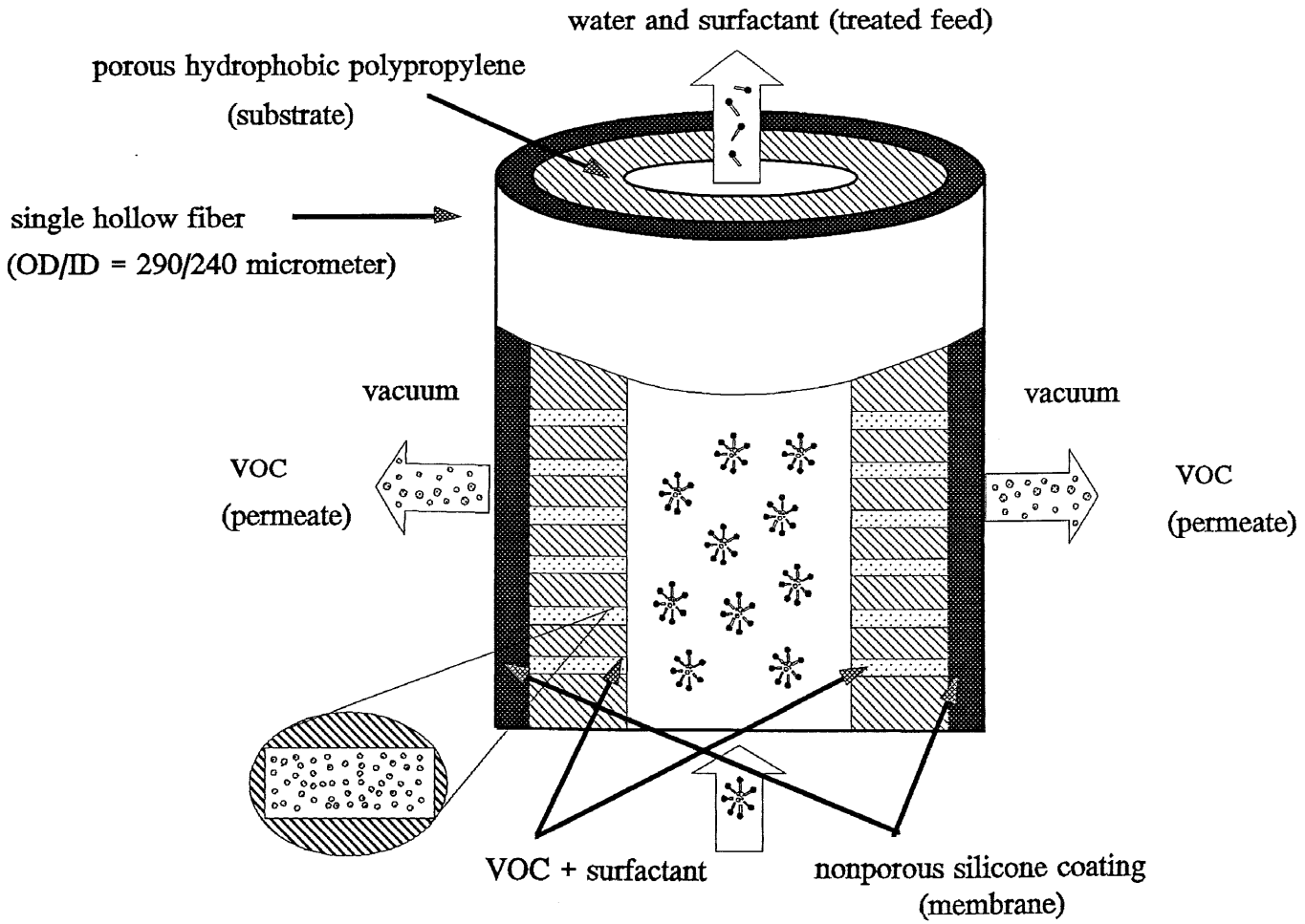

Figure 2.5 Micellar feed of surfactant and VOC into the hollow fiber with dry pores filled with VOC vapor

enter the pores. The situation will become complicated and is going to be influenced by the level of free TCE released by micellar collision with the pore mouth, pore surfaces or thereabouts.

The behavior of the system in operation may be judged by determining the mass transfer coefficient of TCE. For any given overall resistance level, the TCE flux will be proportional to the free TCE concentration at the upstream surface of the membrane (the downstream partial pressure is assumed to be very low). The availability of free TCE will be highest in a surfactant-free system. In efficient micellar systems, the free TCE level may be 2-3 orders of magnitude smaller. Whether micelles continue to exist at the membrane surface or are broken up by collisions with the membrane surface and release the TCE cargo from their core for removal by vaporization, can be determined by the relative magnitudes of the overall mass transfer coefficient experimentally determined, using a fixed concentration driving force of TCE.

CHAPTER 3

MATERIALS AND METHODS

3.1 Chemicals and Gases Used

Trichloroethylene (Purity 99.9%, FW 131.39, Density 1.456 gm/cc), Acetonitrile (HPLC grade, Purity 99.9%), Methanol (Purity 99.9%, FW 32.04), Isopropyl Alcohol (HPLC grade) from Fisher Scientific (Springfield, NJ); Sodium Dodecyl Sulfate (SDS, Purity 99%, FW 288.4), Gum Xanthan (Practical Grade), Dodecane (Purity 99%, FW 170.34), n-Hexane(Purity 99%) from Sigma (St. Louis, MO); Dowfax 8309 kindly supplied by Dow Chemicals Company (Midland, MI); Ultrapure Nitrogen, Helium, Air and Liquid Carbon Dioxide from Matheson Gas Products (E. Rutherford, NJ).

3.2 Hollow Fiber Modules and Module Fabrication Procedure

The hollow fiber membrane modules contained hydrophobic microporous hollow fiber support having a plasma polymerized thin nonporous silicone skin on the outer surface (240 μm/290 μm ID/OD; substrate is polypropylene Celgard X-10, Hoechst Celanese, Charlotte, NC). Four modules were prepared and one module having a Mitsubishi polypropylene substrate was procured from AMT (Minnetonka, MN). The geometrical characteristics of these modules are given in Table 3.1. For each module, 75 fibers were laid out over a polythene sheet on a table. Five fibers were carefully taken at a time from the

Table 3.1 Characteristics of the modules used

Module No.	Fiber Manu-Facturer	Membrane Coating	No. of Fibers	O.D (μm)	Active Length (cm)	Mass Transfer Area Based on O.D (cm^2)	Remarks
1. *	Celgard (X-10)	Silicone	75	290	20.5	140.1	Fabricated in lab.
2. *	Celgard (X-10)	Silicone	75	290	20.5	140.1	Fabricated in lab.
3. *	Celgard (X-10)	Silicone	75	290	28.5	194.7	Fabricated in lab.
4.	KPF-205 Mitsubishi	Fluoro-polymer	106	205	30	204.8	AMT
5.	Celgard (X-10)	Silicone	75	290	28.5	194.7	Fabricated in lab

Module No. 1 & 2 in series = Twins; Module No. 1, 2 & 3 in series = Trio.

* Porosity (ϵ_m) is 0.30 and tortuosity (τ_m) is 3.5 (Prasad and Sirkar, 1988).

spool and cut to the desired length. The fibers were kept in place using scotch tape at both ends. Then scotch tapes at the ends were removed from the fiber mat which was kept wet with water. The fibers were then rolled gently and slowly to form a bundle. Two ends of the mat were tied separately into a tight bundle. The end portions were cut to remove the scotch tape. The cotton threads were tied loosely to keep the fibers together.

The fibers were then pulled into a 1/4" OD seamless stainless steel tube (McMaster-Carr, New Brunswick, NJ) of desired length, connected to a 1/4" stainless steel male run tee (Swagelok, R.S Crum, Mountainside, NJ). During the whole operation of putting the fiber bundle inside the shell, the shell side was filled with water to avoid any friction with the metal. The module was dried by passing filtered air through the shell for two days. The module was then ready for potting of the tube sheet.

One type of epoxy resin and two types of silicone rubber were used for potting the tube sheet. The first layer of potting was done externally with RTV118 silicone rubber (General Electric, Waterford, NY) at the end of the male tee connection. The second layer was made by mixing C-4 resin and D activator (Beacon Chemicals, Mt. Vernon, NY) in 4 to 1 weight proportion. The components were thoroughly mixed in a plastic cup and the mixture was deaerated in a vacuum desiccator. The resin mixture was poured into the shell side of the tube sheet by a disposable pipette. The epoxy was

allowed to harden for 24 hours at room temperature. The third and the final layer was done with a mixture of RTV615A silicone rubber compound and RTV615B silicone curing agent (General Electric, Waterford, NY), in 10 to 1 weight proportion. This layer was used to provide a gas-tight seal between the epoxy resin and the silicone coated hollow fiber. The third layer was also allowed to harden for 24 hours at room temperature and the fiber bundle at the end of the male tee connection was cut with a sharp knife. The entire tube sheet was completely cured in a period of 2 weeks. For preparing the module (# 5, Table 3.1) for experiments with dodecane only two layers of potting were used. The first layer was made of a mixture of A-2 resin and Activator A (Armstrong Products, Easton, MA). The second layer was made of epoxy (C-4 resin and Activator D) used for other modules.

3.3 Experimental Setup

3.3.1 Pervaporation Setup

The experimental setup for pervaporation is shown schematically in Figure 3.1. Feed was pumped into the module by a peristaltic Masterflex pump, model 7518-10 (Cole Parmer, Vernon Hills, IL) from a collapsible Teflon bag (Cole Parmer, Vernon Hills, IL). Teflon bags of two different capacities, 1.2 and 4.7 liters were used depending on the flow rate and duration of the experiment. Transparent 1/4" ID Teflon tubing (Cole Parmer, Vernon Hills, IL) and stainless steel fittings (Swagelok, R. S. Crum, New Brunswick, NJ) were used for the

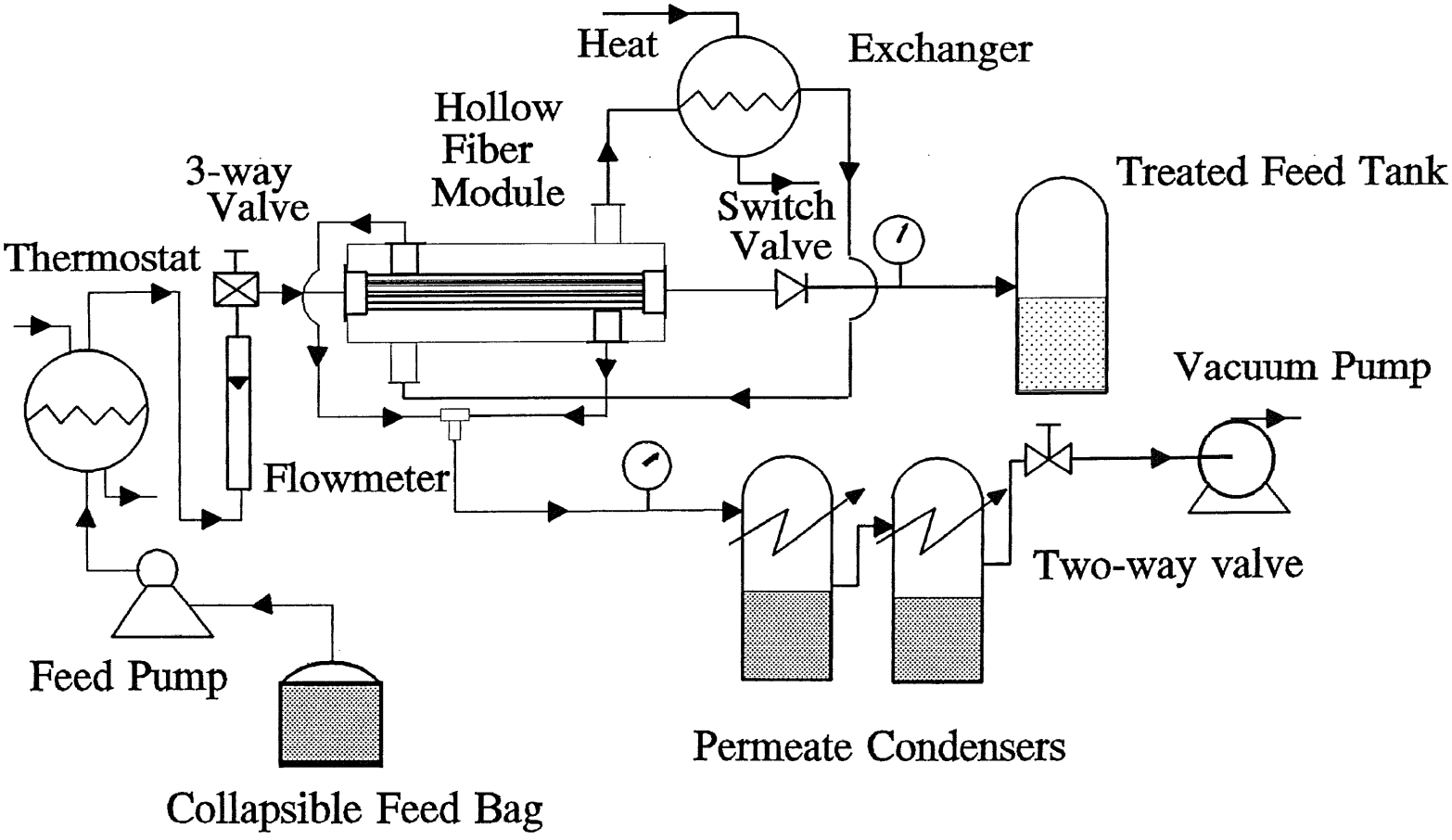

Figure 3.1 Pervaporation experimental unit

feed and all connecting lines to and from the membrane module. The feed line was connected to a three way valve (Swagelok, R.S Crum, New Brunswick, NJ) for collection of feed samples. A micrometering valve (Swagelok, R. S. Crum, New Brunswick, NJ) was connected to the feed line to regulate the feed pressure. An oilless vacuum pump (KNF Neuberger, Trenton, NJ, Model UN 726.112 FTP) was used to maintain a vacuum of -28/-28.5 inch Hg. Convoluted Teflon tubes (Cole Parmer, Vernon Hills, IL) were used for the vacuum line connections to the condensers. The modules were immersed in a polyethylene water bath interfaced to a thermostat (Fisher Scientific, Springfield, NJ) to maintain the desired temperature range between 18°-50°C. One or two condensers (Labglass, Vineland, NJ) with a graduated tip were connected in series to the vacuum line before the vacuum pump. Dry ice and methanol were used as cooling medium in a Dewar flask (Labglass, Vineland, NJ), inside which the condenser was kept to trap the permeate vapor from the module outlet. For experiments at a high feed temperature, a thermostat (Haake, model A81) was employed to heat the feed line. Feed was pumped from the Teflon bag through a heating coil immersed in a heated recirculating oil bath to achieve the desired temperature.

3.3.2 Oil Permeation Setup

The experimental setup for oil permeation is shown schematically in Figure 3.2. Feed was pumped into the module by a peristaltic Masterflex pump, model 7518-10 (Cole Parmer,

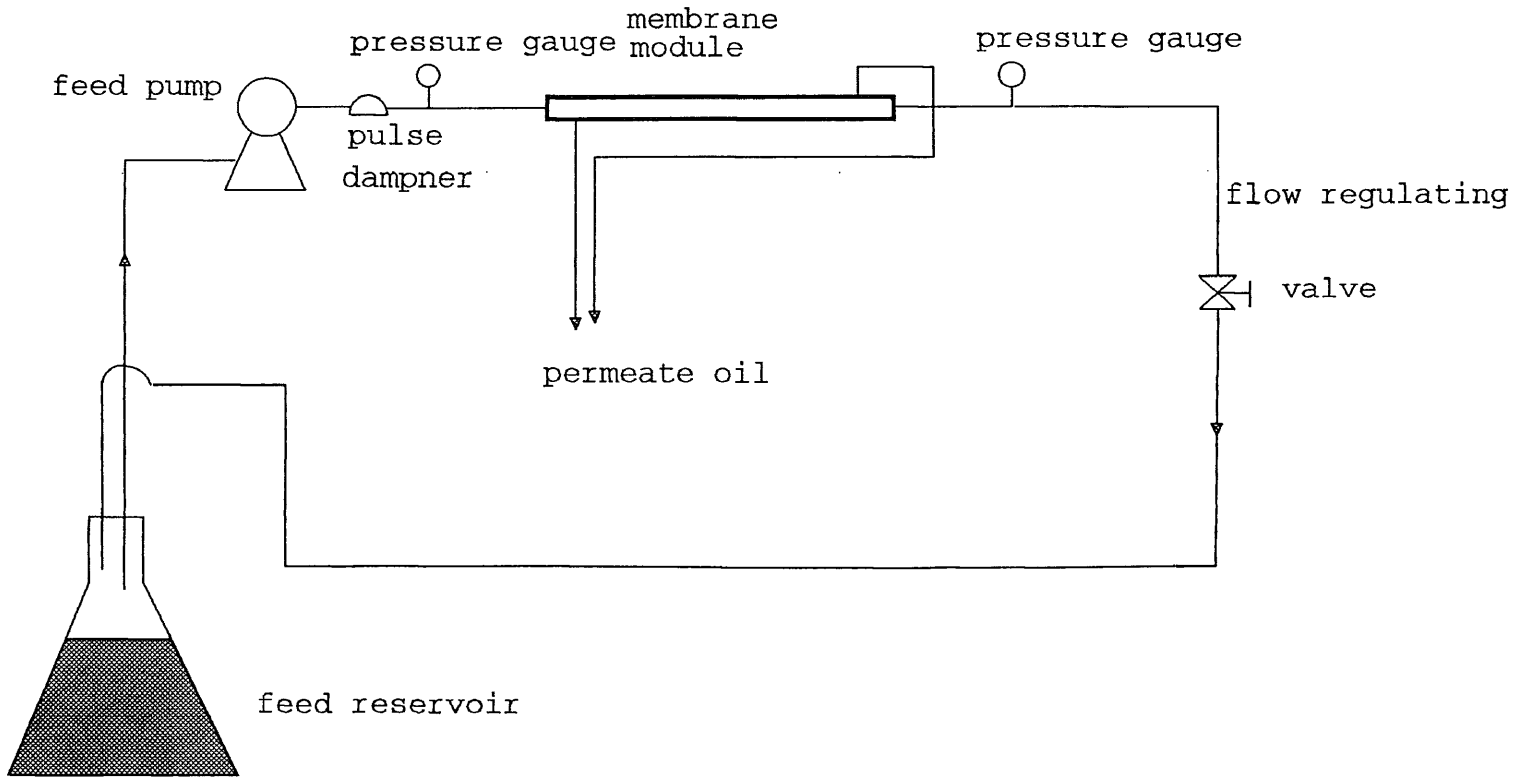

Figure 3.2 Experimental setup for oil permeation

Vernon Hills, IL). The feed solution of dodecane was made in a 4 liter HDPE (Cole Parmer, Vernon Hills, IL) reservoir and was kept under continuous stirring during the experiments. The feed line was connected to the tube side of the membrane module through a pulse dampener (Cole Parmer, Vernon Hills, IL). Two pressure gauges (Cole Parmer, Vernon Hills, IL) were connected before and after the module to monitor the pressure drop along the module length. A flow regulating metering valve (R. S. Crum, New Brunswick, NJ) was connected at the outlet to regulate the flow. The outlet was connected back to the feed reservoir to operate under batch recirculation mode. The shell side was maintained at atmospheric pressure.

3.4 Analytical Procedure

3.4.1 High Pressure Liquid Chromatography

Aqueous TCE concentration was measured in a HP series II 1090 high pressure liquid chromatograph (HPLC) with a HP 3390 integrator and an autosampler (Hewlett Packard, Wilmington, DE). A reverse-phase Hypersil ODS C18 HP column (5 μm, 100 x 4.6 mm, Hewlett Packard, Wilmington, DE) was used. An AltGuard system (Alltech, Deerfield, IL) was used with a Hypersil ODS C18 5 μm Alltech guard column to protect the HPLC column from any damage and contamination without changing the separation efficiency. The composition of the mobile phase used was 60% acetonitrile and 40% deionized and filtered water. TCE concentration was determined using an injection volume of 5 μl at 200 nm wavelength and a mobile phase flow rate of 0.4

cc/min. The HPLC was calibrated for TCE concentration ranging from 0-120 ppm and the response was found to be linear. Calibration was done for TCE in pure water as well as in 0.3%, 1.0%, 3.0%, and 5% of SDS (w/v) solutions; the responses were nearly identical. Figure 3.3 shows the calibration curves of TCE at different concentration levels of SDS. For every sample analyzed, two injections were made to avoid any error and the average was taken as the actual response. A wash cycle with deionized water was programmed so that three injections of deionized water were run automatically for 5 minutes each after analysis of every sample. Calibration was checked every week by analyzing freshly prepared standards.

3.4.2 Gas Chromatography

Aqueous TCE concentration was also measured in a HP 6890 series gas chromatograph (GC) using a HP 7694 Headspace Sampler and HP 6890 series integrator (Hewlett Packard, Wilmington, DE). TCE was analyzed by a flame ionization detector (FID) using a HP-5 capillary column (crosslinked 5% PH ME Siloxane) of 30 m length, 320 μm dia and 0.25 μm film thickness (Hewlett Packard, Wilmington, DE). Ultrapure nitrogen was used as the carrier gas. Analysis of TCE in aqueous solutions of varying surfactant concentrations posed difficulties in reproducing results using the direct liquid injection headspace techniques because of their sensitivity to matrix variation. It also required proper calibration curves for each sample matrix. This was extremely difficult as the

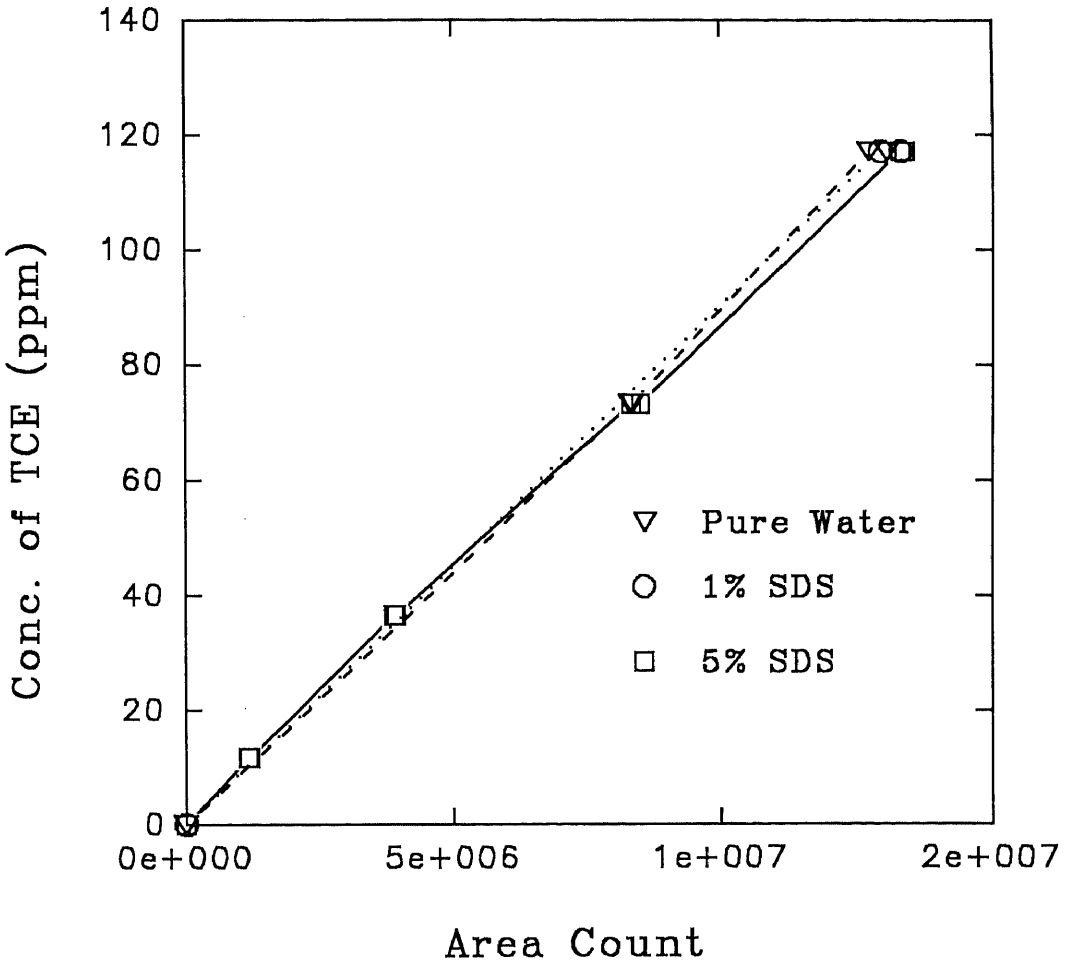

Figure 3.3 Calibration curve for TCE

compositions of the samples varied widely or were unknown. The methodology of Full Evaporation Technique (FET) was used to overcome the matrix effect (Markelov and Guzowski, 1993).

This technique was based on a near-complete transfer of analytes from a condensed matrix into a vapor phase. This transfer eliminated the possibility of contamination from any nonvolatile component in the sample such as SDS, and also the calibration was not affected by the sample matrix. The concept behind the full evaporation technique was to reduce the sample size and increase the temperature to eliminate the matrix effect. Reproducible results were obtained by using 13 μl of sample in a 22.5 ml headspace vial. The optimum Headspace oven temperature (100°C), sample volume (13 μl) and sample equilibration time (7 min) were determined after an extensive study by varying each of these parameters one at a time. Figure 3.4 shows the effect of equilibration time on TCE output signal. The curve reached a plateau after a certain time (6 minutes) indicating that the peak area became independent of the equilibration time at that time zone. Sample vials were thermostated in the headspace analyzer for 7 minutes at 100°C. Headspace vapors were analyzed by pressurizing the vials for 0.15 minute followed by a timed injection of the vapors for 1 minute into the gas chromatographic column. A temperature program was fixed for the GC in order to get clear separation of TCE. The initial oven temperature of the GC was set at 40°C for 1.5 min. In the next step, temperature was ramped at 25°C per min until it

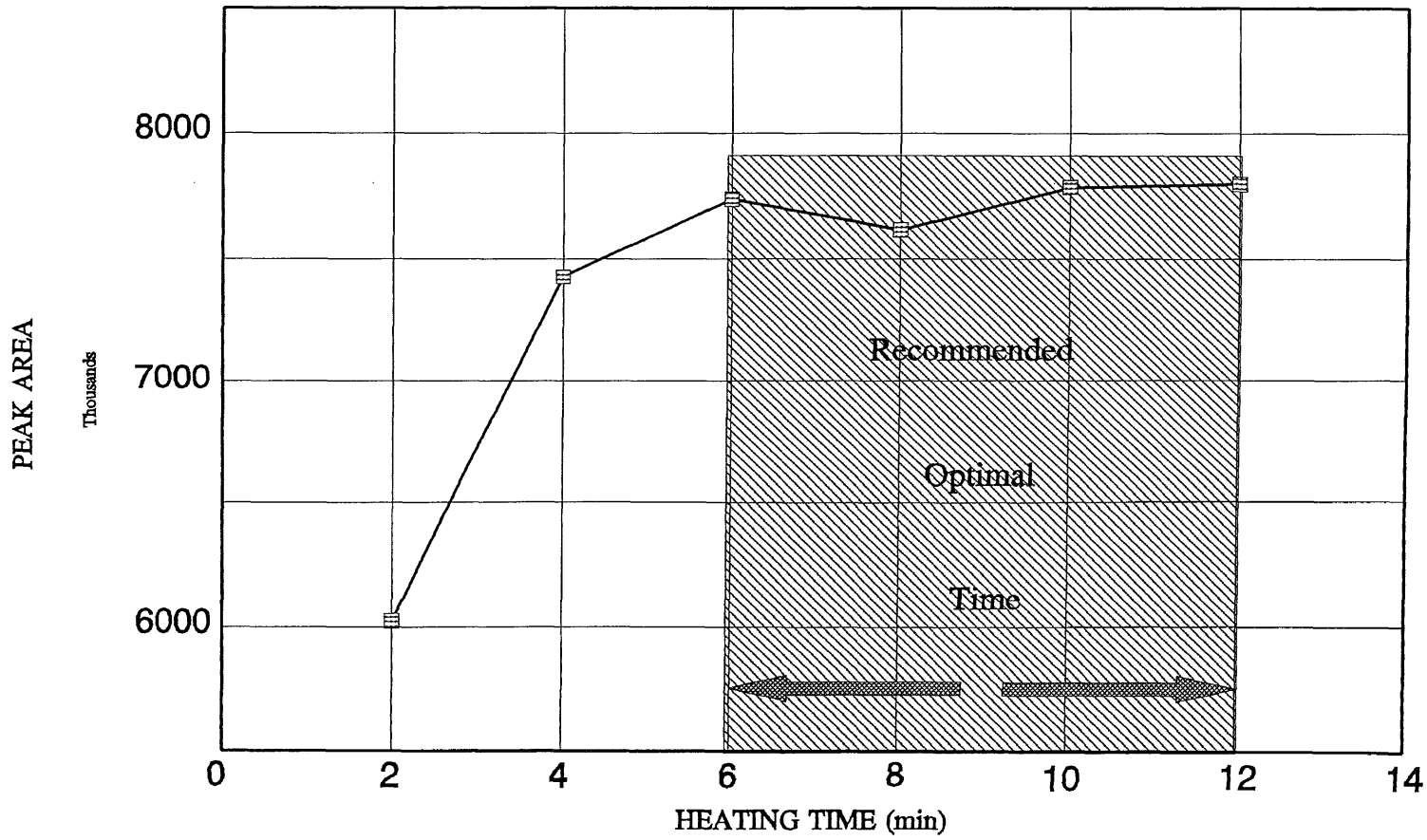

Oven=75C;Det=250C;N2=10mL/min;HS-Oven=65C 1%SDS & 75 ppm TCE

Figure 3.4 Effect of equilibration time on TCE output

reached 75°C, where it was kept for 1 min. In the final step, the temperature was ramped at 40°C per min., until it reached the final temperature of 160°C, which was maintained for 3 min.

A similar procedure was used for analyzing dodecane in the GC Headspace device. The volume of sample collected from the feed reservoir of dodecane-water mixture was 2 ml. Dodecane was extracted into the hexane phase by using a Centrifuge (model no. IEC 438, International Equipment, Needham Hts., MA). A 5μl sample for analysis was taken from the hexane phase and was analysed in the GC-Headspace. A temperature program similar to that adopted for TCE analysis was employed. Only the final temperature was changed to 220°C as the boiling point of dodecane is 215°C. Figures 3.5 and 3.6 show the equilibration time curve and the dodecane calibration curve respectively.

3.5 Experimental Procedure

3.5.1 Preparation of Feed

Fresh feed for pervaporation experiments was prepared before each experiment to avoid volatilization of TCE. A stock solution of desired surfactant concentration was prepared at least 48 hours before the experiment for proper micelle formation. To prepare a desired concentration of surfactant (w/v), deionized water was heated just above the Krafft Point of SDS (18°-20°C) before adding the surfactant. This enhanced instant solubilization of the surfactant and micelle formation

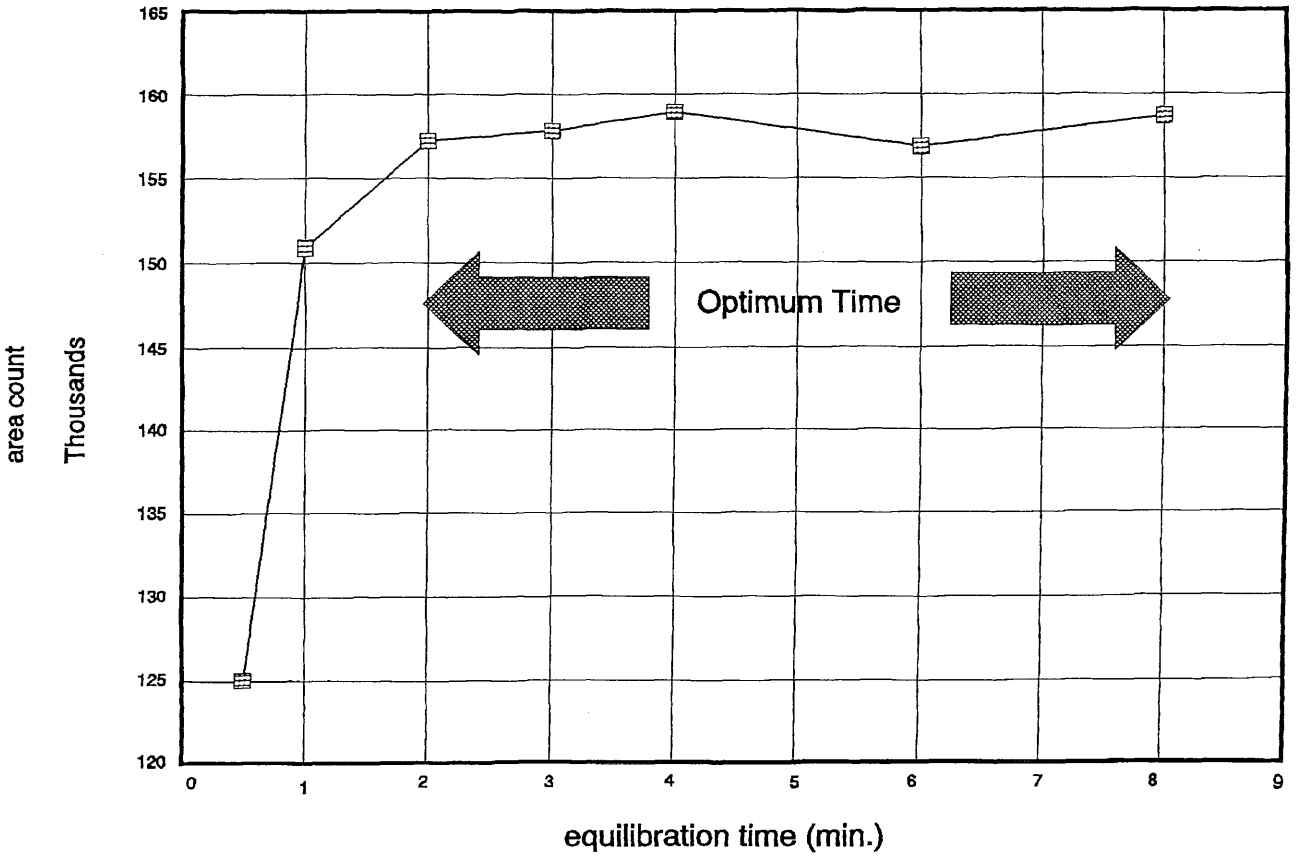

Figure 3.5 Equilibration time for dodecane in headspace

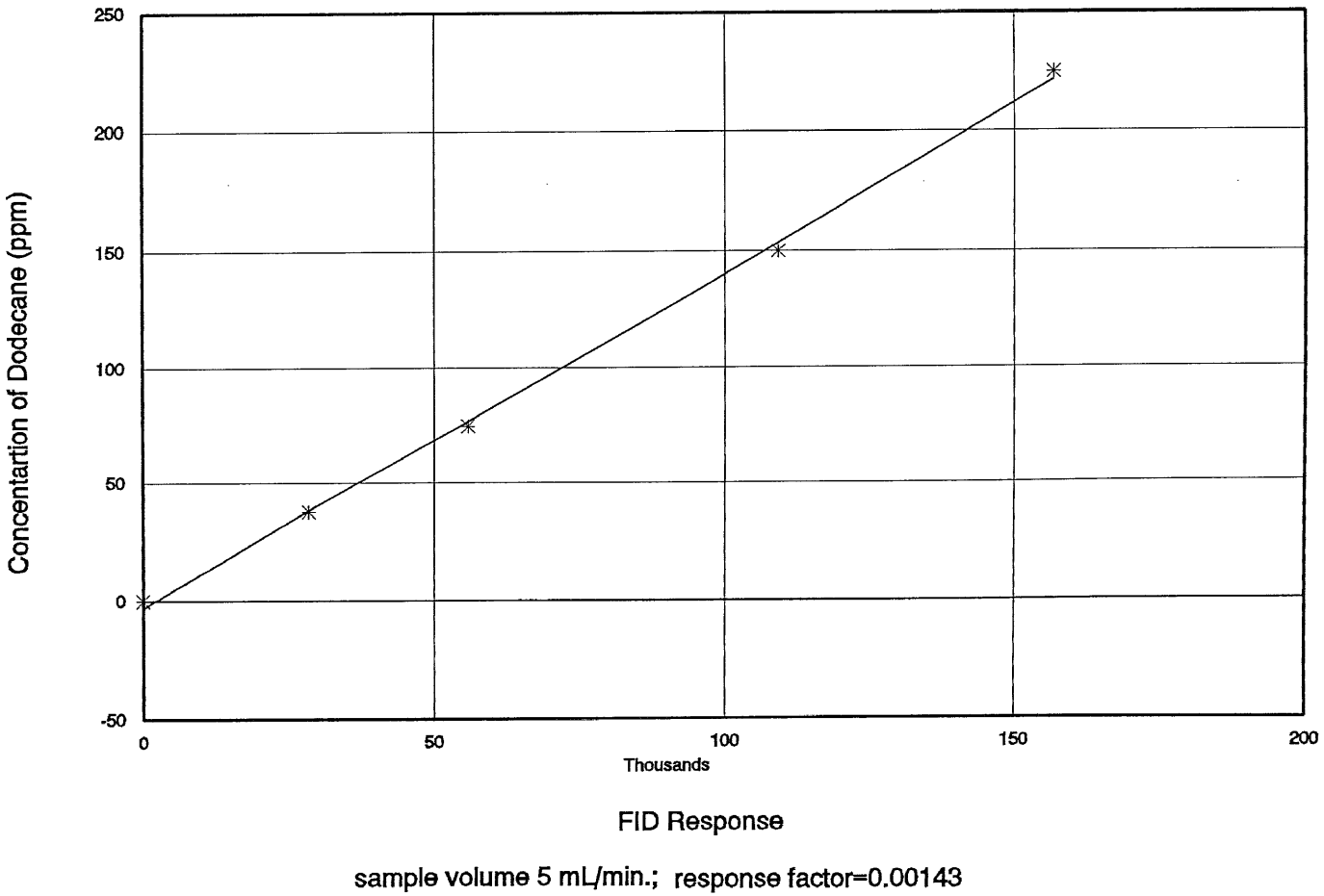

Figure 3.6 Calibration of the FID response for n-dodecane

instead of dissociation into ions. This surfactant solution was kept in slow stirring condition for a minimum of 48 hours before adding the TCE. The feed was prepared in a glass vessel with a minimum headspace to avoid volatilization of TCE.

For preparing the feed for the oil permeation experiments dodecane was added to a specific volume of water in the reservoir. The feed was kept under rapid stirring, using a magnetic stirrer overnight to achieve an oil-in-water emulsion.

3.5.2 Sampling

Sampling of feed and retentate in pervaporation experiments was done very carefully to avoid any kind of loss during sample collection and dilution. The feed line was connected to a three-way valve for collection of feed sample. Feed and retentate samples were tested every half hour in the GC/Headspace and every one hour in the HPLC. At the time of feed sample collection, the three-way valve was opened and the feed was allowed to flow for a minute to avoid any error arising from any stagnant feed in the collection line. Samples were collected in a small 2 ml glass vial and capped immediately with a Teflon-lined cap to avoid TCE loss. For analysis in the GC/Headspace, 13 μl of the sample was taken in a high precision Hamilton microsyringe and was directly injected to a headspace vial of volume 22.5 ml. For HPLC analysis, feed sample was diluted 50-100 times depending on the feed concentration, in a Hamilton Diluter (Fisher

Scientific, Springfield, NJ). Same procedure was followed for the retentate sample for the GC. For HPLC analysis the retentate sample was diluted 2-12.5 times or directly injected depending on the absolute concentration of the sample. The diluted samples were thoroughly mixed in a vortex mixer (Fisher Scientific, Springfield, NJ) before analysis.

3.5.3 Experiment

For pervaporation experiments, feed solution was pumped into the collapsible Teflon bag which prevented formation of headspace during an experimental run and kept the feed concentration nearly constant. Feed was kept at a pressure range of 7-10 psig by using a micrometering flow control valve (Swagelok, R. S. Crum, New Brunswick, NJ) in the retentate line. Feed pressure was monitored by using a dial pressure gauge (Cole Parmer, Vernon Hills, IL). Vacuum was tested at -28" Hg before starting the system. The temperatures of the water bath and the thermostat were fixed at the desired set point before start-up. Dry ice was prepared in a dry ice machine using liquid carbon dioxide. Dewar flasks were filled with dry ice and methanol after putting in the condenser to achieve a low cooling temperature (approx. -50°C). The condenser and the feed lines were insulated with glasswool and aluminum foil. Samples were taken every half hour and analyzed. The experiment generally reached steady state after 3 hours and normal runs were carried out for 6-7 hours. The experiment was stopped once consistent results were obtained

from 4 consecutive samples. The volume of the permeate was observed and noted from the collection in the condenser. The volume of water and the VOC could be easily noted as the permeate separated into two distinct organic and aqueous phases. After every experiment the module was washed for a few hours with deionized water and filtered nitrogen was passed overnight to dry it before another experiment.

In oil permeation experiments the oil-in-water emulsion was fed to the module by a masterflex model pump. The outlet from the module was recirculated back to the feed reservoir. The feed in the reservoir was kept under constant stirring during the experimental run to get a homogeneous emulsion. The flow rate and the pressure drop along the module were noted every hour. Samples from the reservoir were taken every hour to determine the decrease in concentration of oil in the reservoir. The permeate was collected during the experimental run in a graduated cylinder. In the experiments with SDS, the surfactant solution was prepared first before adding dodecane. Although the emulsion was much more stable in the presence of surfactant, the reservoir was kept under constant stirring during the experimental runs. After every set of run the module was washed with deionized water and 25% isopropyl alcohol (IPA) solution and dried overnight by passing nitrogen and filtered air.

The TCE pervaporation experiments were planned in four phases. In the first phase (phase 1) the experiments were started with a home-made small module (#1, Table 3.1) at

different concentrations of SDS and TCE. Some experiments were also carried out using the AMT module (# 4, Table 3.1). After getting the basic data on the performance of the module, experiments with modules in series were planned for the next phase (phase 2). The schematic diagrams of the series connections are shown in Figure 3.7. Two (# 1 & 2, Table 3.1) or three (# 1, 2 & 3, Table 3.1) modules were connected in series to carry out experiments under conditions similar to those in phase 1 to achieve higher TCE removal and to observe the performance of the system using more than one module. In the subsequent phase (phase 3), performance of the system was tested using Dowfax 8390 as the surfactant under same conditions of experiments with SDS. A couple of experiments were also done with SDS, Xanthan Gum and TCE as the feed matrix. In the fourth and the final phase, experiments were done with one small module (# 1, Table 3.1) using a system of only TCE and water. These experiments were done to compare the performance of the module under the same conditions with or without the surfactant. The experimental parameters for pervaporation in the different phases are given in Table 3.2.

At the very end of phase 4, a few experiments were done for oil permeation using dodecane as a model oil. Experiments were done to determine the performance of the module by passing the feed both from the tube side and the shell side. A couple of experiments were also done to determine the effect of feed pressure and flow rate on the oil flux. Table 3.3 provides the experimental parameters for dodecane experiments.

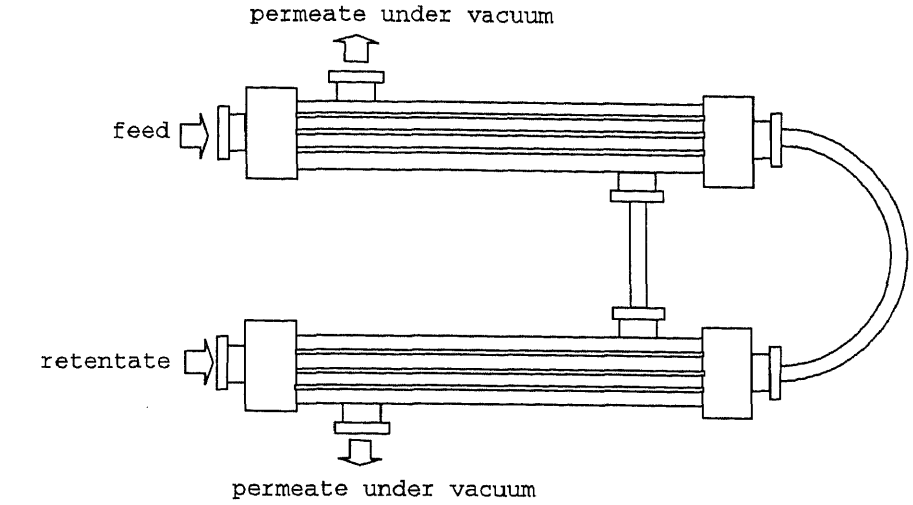

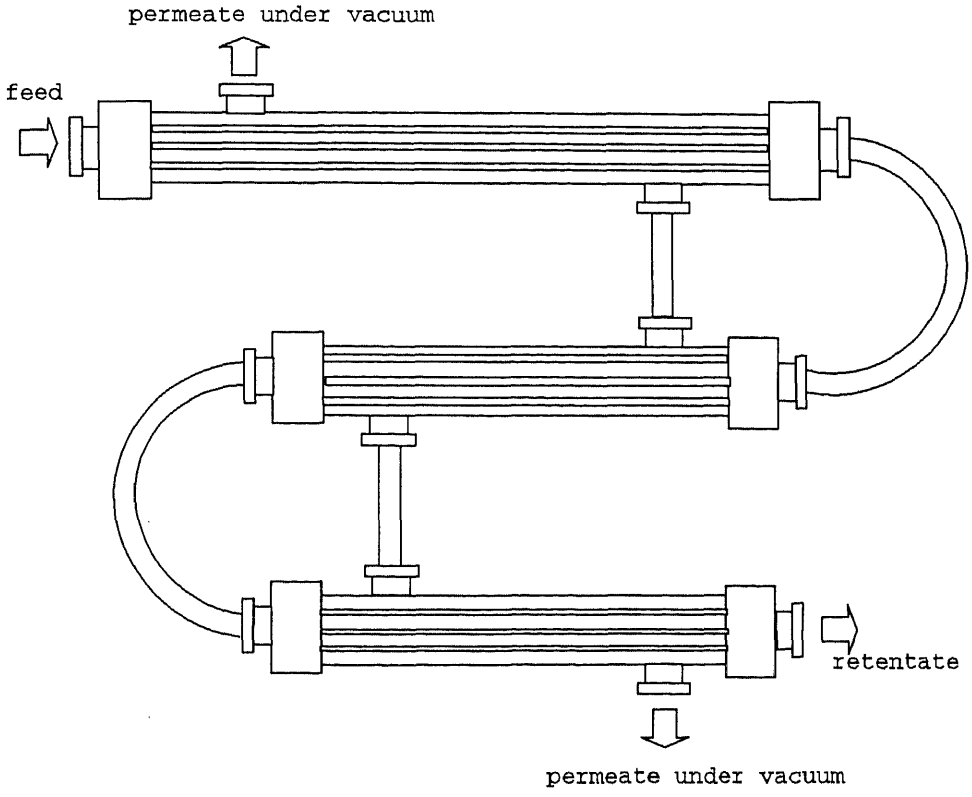

Figure 3.7 Modules in series with feed in tube

Table 3.2 Experimental parameters for TCE pervaporation

	Feed flow rate (ml/min.)	Feed Temperature (°C)	Feed pressure (psig)	Vacuum (mm Hg)
phase 1	2.0-8.0	18	7-10	-27 to -28.5
phase 2	2.0-15.0	18-35	7-10	-27 to -28.5
phase 3	2.0-3.0	18	7-10	-27 to -28.5
phase 4	2.0-20.0	18	7-10	-27 to -28.5

Table 3.3 Experimental parameters for dodecane permeation

Feed Pressure (psi)	Feed flow rate (ml/min)	Dodecane conc. (ppm)	SDS conc. (%)
7-15	9-19	4000-10000	0-0.5

The properties of the surfactants and TCE are given in Tables 3.4 and 3.5.

3.5.4 Reproducibility of Experiments

In this research, each experiment in pervaporation was repeated twice to avoid any experimental error. An experiment was reported if both results were consistent. For reporting purpose, data from one of the experiment from each set and not the average value were taken.

Table 3.4 Properties of surfactants used *

	SDS	Dowfax 8390
1. Chemical name	Sodium Dodecyl Sulfate	Dialkylated Diphenyl Ether Disulfonate
2. Source	Sigma Chemicals	Dow Chemicals
3. Type	Anionic	Anionic
4. Formula Weight	288.4	900 (100%) 643 (avg. M. W)
5. Formula	$C_{12}H_{25}O_4SNa$	$[2(C_6H_4)+(C_{16}H_{33})+(NaSO_3)]+O$
6. Active component	99%	35% (min.)
7. CMC, 0.1 M electrolytes	0.28	0.014
8. Free energy of micellization ΔG°		
DDI water (KJ/mole)	-22.27	-26.42
0.1 M electrolyte	-28.77	-39.19
9. Area per molecule ($Å^2$)	43.70	93.83
10. Density (g/cc) @25° C		1.03-1.15
11. Viscosity (cps) @25° C		10

* source: Rosen (1989), Dow Chemical Company(Michigan).

Table 3.5 Physical and chemical properties of TCE *

molecular weight (g/mol)		131.39	
melting point (°C)		-87.10	
boiling point (°C)		86.70	
density (g/cc), liquid 20° C		1.465	
viscosity, mPa.s			
20° C		0.58	
60° C		0.42	
critical properties			
temperature (°C)		271.0	
pressure (MPa)		5.02	
heat capacity, (J/kg.K)			
liquid		941.0	
vapor at boiling point		653.0	
dipole moment, debye		0.77	
dielectric constant ϵ		3.43	
vapor pressure (kPa)[a]	A	B	C
Antoine constants	5.94606	1187.51	214.474
solubility (mg/L)		1100.0	

[a] $\log_{10} P = A-[B/(T+C)]$
* source: Kirk-Othmer, Encyclopedia of Chemical Technology. Vol. 3, 1983, Wiley & Sons.

CHAPTER 4

RESULTS AND DISCUSSION

To achieve the goals mentioned in Chapter one of this thesis, several series of experimental runs were carried out to investigate the performance of various hollow fiber modules singly or in series: thus the mass transfer area was varied considerably. Three basic parameters were taken as a measure of the module performance and its efficiency. They are: percent removal of TCE, TCE flux and water flux. As mentioned in section 3.6 of this thesis, experiments were carried out in four different phases. In this chapter the results of each phase will be discussed separately. Further the results of the preliminary permeation experiments of dodecane-water emulsions will also be presented and discussed.

4.1 Phase One

In phase one of this research initial exploratory experiments were done with different concentrations of TCE and SDS using one small module (# 1, Table 3.1). Experiments were planned with different concentrations of SDS keeping the flow rate of the feed constant. All experiments in phase one were carried out at a temperature of 18°C.

The first set of experiments utilized a very high concentration of SDS of 5% (weight by volume), which is approximately 20 times the CMC value. In all experiments done

with 5% SDS, the feed was in the shell side of the module. The concentration range of TCE in the feed was 7600-8200 ppm. The experiments were carried out at two different flow rates of 2.5 and 7.5 ml/min. Figure 4.1 shows the results of these runs. It was observed that with increase in flow from 2.5 to 7.5 ml/min., the removal of TCE came down from 28% to 13% whereas the flux of TCE increased considerably. This was due to the fact that with an increase in flow rate the residence time of the feed in the module was lower which resulted in a drop in the percent removal; but as a higher concentration of TCE was fed to the module, the flux of TCE was increased. TCE flux was also likely to be affected by the feed Reynolds number. The removal of TCE was calculated based on the inlet feed concentration and the concentration of the retentate. The flux of TCE was calculated based on the procedure shown in Appendix A.

Since the experiments were done under the condition of a constant feed concentration and flow rate, the volume of water collected in the condensers represented the accumulated volume during the whole experiment. Water flux was obtained by measuring the water volume (V_{H2O}) collected in the condensers, and the operating time (t) according to the following equation:

$$water\ flux = \frac{V_{H_2O} * \rho_{H_2O}}{A_m * t} \qquad (4.1)$$

where A_m is the mass transfer area based on the outer diameter of the hollow fiber.

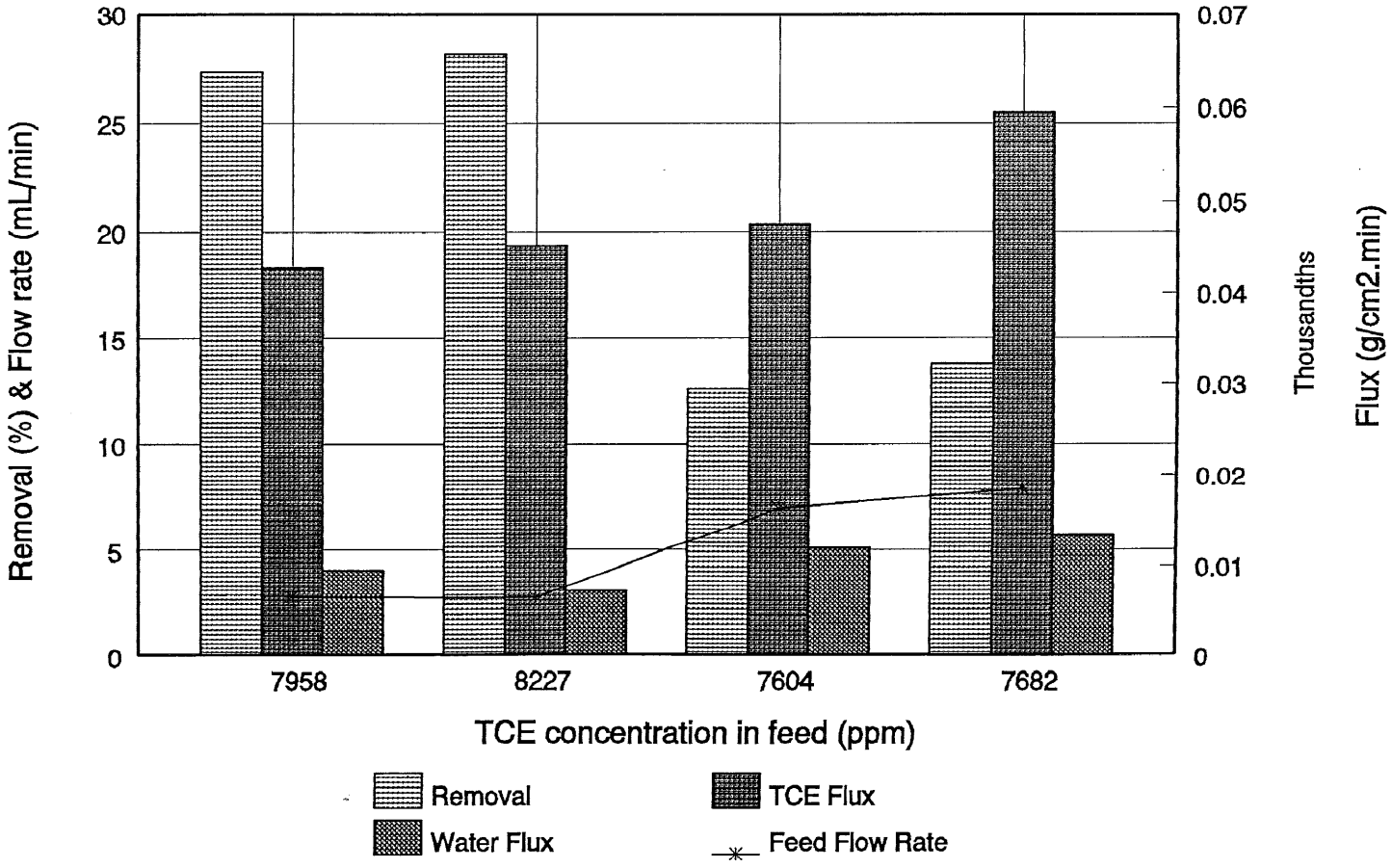

Figure 4.1 TCE removal with 5% SDS

For these experiments, in order to express the separation efficiency between the two permeating species, "i" (solute) and "j" (solvent), a separation factor (α_{ij}) was defined as follows (Zhu et al., 1983):

$$\alpha_{ij}=[y_i/(1-y_i)][(1-x_i)/x_i]=\left[\frac{J_i}{J_j}\right] * \left[\frac{C_j'}{C_i'}\right] \qquad (4.2)$$

where J_i is the permeation flux and C_i' is the feed concentration of species i and similarly for species j. The percent removal, selectivity, TCE flux and water flux for all experiments were calculated following the above mentioned methods. Table 4.1 gives the results of this series of experiments for 5% SDS-containing solution and TCE.

In the next series of experiments the concentration of SDS was lowered to 3%. For the first time feed was passed through the tube side of the module, exposing TCE and SDS directly to the pores of the substrate. For a similar concentration range (7500-8200 ppm) of TCE used in shell side experiments with 5% SDS, the behavior of the module was observed. For a flow rate of around 2.5 ml/min, the percent removal and TCE flux were significantly higher than those observed in the 5% shell side experiments. Table 4.1 provides also the results of these experiments.

The next set of experiments were done with 1% SDS with a wide range of TCE feed concentrations. Figure 4.2 shows the results of experiments for a concentration range of 1800-3100 ppm of TCE at a flow rate of around 2.5 ml/min. It was

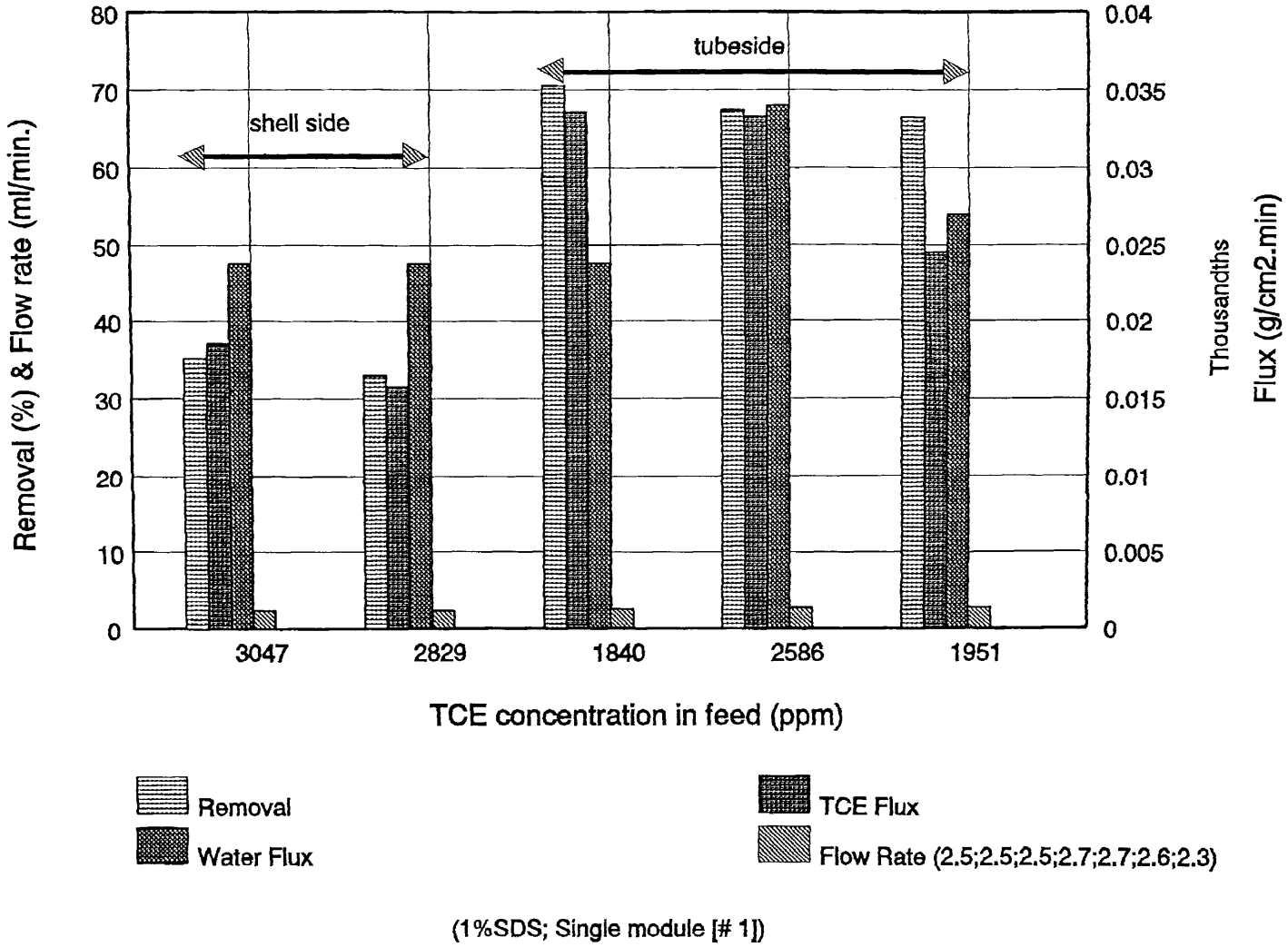

Figure 4.2 TCE removal with 1% SDS

observed that in this concentration range, the TCE removal in the experiments with feed in the shell side(30-32%) were half the removal obtained when the feed was in the tube side (68-71%). This was due to the fact that when micelles hit the substrate in the tube side TCE was released and was directly exposed to the pores of the hydrophobic substrate and vaporized immediately. Also when fed from shell side there could be a drop in the driving force as the effective vacuum in the tube side could be less due to the increased pressure drop in the pores and the tube side compared to the tube-side feed operation.

Figure 4.3 shows the effect of TCE concentration in feed with 1% SDS concentration. It was observed that as the TCE concentration went up from 283 to 2586 ppm, the percent removal dropped from 81.3 to 67.4. However TCE flux increased almost linearly with TCE concentration from 3.5e -6 gm/cm^2-min. for 283 ppm TCE to 3.4 e -5 gm/cm^2.min. for 2586 ppm TCE.

The next set of experiments in phase one was carried out with 0.3% SDS, which is slightly higher than its CMC value. Figure 4.4 shows the results of experiments done with flow rates around 2.6 ml/min. for a TCE concentration around 900 ppm. Experiments were carried out with feed in both shell and tube side; similar results were obtained as in earlier experiments with 1% SDS. Percent removal and TCE flux were doubled in the tube side experiments. One experiment was done in the tube side with a TCE concentration of 920 ppm for a very low flow rate of 2.3 ml/min., which showed a TCE removal

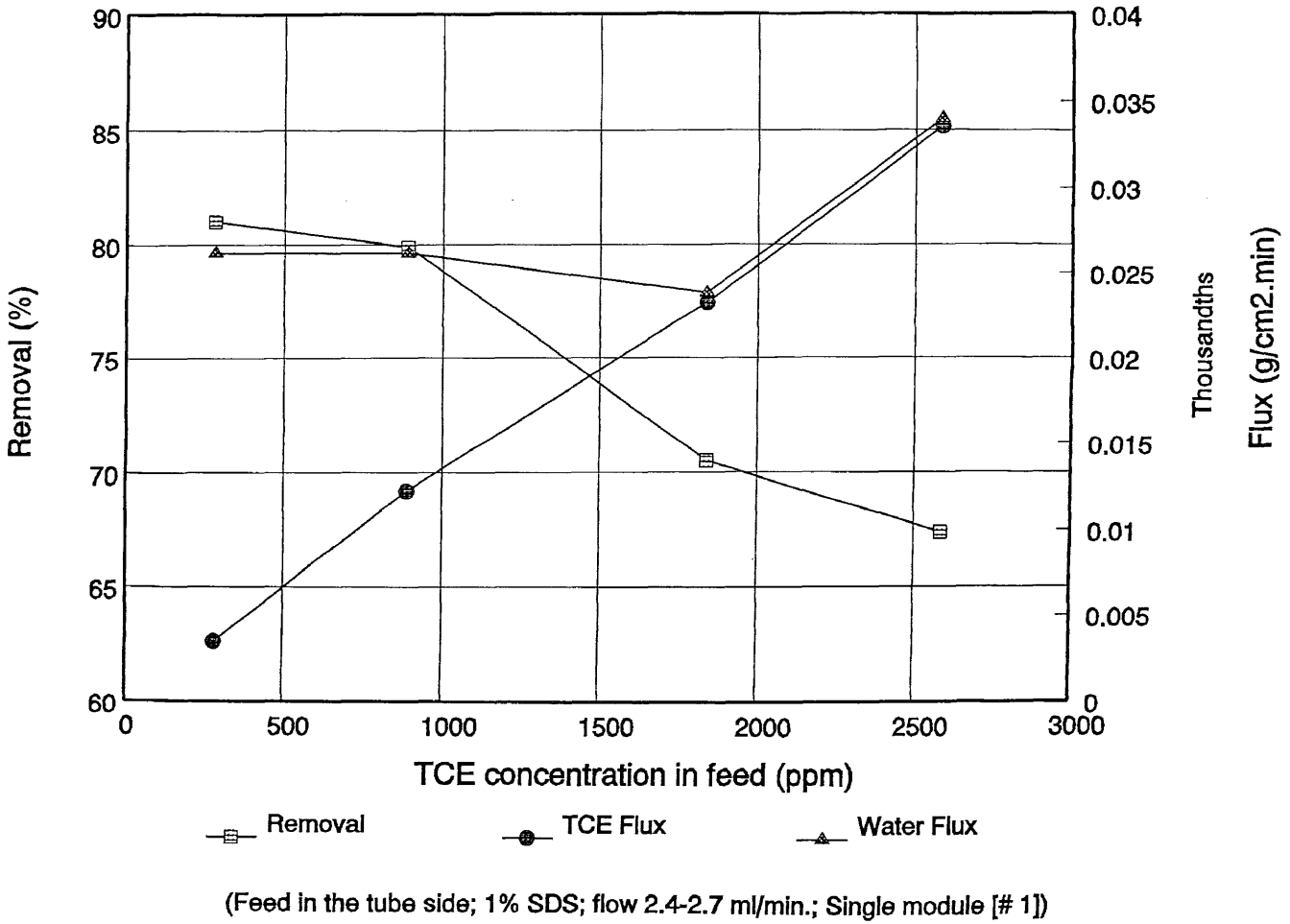

Figure 4.3 Effect of feed TCE concentration on TCE removal with 1% SDS

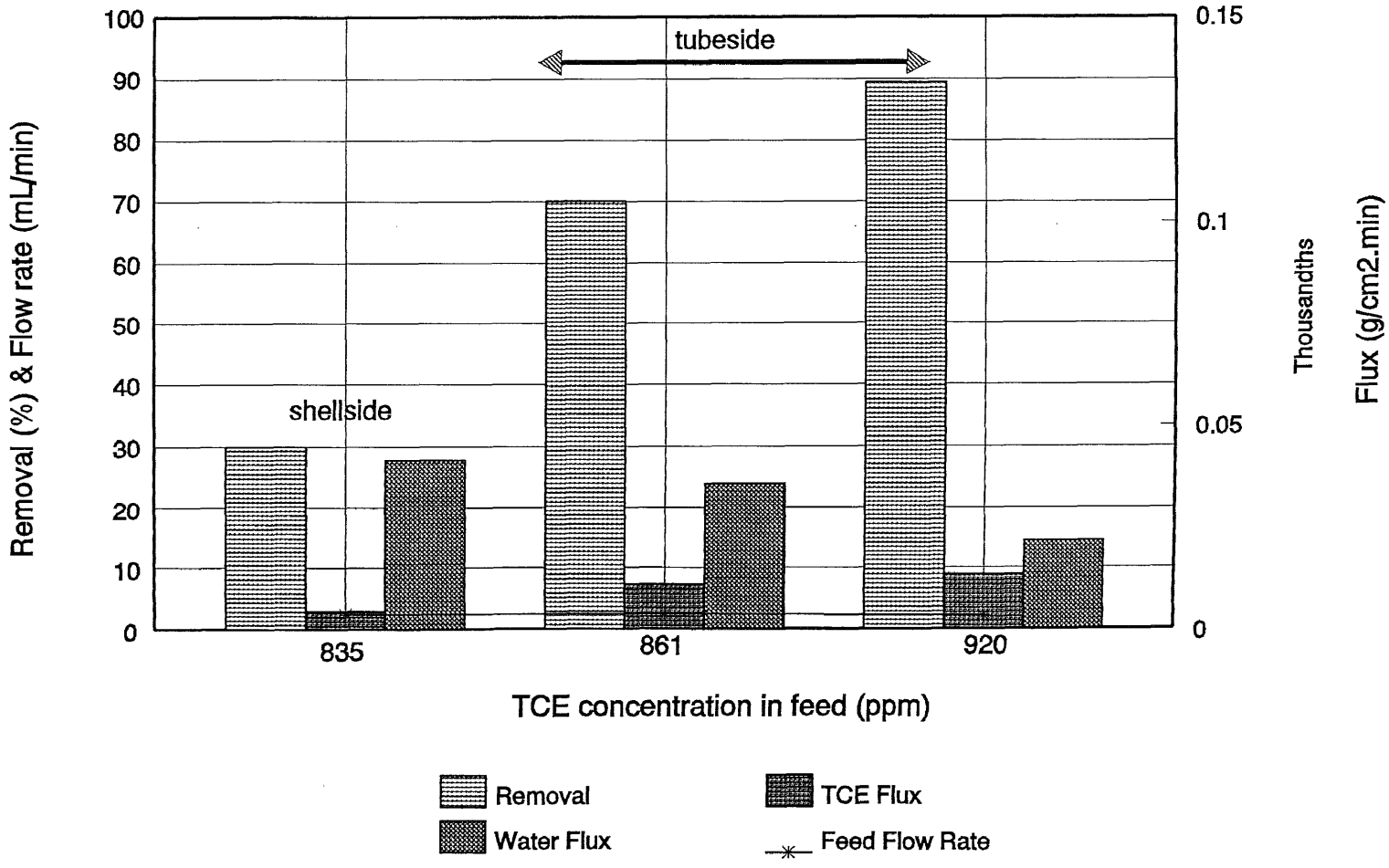

Figure 4.4 TCE removal with 0.3% SDS

Table 4.1 Experimental data for TCE removal in module # 1 for 5% and 3% SDS

feed conc. (ppm)	flow rate (ml/min)	run time (min)	removal (%)	TCE flux (g/cm^2-min)	water flux (g/cm^2-min)	% SDS	select-ivity
7958*	2.76	300	27.4	4.3e -5	9.5e -6	5	565
8227*	2.73	300	28.2	4.5e -5	7.1e -6	5	770
7604*	7.0	240	12.6	4.8e -5	1.2e -5	5	525
7682*	7.9	240	13.8	6.0e -5	1.3e -5	5	578
8132**	2.4	340	42.5	5.9e -5	2.5e -5	3	288
7479**	2.35	245	44.8	5.6e -5	3.8e -5	3	198

* shell side; ** tube side

Table 4.2 Experimental data for the flouropolymer module

feed conc. (ppm)	flow rate (ml/min)	run time (min)	removal (%)	TCE flux (g/cm^2-min)	water flux (g/cm^2-min)	% SDS	select-ivity
645*	2.4	320	52.3	4.0e -6	9.5e -5	1	65
1100*	2.42	335	51.3	6.6e -6	3.9e -5	1	152
1165*	2.5	320	57.0	7.8e -6	1.0e -4	1	64
1089**	2.46	300	95.8	1.2e -5	8.8e -5	1	128
1150**	2.43	300	97.3	1.3e -5	8.5e -5	1	135
2137**	2.42	300	92.5	2.3e -5	1.2e -4	1	90

* shell side; ** tube side

of 89.4%. Figure 4.5 shows the effect of SDS concentration on the performance of the membrane module under similar experimental conditions. Experiments with 1% SDS with a TCE concentration level of 891 ppm shows lower removal and TCE flux than those observed in the experiments done with 0.3% SDS under similar conditions. This showed that the presence of surfactants affected the performance of the module adversely.

After obtaining the preliminary data about the behavior of a single module (#1, Table 3.1), a few experiments were done with two other modules (# 2 and # 3, Table 3.1) and similar performance was observed. In the last stage of phase one the fluoropolymer module from AMT (# 4, Table 3.1) was tested and the results are shown in Figure 4.6. This module performed better than module # 2 and 3 in so far as removal of TCE was concerned. A removal of 97.3 % was obtained for TCE concentration of 1150 ppm with 1% SDS, whereas module # 1 and 2 could achieve only 70 % removal of TCE under similar condition. But the water flux in this fluoropolymer module was 3 times higher than the corresponding water fluxes in experiments with 1% and 0.3% SDS. This could be due to the very thin polymer coating on the Mitsubishi fibers. The thin coating facilitated the TCE flux but also allowed water to permeate more freely. As a result, the selectivity obtained were in the low range of 64-152. Table 4.2 provides the data from this series of experiments. After this set of experiments the module developed leaks which were tested and confirmed by pressurizing the module with water in the shell side.

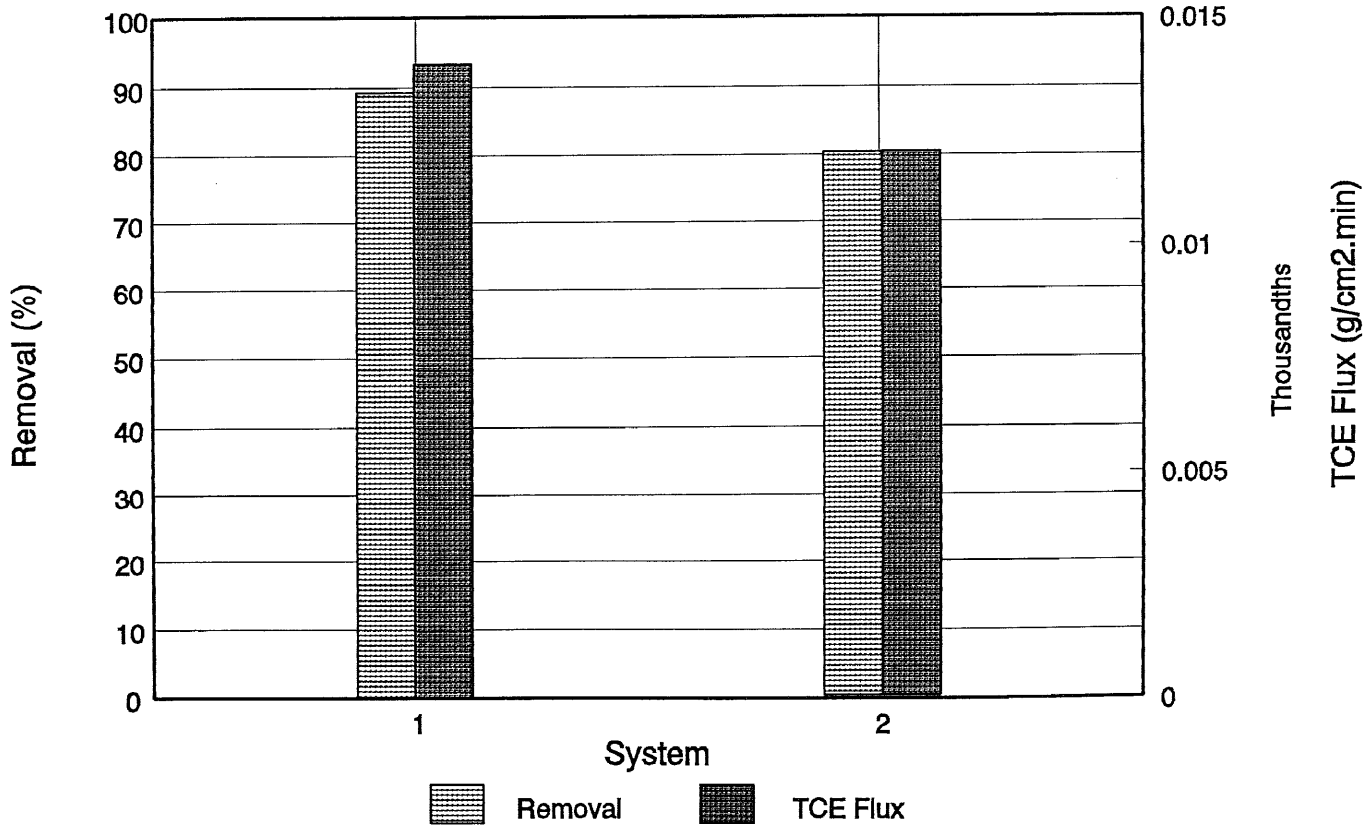

System 1: 0.3% SDS, 2.3 ml/min. Flow rate, feed concentration 920 ppm
System 2: 1% SDS, 2.42ml/min. Flow rate, 891 ppm feed concentration

(Feed in the tube side; Single module [# 1])

Figure 4.5 Effect of SDS concentration

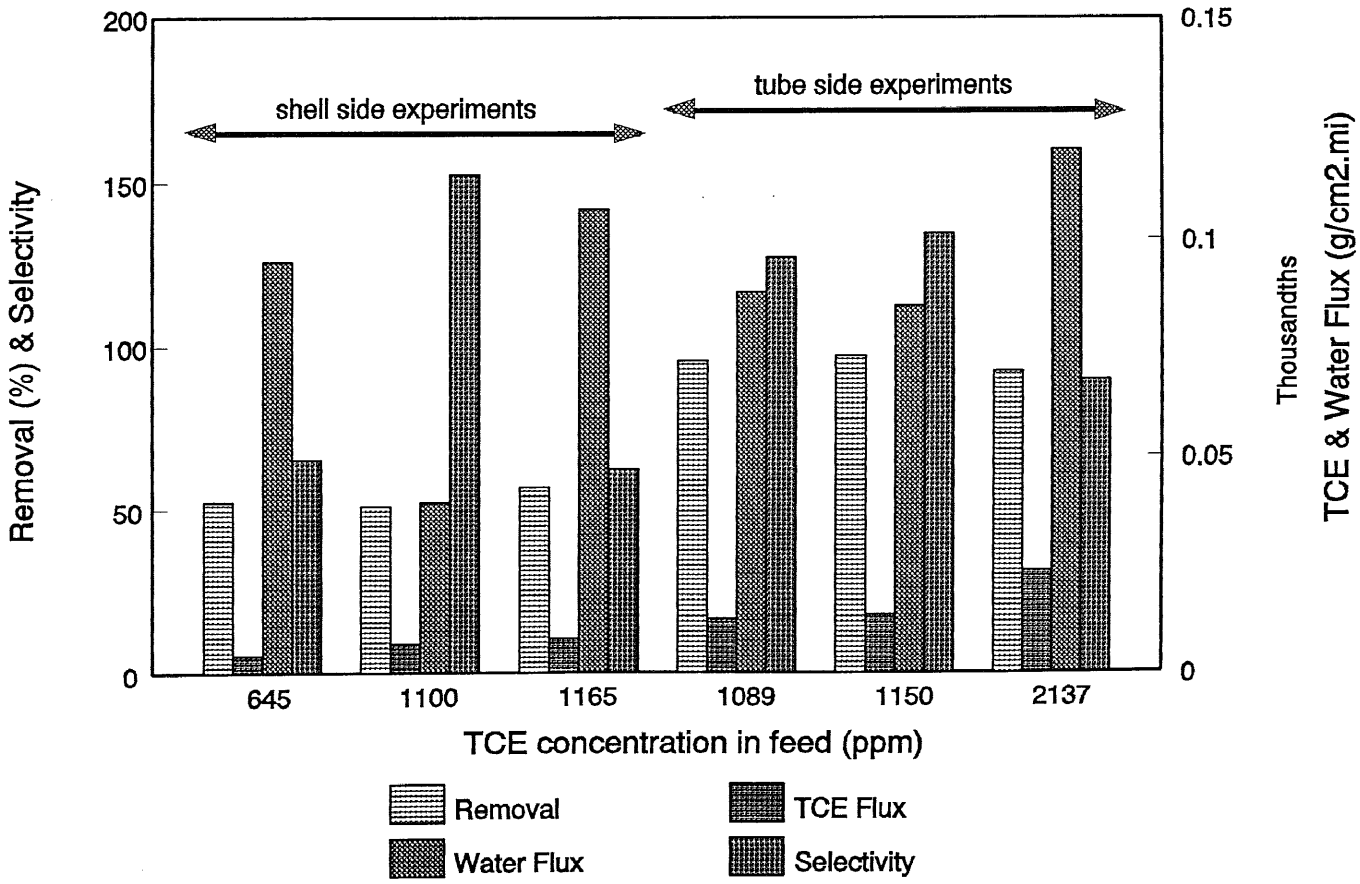

(1%SDS; 2.5 mL/min; Temp=18 C)

Figure 4.6 TCE removal in fluoropolymer module

4.2 Phase Two

In phase two, experiments were carried out with two or three Celgard fiber-based modules connected in series as shown in Figure 3.7. The effects of feed flow rate and feed temperature were also explored in this section. All sets of experiments were carried out at two different concentrations of SDS such as 1% and 0.3%. The results of mass transfer calculations will also be shown in this section for both concentrations of SDS.

The first set of experiments were done with 1% SDS. To study the effect of TCE concentration in feed, experiments were carried out at a constant feed flow rate of 2.5 ml/min; the concentration of TCE was varied from 525 ppm to 2980 ppm. Figure 4.7 shows the results with two modules in series (twins system). The removal of TCE shows a decreasing trend with increase in TCE feed concentration from 525 ppm to 2980 ppm. However the drop in percent TCE removal was not very high and even at a high TCE concentration of 2980 ppm, 84% removal could be achieved. As shown in the plot TCE flux increased linearly with an increase in concentration. Both these observations were in agreement with the experimental results in phase one shown in Figure 4.3.

The water flux did not show any clear trend in this plot which was also evident in Figure 4.3. This could be due to the error in collection of the water in the condenser. The flux of water calculated is dependent on the volume of water actually collected in the whole duration of the experiment; it therefore includes the water collected during the unsteady

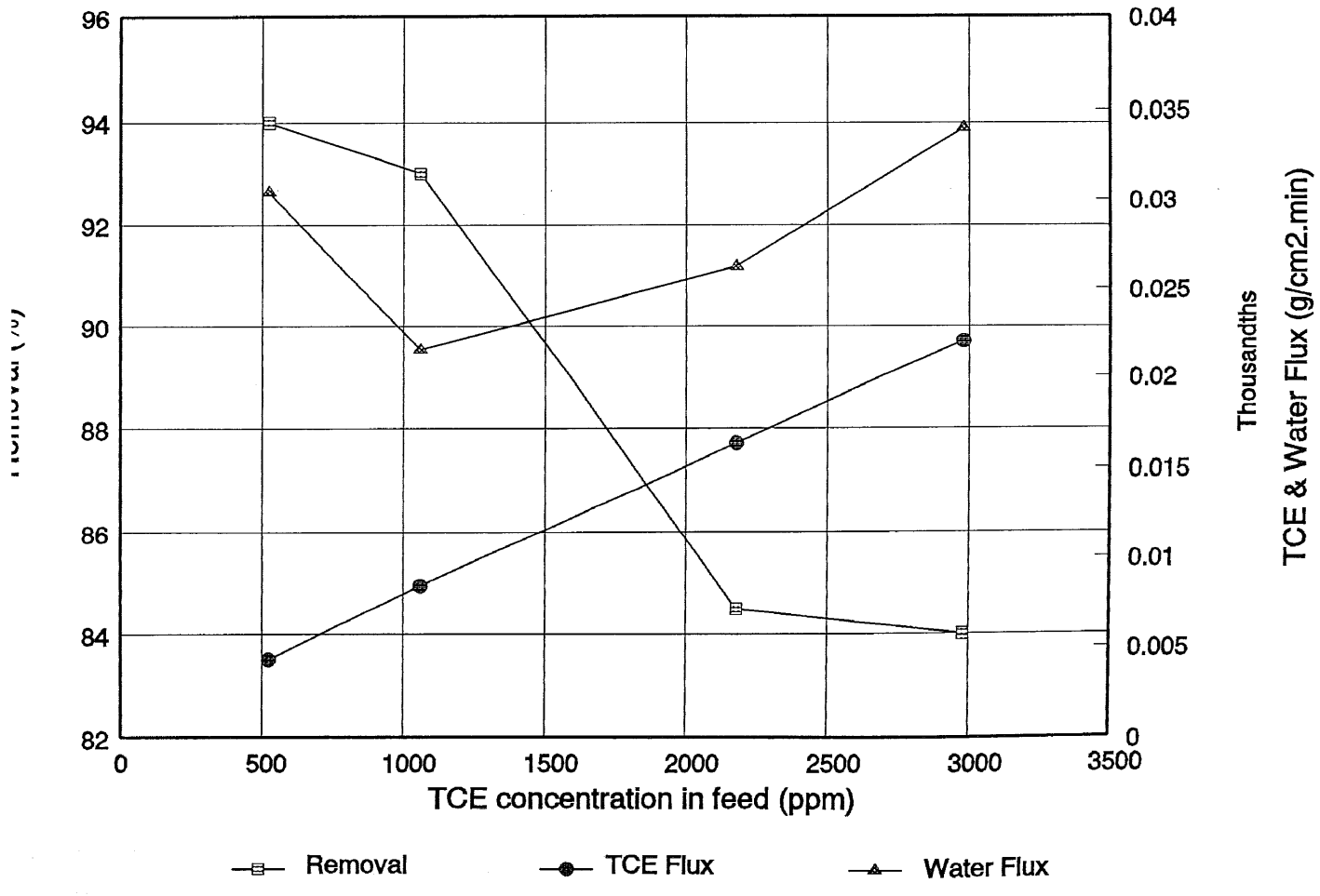

Figure 4.7 Effect of TCE concentration in feed with Twins module

state at the beginning of the experiments. This volume was also influenced by the efficiency of the cooling system of dry ice and methanol which could have involved manual error in setting up the system before startup of experiments. Table 4.3 gives the experimental data for this series of experiments.

The next series of experiments were carried out to determine the hydrodynamic effect on the performance of the module at 1% SDS concentration. The experimental results are shown in Figure 4.8 and the data are provided in Table 4.4. As the feed flow increased from 2.4 ml/min. to 7.5 ml/min., the removal dropped from 93% to 65.5% due to a decrease in the residence time. However TCE flux showed an increasing trend as the concentration of TCE exposed to every section of the module was higher. The selectivity increased from 372 to 505 with an increase in the flow rate. These experiments were carried out at a constant concentration of TCE of around 1000 ppm.

This set of experiments with 1% SDS was also used to calculate the overall mass transfer coefficient and the boundary layer mass transfer coefficient; the calculation procedure is given in Appendix A. The overall mass transfer coefficient for the pervaporation module was found to be an increasing function of Reynolds number as shown in Figure 4.9. This was in agreement with the results from Yang et al. (1995) and Lipski and Cote´ (1990). The overall mass transfer coefficient, K_{ov}, was calculated using the logarithmic mean

Table 4.3 Effect of feed concentration on TCE removal for 1% SDS

feed conc. (ppm)	flow rate (ml/min)	run time (min)	removal (%)	TCE flux (g/cm^2-min)	water flux (g/cm^2-min)	selectivity
525	2.44	270	94	4.3e -6	3.0e -5	269
1060	2.4	365	93	8.4e -6	2.2e -5	370
2178	2.5	360	84.5	1.6e -5	2.6e -5	285
2980	2.4	425	84	2.2e -5	3.4e -5	217

Table 4.4 Effect of feed flow rate on TCE removal for 1% SDS

feed conc. (ppm)	flow rate (ml/min)	removal (%)	TCE flux (g/cm^2-min)	water flux (g/cm^2-min)	k_b (cm/sec)	K_{ov} (cm/sec)	selec-tivity
1060[a]	2.4	93	8.5e -6	2.2e -5	8.2e -4	3.8e -4	372
1064[b]	5.0	73.5	1.4e -5	3.0e -5	1.0e -3	3.9e -4	430
1041[c]	7.5	65.5	1.8e -5	3.5e -5	1.2e -3	4.7e -4	505

run time (min): [a] =365; [b] =375; [c] =390

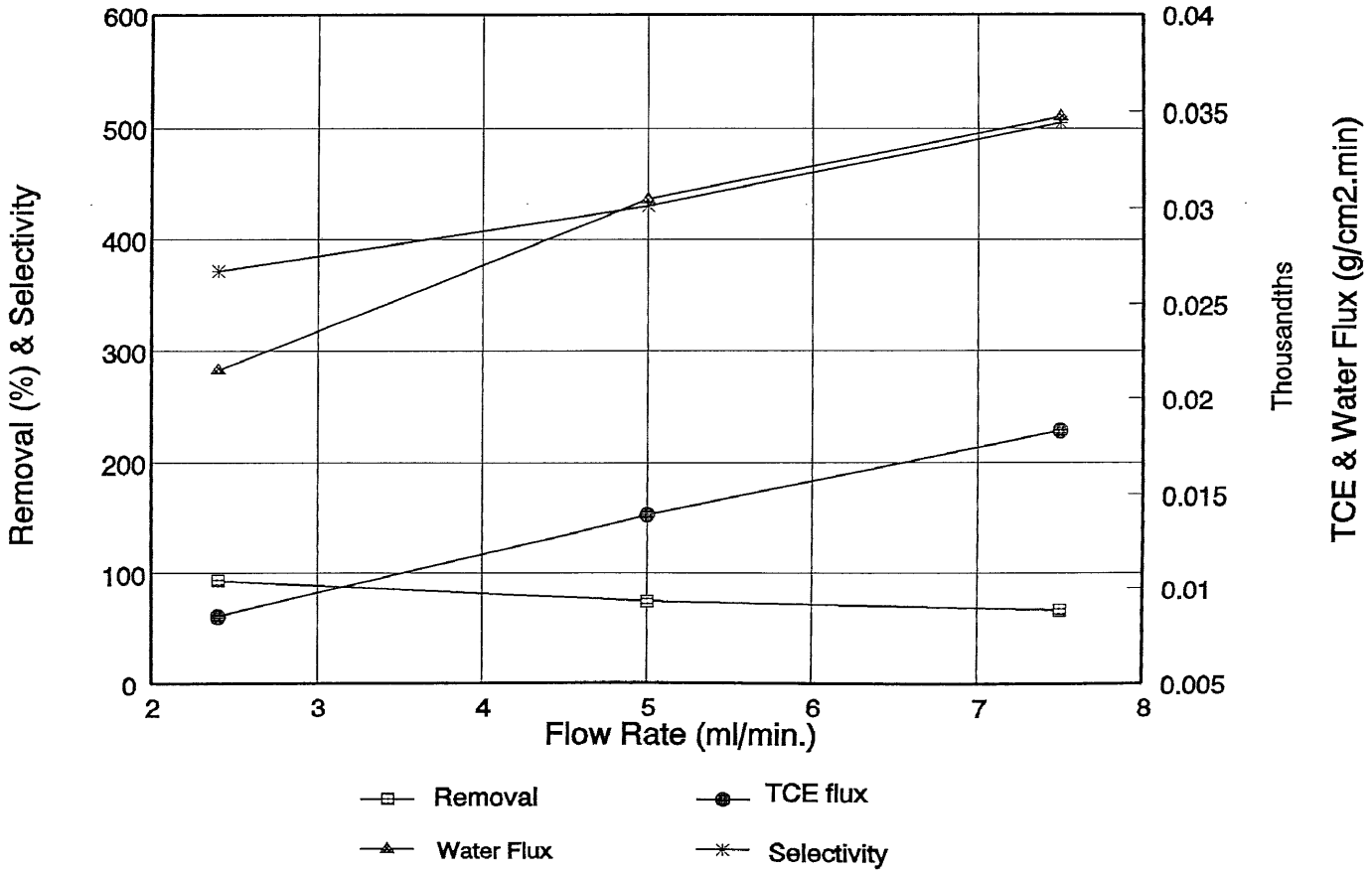

(1% SDS; temp = 18C; Conc.= 1060-1064-1041 ppm; Twins module [# 1 & 2])

Figure 4.8 Effect of feed flow rate with 1% SDS

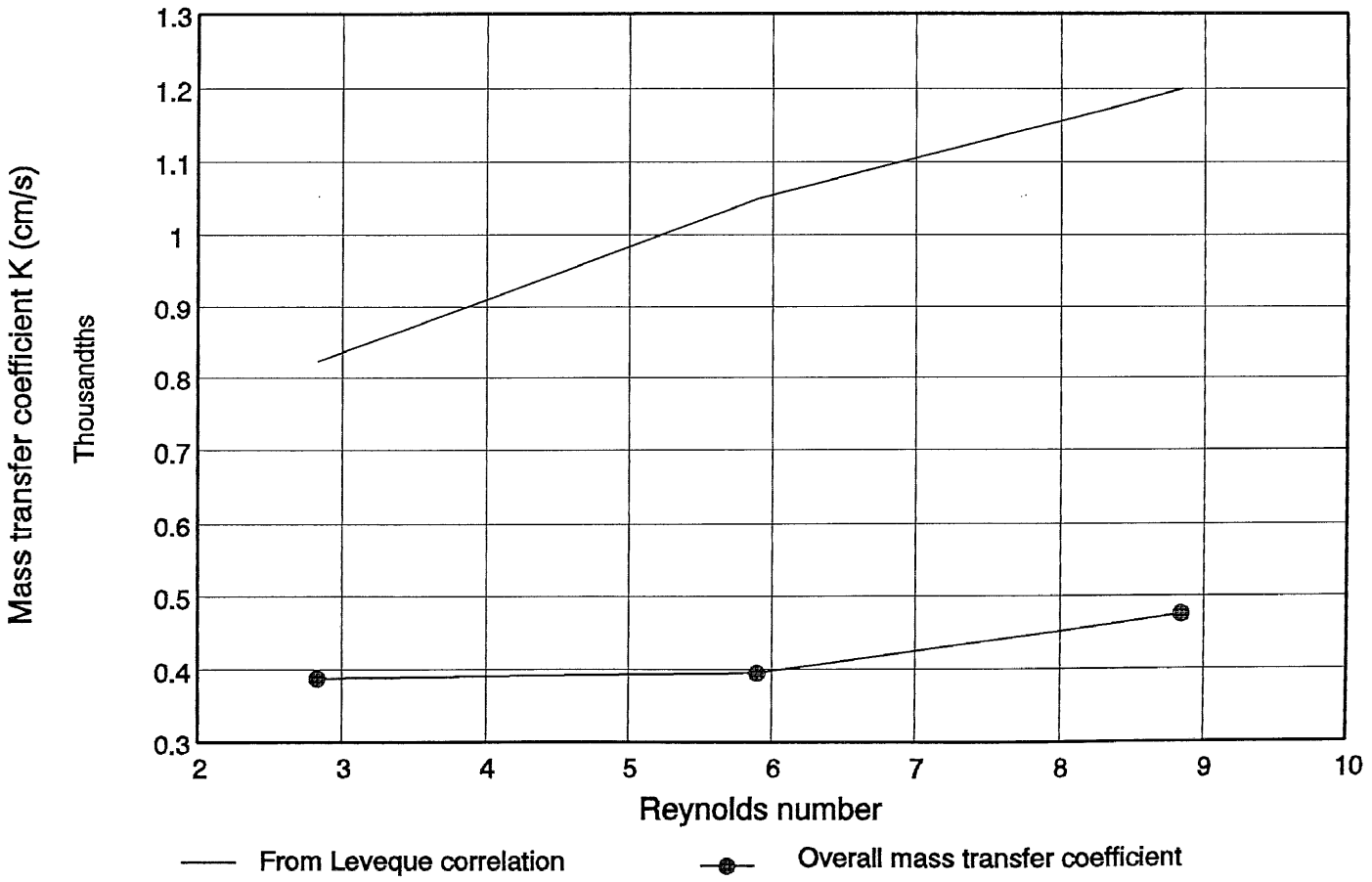

Figure 4.9 Mass transfer coefficients with 1% SDS

concentration difference. The boundary layer mass transfer coefficient, k_b, was calculated based on the Leveque correlation (Wickramasinghe et al., 1992). The dependency of the overall mass transfer coefficient on the Reynolds number indicates that the liquid film resistance ($1/k_b$) is significantly larger than that predicted by the Leveque correlation. Reynolds number was calculated based on the average feed solution velocity u, and the inner fiber diameter d_i as the characteristic length:

$$Re = \frac{d_i * \rho_{H_2O} * u}{\mu_{H_2O}} \tag{4.3}$$

where

$$u = \frac{Q}{60 * N * S} \tag{4.4}$$

N = Number of fibers

s = Fiber cross sectional area = $(\pi/4)d_i^2$.

The experimentally obtained values of mass transfer coefficients are presented in Table 4.4 and Figure 4.9. Based on the resistance-in-series theory (Liu et al., 1996) the following equation was used to calculate the membrane mass transfer resistance:

$$\frac{1}{K_{ov} d_o} = \frac{1}{k_m d_o} + \frac{1}{k_b d_i} \tag{4.5}$$

where,

d_o = outside diameter of the fiber

d_i = inside diameter of the fiber.

To develop an estimate of additional boundary layer resistance encountered in surfactant-based systems, the following strategy was adopted. It was assumed that the boundary layer resistance could be described by the Leveque correlation. Then the estimate of membrane resistance obtained from K_{ov} data will indicate the effect of the surfactant solution via modified estimates of the membrane resistance. In reality membrane resistance is unaffected by surfactants; what changes due to the surfactant is the effective boundary layer resistance. A linear regression was then performed on the values of $1/(K_{ov}d_o)$ and $1/(k_b d_i)$ and the value of k_m obtained was 7.55e -4 cm/sec. This value is one order lower than the value obtained by Yang et al. (1995) indicating some additional resistance due to the presence of surfactant in the boundary layer. The data taken for regression are provided in Appendix A, Table A.2.

The next series of experiments were done with 0.3% SDS concentration. Similar experiments were carried out with twins system to determine the hydrodynamic effect. The results are shown in Figure 4.10. It was observed that with an increase in flow rate from 2.4 ml/min. to 15 ml/min., the removal of TCE dropped from 95.8% to 67.7%. Compared to the drop in removal with 1% SDS under similar conditions, the drop of 28.1% is relatively low. This improvement in performance was due to the low concentration of SDS. At such low concentrations of SDS, the number of micelles are much less than the number at 1% SDS concentration. In the model postulated in Chapter 2, the

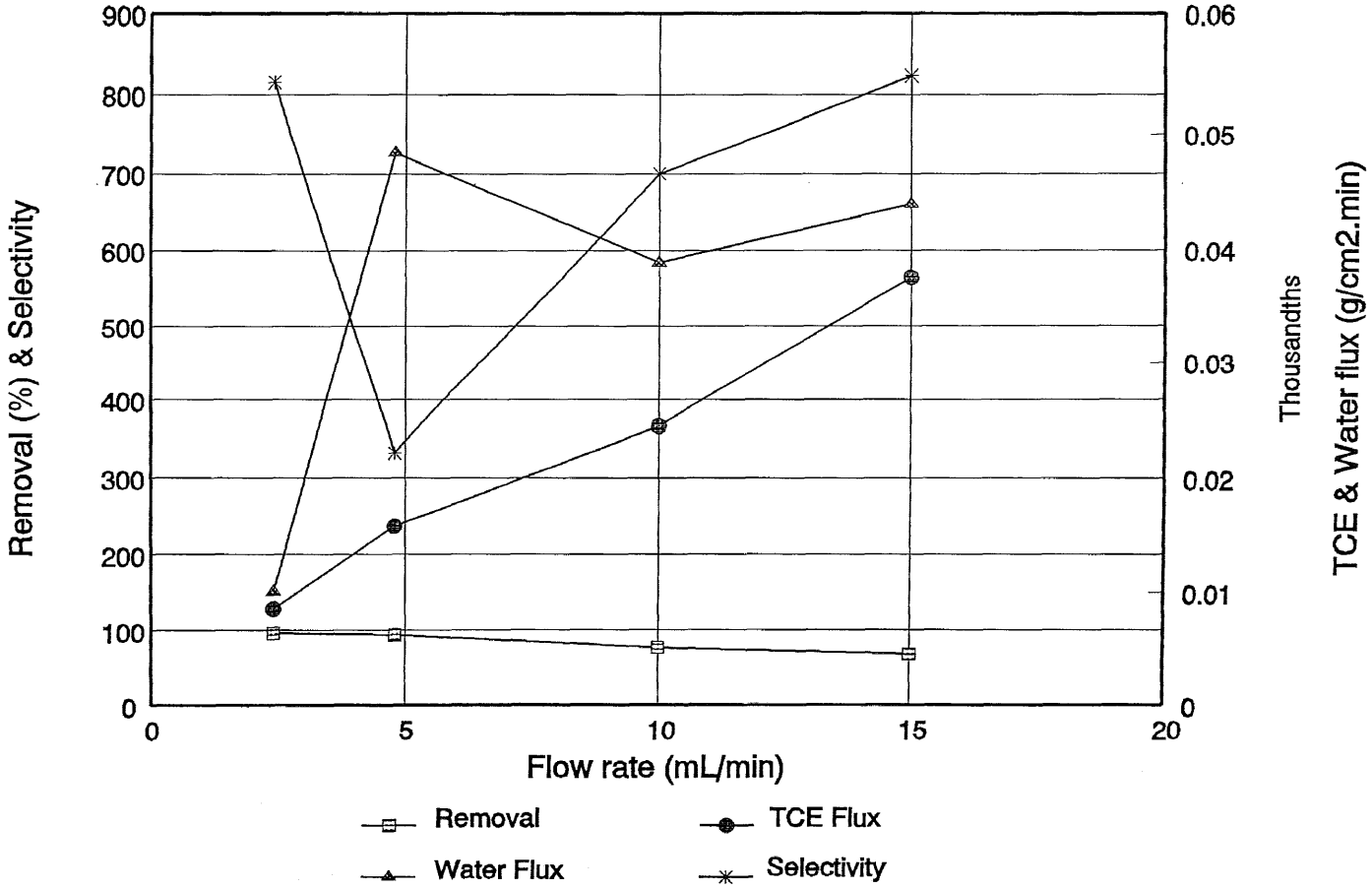

(0.3% SDS; Temp= 18C; TCE Conc= 1043-984-894 ppm; Twins-module [# 1 & 2])

Figure 4.10 Effect of feed flow rate with 0.3% SDS

release of TCE will be much more probable with a lower concentration of SDS. TCE flux also shows higher values with 0.3% SDS concentration. In the higher range of flow rates, the TCE flux was double compared to the flux with 1% SDS concentration. The experimental data for this set of experiments are given in Table 4.5. The water flux in Figure 4.10 again does not show any definite trend. The selectivity calculated for this set of experiments was in the high range of 700-830 with the exception of the experiment at a flow rate of 4.8 ml/min., as shown in Figure 4.10. The selectivity obtained from these experiments were mostly above 700, which was higher than the values for a 1% SDS system.

Mass transfer calculations were done in the manner followed in earlier experiments. The overall mass transfer coefficient was at least 50% higher than the corresponding value with 1% SDS indicating a decrease in resistance due to the lower concentration of SDS. The values of the mass transfer coefficients are shown in Figure 4.11. The value of k_m obtained from the linear regression was 1.0e -3 cm/sec. Even though this is still lower than the value obtained by Yang et al. (1995) for a system without surfactant, it is 30% higher than the value of k_m obtained in the system with : SDS. The regression data for the calculation of k_m a: provided in Appendix A, Table A.3.

The next series of experiments were done with twi: system and 0.3% SDS concentration to determine the effect c feed temperature on pervaporation. The experiments we:

Table 4.5 Effect of feed flow rate on TCE removal for 0.3% SDS in a Twins module

feed conc. (ppm)	flow rate (ml/min)	removal (%)	TCE flux (g/cm^2-min)	water flux (g/cm^2-min)	k_b (cm/sec)	K_{ov} (cm/sec)	sele-ctivity
1043[a]	2.4	95.8	8.6e -6	1.0e -5	8.2e -4	4.5e -4	815
984[b]	4.8	93.8	1.6e -5	4.8e -5	1.0e -3	7.9e -4	332
895[c]	10.0	76.0	2.4e -5	3.9e -5	1.3e -3	8.5e -4	700
1039[d]	15.0	67.7	3.8e -5	4.4e -5	1.5e -3	1.0e -3	823

run time (min): [a]=390; [b]=280; [c]=385; [d]=292

Table 4.6 Effect of feed temperature on TCE removal for 0.3% SDS in a Twins module

feed conc. (ppm)	flow rate (ml/min)	run time (min)	removal (%)	TCE flux (g/cm^2-min)	water flux (g/cm^2-min)	feed temp. (°C)	select-ivity
898	4.8	280	93.1	1.4e -5	4.8e -5	18	329
796	5.0	525	98.7	1.4e -5	8.4e -5	28	205
874	4.7	525	96.5	1.5e -5	2.4e -4	38	68

Table 4.7 Effect of feed flow rate for 0.3% SDS and the Trio module arrangement

feed conc. (ppm)	flow rate (ml/min)	run time (min)	removal (%)	TCE flux (g/cm^2-min)	water flux (g/cm^2-min)	feed temp. (°C)	sele-ctivity
1068	5.0	430	100.0	1.1e -5	1.4e -4	38	72
1002	7.3	290	99.0	1.5e -5	3.1e -4	38	48
981	10.0	350	97.8	2.0e -5	2.8e -4	38	72

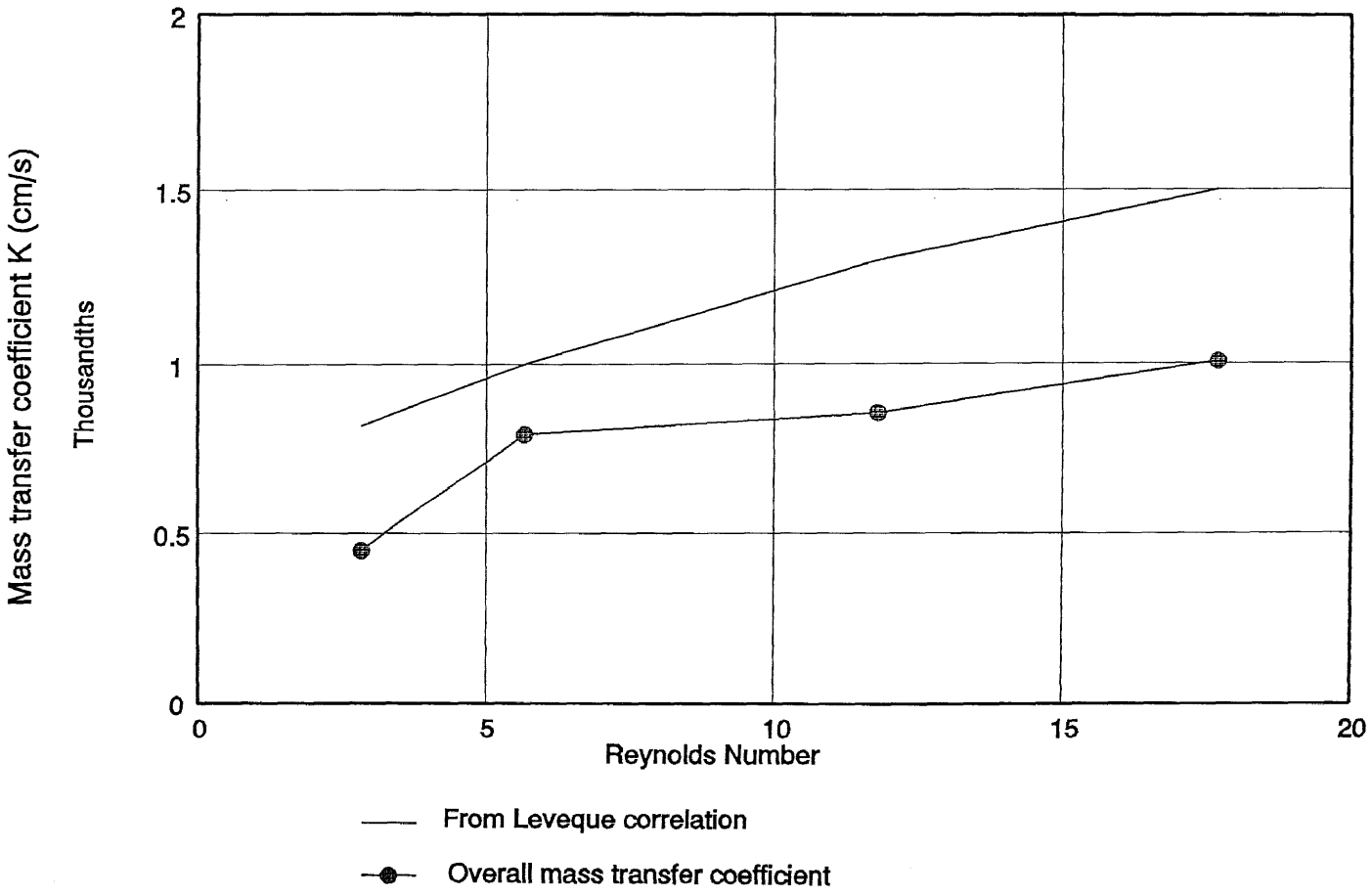

Figure 4.11 Mas:

carried out at different temperatures at a TCE concentration of 800-900 ppm and a feed flow rate of 5 ml/min. The results are shown in Figure 4.12 and the data are given in Table 4.6. The removal of TCE increased from 93% to nearly 99% with an increase in temperature from 18°C to 38°C. Interestingly TCE flux did not show any substantial increase.

Water flux increased very rapidly with an increase in feed temperature. This was expected as the vapor pressure of water increased with higher temperature and more water would permeate under vacuum on the permeate side. With an increase in temperature the selectivity came down from 329 to 68.

Till this point the maximum removal which could be achieved was 98.7% at 28°C at a flow rate of 5.0 ml/min. for a SDS concentration of 0.3%. In the last section of phase two, experiments were carried out with three modules (# 1, # 2 and # 3, Table 3.1, Trio system) in series to achieve complete removal of TCE. These results are shown in Figure 4.13. Experiments were again carried out at 0.3% SDS concentration and at a TCE concentration of about 1000 ppm. With the trio system at 38°C, 100% removal of TCE was achieved at a flow rate of 5 ml/min. A very high removal of 98.5% was obtained even at a very high flow rate of 10 ml./min.. The experimental data are given in Table 4.7.

4.3 Phase Three

In this phase different types of systems were tested in a single module (#1, Table 3.1) or twins module. The removal of

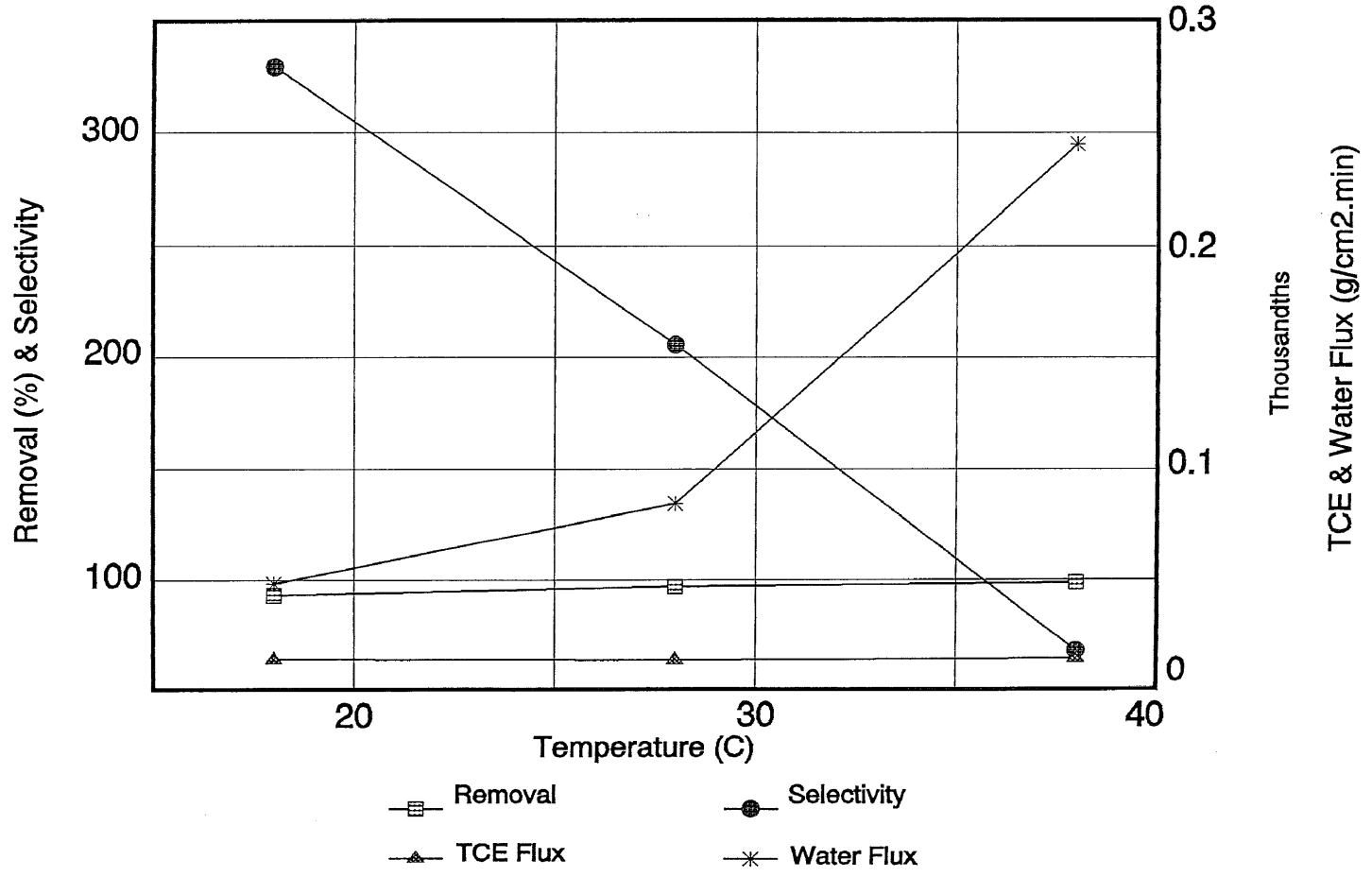

Figure 4.12 TCE removal by pervaporation precess; effect of temperature

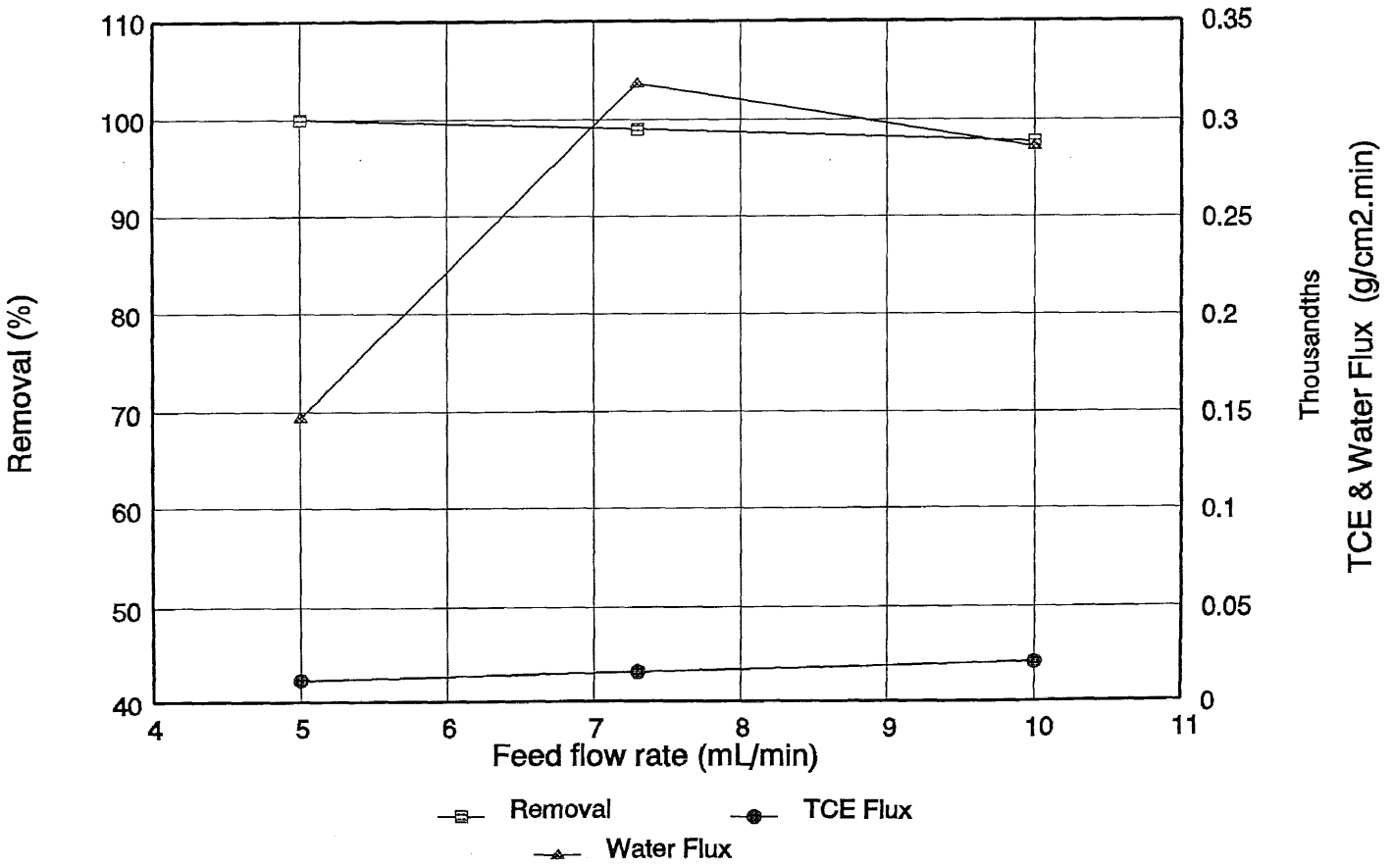

(0.3% SDS; Temp= 38C; TCE Conc=1068; 1002; 981 ppm; Trio-module [# 1, 2 & 3])

Figure 4.13 Effect of feed flow rate in Trio module

TCE was studied in the presence of surfactants other than SDS. A few experiments were done with the surfactant SDS and xanthan gum, a high molecular weight polymer. This system was studied as U.S. Navy (sponsor of this research) has several contaminated ground water sites under study where surfactant flushing proposes to employ xanthan gum.

The comparison of the performance of the module under same conditions with SDS and Dowfax is given in Figure 4.14. A similar system with a TCE concentration around 1000 ppm and a flow rate of 2.5 ml/min. was taken for comparison. The removal of TCE from the 0.5% Dowfax system (system 2) was found to be 100% compared to 95.8% removal in the system with 0.3% SDS (system 1). It was observed that water flux was doubled in the Dowfax system compared to the SDS system. But the TCE flux was reduced by about 15% in the Dowfax system (due to a lower TCE level). So the improvement in TCE removal was actually obtained with a decrease in the selectivity which came down from 815 (system 1) to 395 (system 2).

The next experiment was done with 0.3% SDS and 125 ppm of xanthan gum. Figure 4.15 shows the comparison between the two systems with or without xanthan gum. Again TCE concentration in both systems was chosen around 1000 ppm with a flow rate of 2.3-2.4 ml/min. Surprisingly it was found that the presence of the high polymer did not influence the TCE removal and flux, as is evident from the figure. Furthermore a 30% reduction in the flux of water could be achieved which gave a high

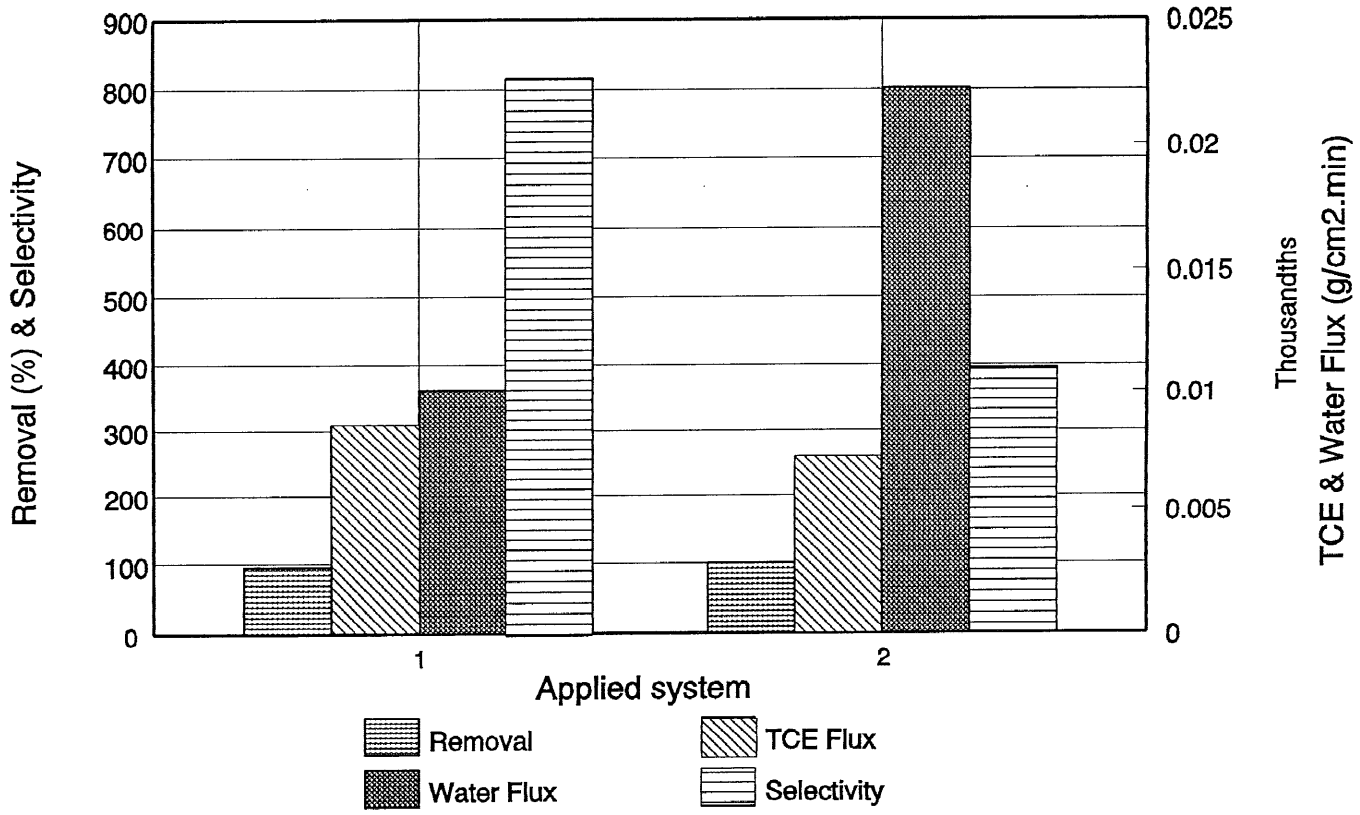

1: 0.3% SDS;
2: 0.5% DOWFAX 8390.

(0.3% SDS/TCE 1043 ppm; 0.5% DFX/ TCE 819 ppm; Temp= 18C; Twins-module [# 1 & 2])

Figure 4.14 Comparison of system performance using different surfactants

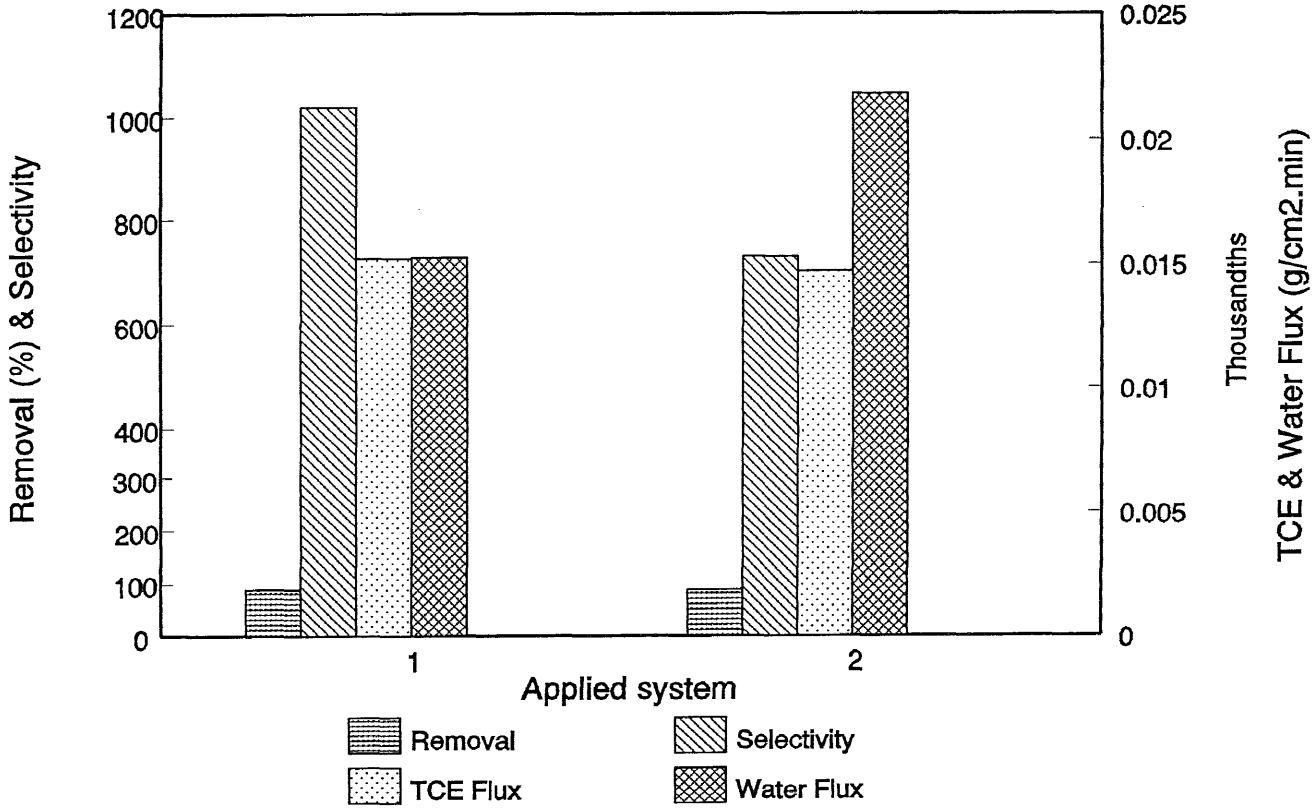

1: 0.3% SDS, 125 ppm Xanthan Gum, 977 ppm TCE, 2.46 ml/min. flow.
2: 0.3% SDS, 920 ppm TCE, 2.3 ml/min. flow.

Figure 4.15 Effect of xanthan gum

selectivity of 1019 compared to 734 in the system with only 0.3% SDS.

4.4 Phase Four

In the fourth and the final phase of this work on TCE pervaporation, the behavior of the membrane module without any surfactant was studied to get a clearer idea about the influence of surfactant on the performance of the module.

The first set of experiments were done to understand the effect of TCE concentration in the feed. Experiments were done with TCE concentration varying from 200 ppm to 1000 ppm which is approximately the solubility limit for TCE in water. Figure 4.16 shows the results of these experiments. TCE flux increased linearly with an increase in concentration although percent removal was almost constant at around 80%-85% over a concentration range of 200-1000 ppm. The water flux again showed no clear trend. The experimental data are provided in Table 4.8 for module # 1.

The next set of experiments were done to determine the effect of feed flow rate in a system without surfactant. Figure 4.17 shows the results of these experiments. TCE flux increased considerably with an increase in flow rate from 2.6 to 35.7 ml/min. The removal came down from 96% to 30% with an increase in the flow rate. The water fluxes in this set of experiment did not vary much over the flow rate range of 2.6 to 25.3 ml/min. This constant water flux over a wide range of feed flow rate was also observed by Psaume et al. (1988) and

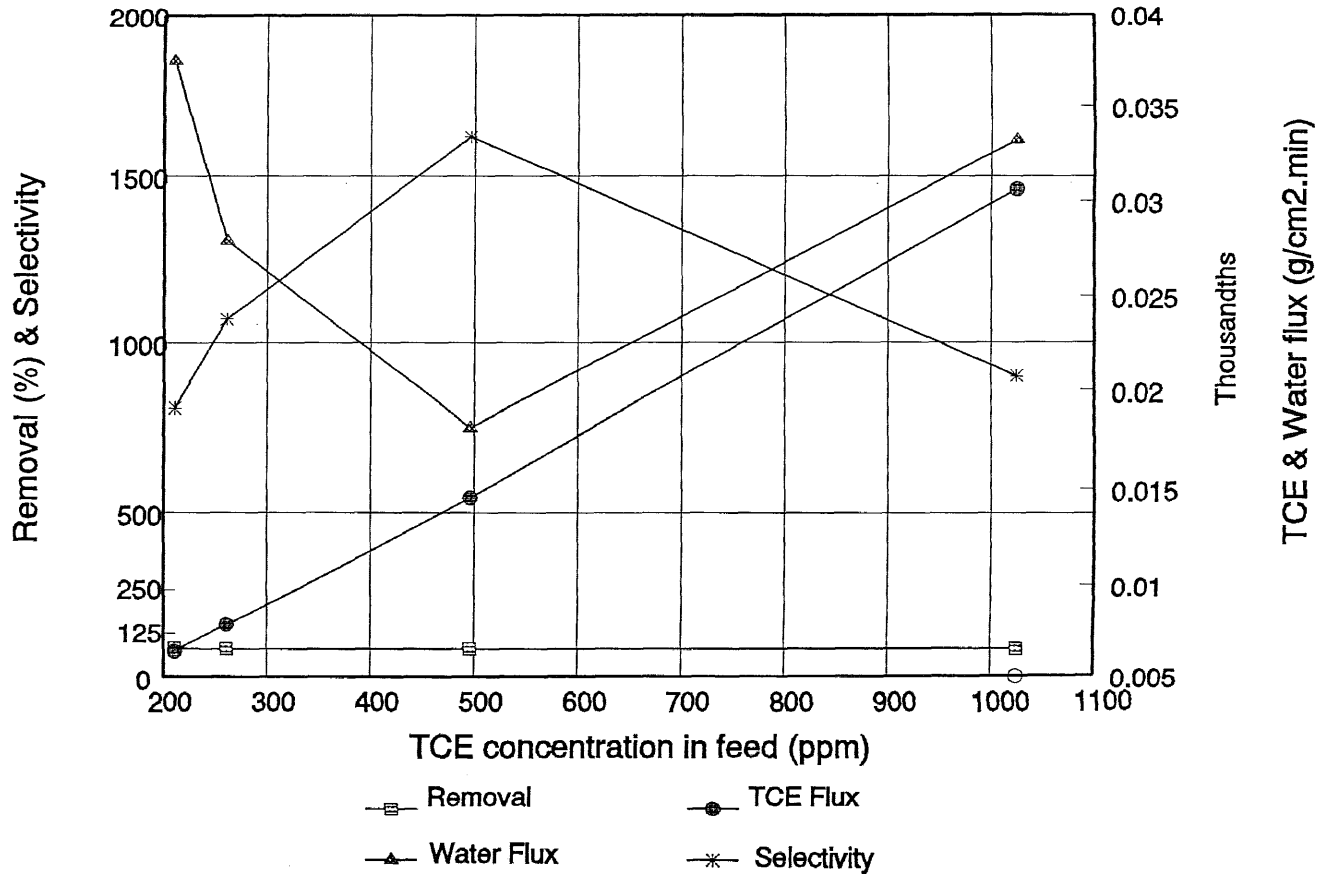

(TCE/water system; Temp= 18C; Flow rate= 5mL/min; TCE Conc= 211-261-496-1025 ppm; Single Module [# 1])

Figure 4.16 Effect of feed concentration in surfactant-free system

Table 4.8 Effect of feed TCE concentration on TCE removal in a surfactant-free system

feed conc. (ppm)	flow rate (ml/min)	run time (min)	removal (%)	TCE flux (g/cm^2-min)	water flux (g/cm^2-min)	sele-ctivity	tube side/ shell side
211	4.9	400	85.7	6.3e -6	3.7e -5	899	tube
261	5.0	435	83.9	7.8e -6	2.8e -5	1620	tube
496	4.9	395	83.7	1.5e -5	1.8e -5	1073	tube
1025	5.0	430	83.6	3.1e -5	3.3e -5	802	tube

Table 4.9 Effect of feed flow rate on TCE removal in a surfactant-free system

feed conc. (ppm)	flow rate (ml/min)	run time (min)	removal (%)	TCE flux (g/cm^2-min)	water flux (g/cm^2-min)	selec-tivity	tube side/ shell side
678	2.6	445	95.5	1.2e -5	3.5e -5	506	tube
826	5.0	370	80.5	2.4e -5	3.9e -5	744	tube
760	10.5	395	60.0	3.3e -5	4.3e -5	1011	tube
754	15.6	390	44.6	3.8e -5	4.8e -5	1050	tube
896	25.3	360	55.3	5.9e -5	4.4e -5	1506	tube
857	35.7	415	36.3	6.6e -5	5.8e -5	1308	tube

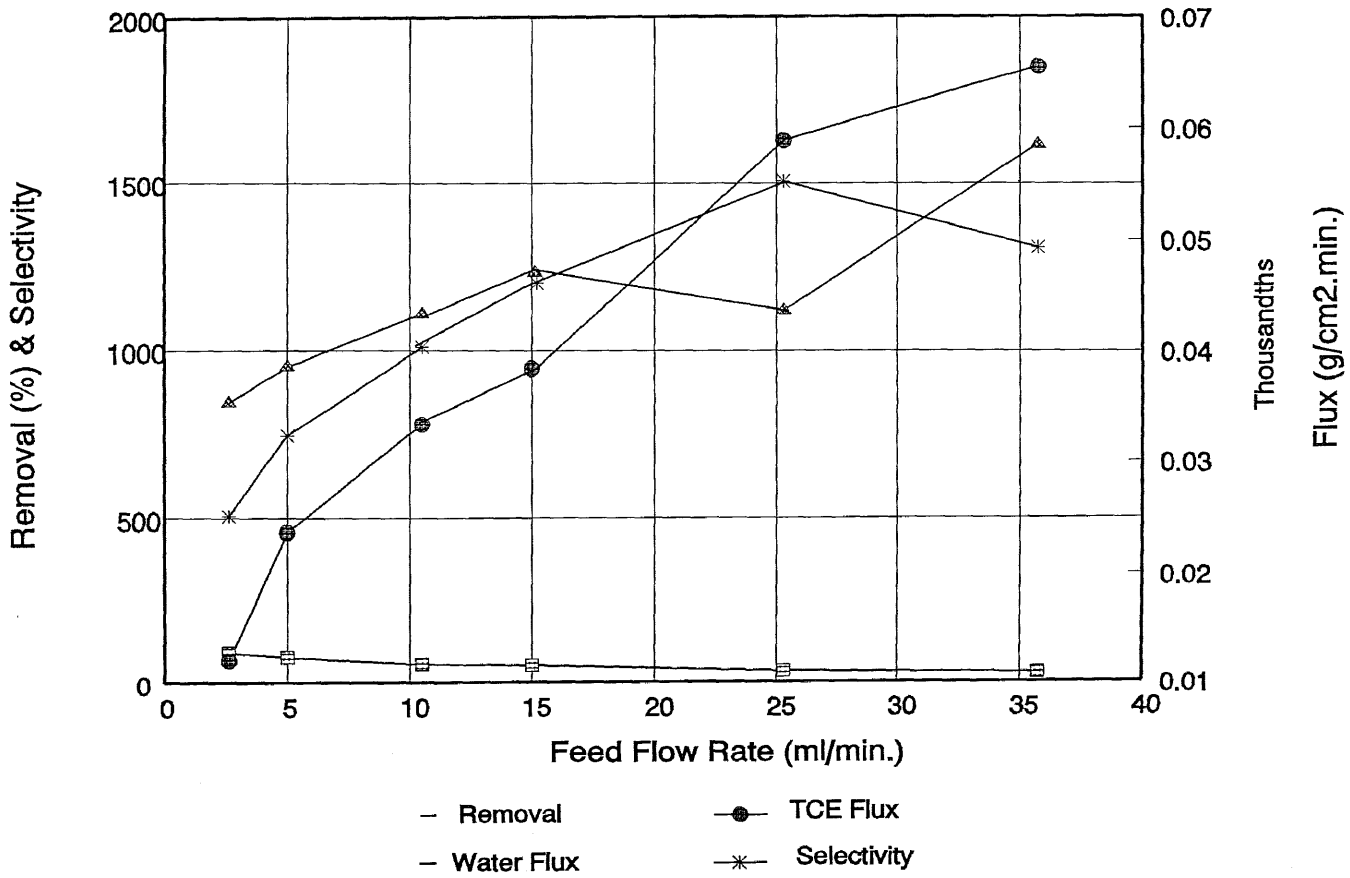

R; feed conc. 700-900 ppm); Temp=18C; single module [# 1])

ect of flow rate in surfactant-free syste

Lipski and Cote´ (1990). The selectivity obtained from this set of experiments increased from 506 to a very high value of 1506 with an increase in feed flow rate. The calculated values of the overall mass transfer coefficient and the boundary layer mass transfer coefficient according to the Leveque correlation are plotted in Figure 4.18. The procedure for calculating the boundary layer mass transfer coefficient is provided in Appendix A. The experimental data for this set of experiments are provided in Table 4.9. The value of k_m obtained from linear regression was 3.00e -3 cm/sec, which was more than three times higher than the values for systems with 1% and 0.3% surfactant. This surely indicated considerable additional boundary layer resistance in the presence of surfactant. The regression data for calculating k_m are provided in Table A.4, Appendix A.

Table 4.10 shows a comparative study of the TCE flux and overall mass transfer coefficient for systems with or without surfactant. As seen in this table TCE flux was almost doubled for a system without surfactant compared to that for a system with 1% SDS . In the presence of the surfactant almost all the TCE is solubilized within the micelle and very little free TCE is available in the bulk feed. If this situation prevailed at the boundary of the membrane then the flux of TCE would have been drastically reduced compared to the system with no surfactant. These observations and results support the postulation given in Chapter two, that the micelles collide with the membrane wall, thereby releasing the TCE trapped in

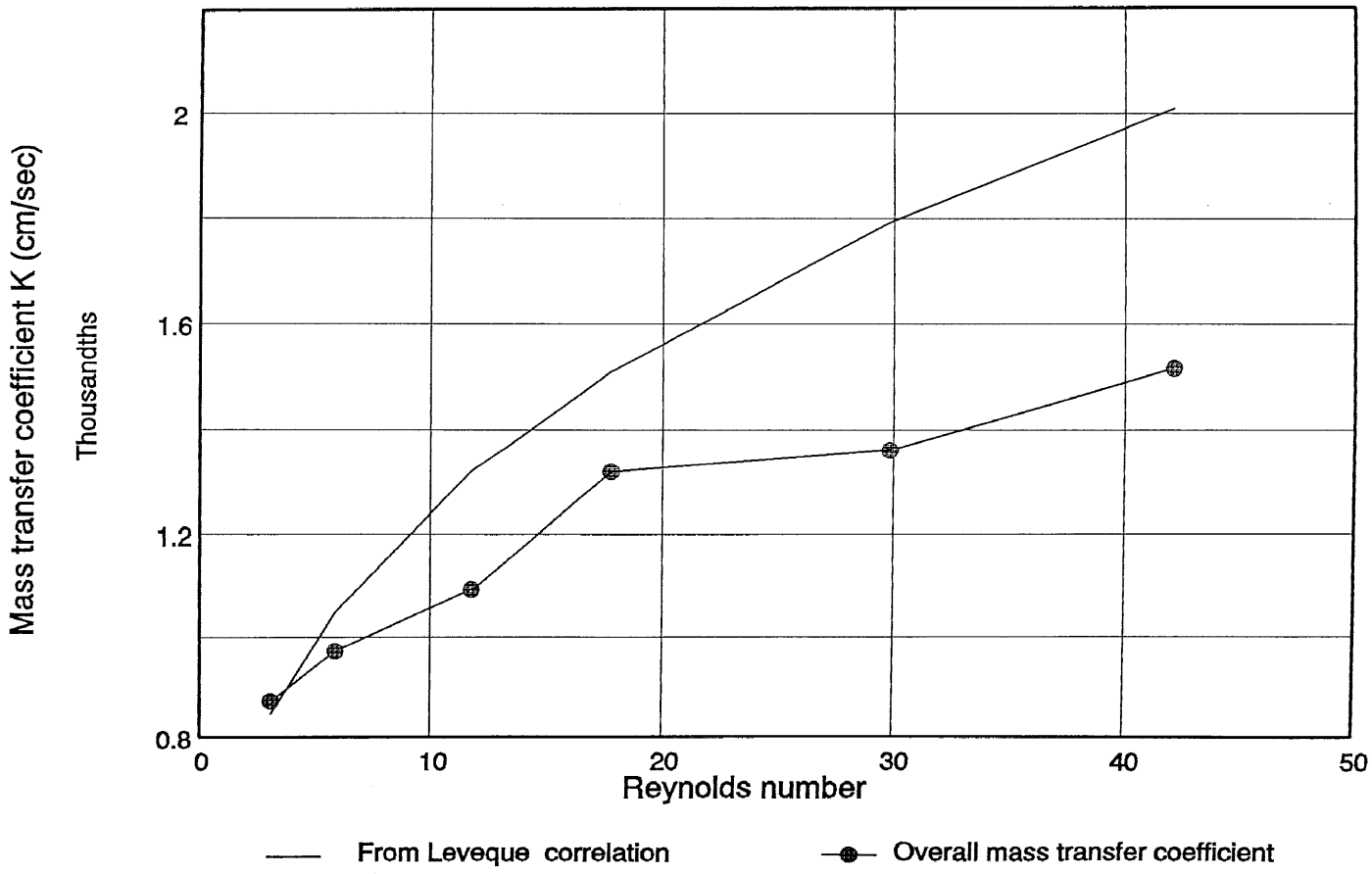

Figure 4.18 Effect of flow rate in surfactant-free system

the core of the micelle. So free TCE is available at the membrane wall giving a TCE flux comparable with those in systems without any surfactant. Figure 4.19 shows the mass transfer coefficients for different SDS concentrations.

Table 4.10 Comparison of TCE flux and mass transfer coefficient with or without a surfactant

% SDS	Flow rate (ml/min)	feed conc. (ppm)	TCE flux (g/cm^2-min)	K_{ov} (cm/sec)	select-ivity
1	5.0	1064	1.4e -5	3.9e -4	430
0.3	4.8	984	1.6e -5	7.9e -4	332
nil	5.0	1025	3.1e -5	1.0e -3	802
0.3	10	895	2.4e -5	8.5e -4	900
nil	10	837	3.6e -5	1.1e -3	1011

4.4.1 Oil Permeation Experiments

In the last part of phase 4, a few experiments were done to explore permeation of dodecane in a coated hydrophobic hollow fiber module (# 5, Table 3.1). Water and dodecane emulsion was first fed to the tube side of the module and oil fluxes were calculated based on the reduction in the oil concentration in the reservoir. All experiments were carried out in the batch recirculation mode, i.e. the outlet from the membrane module was fed back to the feed reservoir. Figure 4.20 shows the results of these experiments with the emulsified feed on the tube side. It is observed that with an increase in the oil concentration from 4780 ppm to 7812 ppm, the flux of dodecane

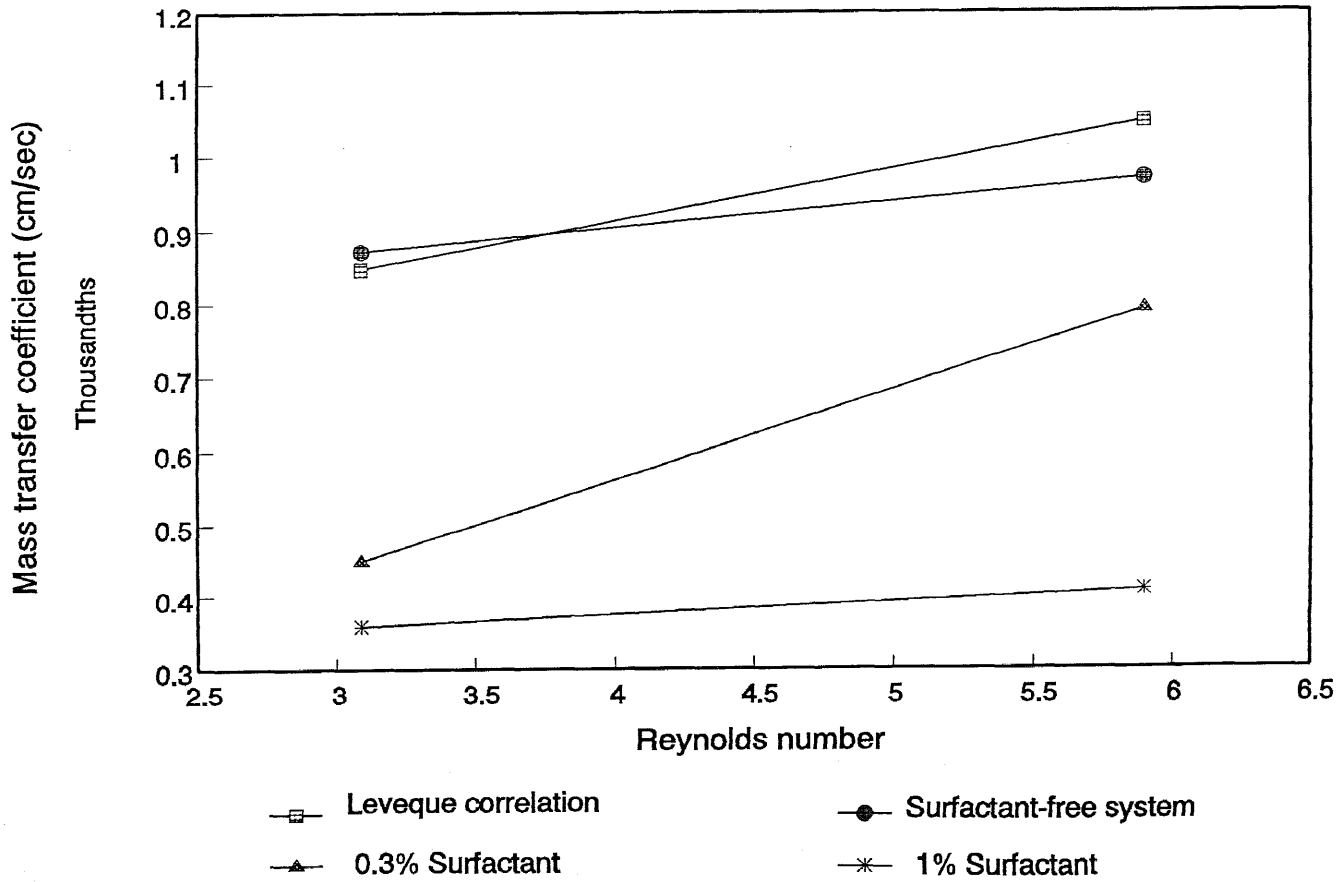

Figure 4.19 Comparison of mass transfer coefficients for different systems

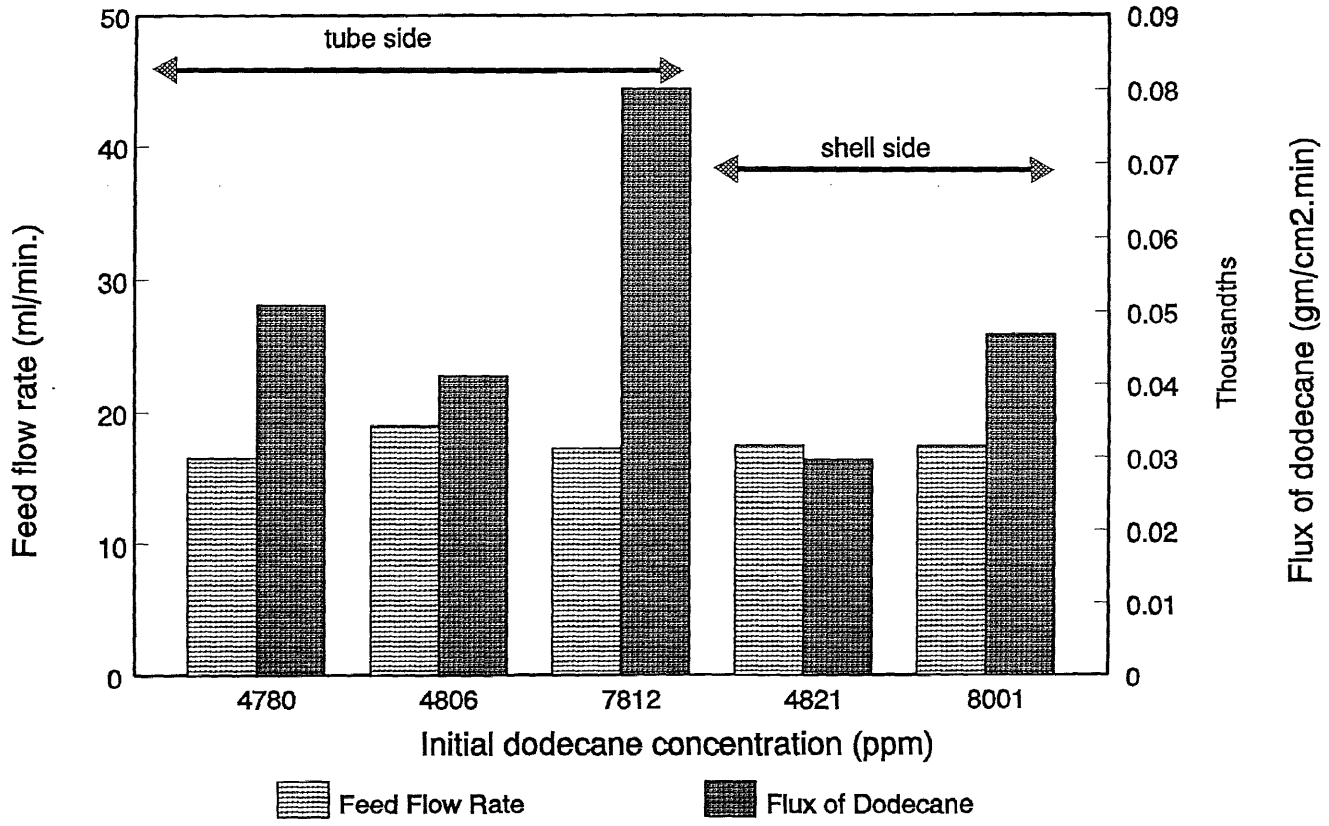

Figure 4.20 Permeation of dodecane

increased from 1.03e -4 gm/cm^2.sec. to 1.6e -4 gm/cm^2.sec. These experiments were carried out in a flow rate range of 17-19 ml/min. This phenomenon was also observed at a low concentration of oil by Magdich and Semmens (1988) and Tirmizi et al. (1996). The results are given in Table 4.11.

During the tube side experiments small drops of permeate were noticed in the tubes connected to the permeate. Before switching to the shell side experiments, the module was washed thoroughly to remove any remaining oil. Isopropyl alcohol solution was passed through the module both on the tube and shell side for several hours and the wash water was tested for dodecane and a positive detection of the oil indicated oil permeation in the shell side. The module was then dried by passing nitrogen and filtered air overnight.

In the next set of experiments the feed was passed from the shell side of the module under conditions similar to those of the tube side experiments. It was observed that at both concentration levels of dodecane, 40-45% reduction in flux was obtained when feed was passed from the shell side. These initial experiments were done at a flow rate of 16.5-19 ml/min. The experimental data are provided in Table 4.11 and the results are shown in Figure 4.20.

Figure 4.21 shows the decrease in dodecane flux with a decrease in concentration of the oil in the reservoir with time, as more oil is removed.

Table 4.11 Experimental data for dodecane permeation

initial feed conc. (ppm)	run time (min)	oil flux (g/cm^2-min)	flow rate (ml/min)	tube side /shell side
4780	360	5.1e -5	16.5	tube
4806	420	4.1e -5	19.0	tube
7812	360	8.0e -5	17.25	tube
4821	420	3.0e -5	17.5	shell
8001	420	4.7e -5	17.5	shell

The next set of experiments were done to establish pressure and feed flow rate effects on dodecane permeation. Experiments were done with two different flow rates of 18 and 10 ml/min by passing the feed from both shell and tube side. Table 4.12 provides the results of these experiments. A 25-30% reduction of dodecane flux was obtained by decreasing the flow rate from 18 ml/min to 9 ml/min. To detemine the effect of pressure on dodecane flux, experiments were carried out at two different feed pressures of 8 and 15 psi keeping the dodecane concentration and feed flow rate constant at 8000-9000 ppm and 18 ml/min respectively. The feed was in the tube side for these experiments. Dodecane flux was found to be linearly increasing from 8.0e -5 to 1.58e -4 gm/cm^2-min with an increase in pressure from 8 to 15 psi.

Finally an experiment was carried out at an oil concentration of 7700 ppm in presence of 0.5% SDS concentration. The dodecane flux obtained at a flow rate of around 18 ml/min was found to be lower by almost one order of

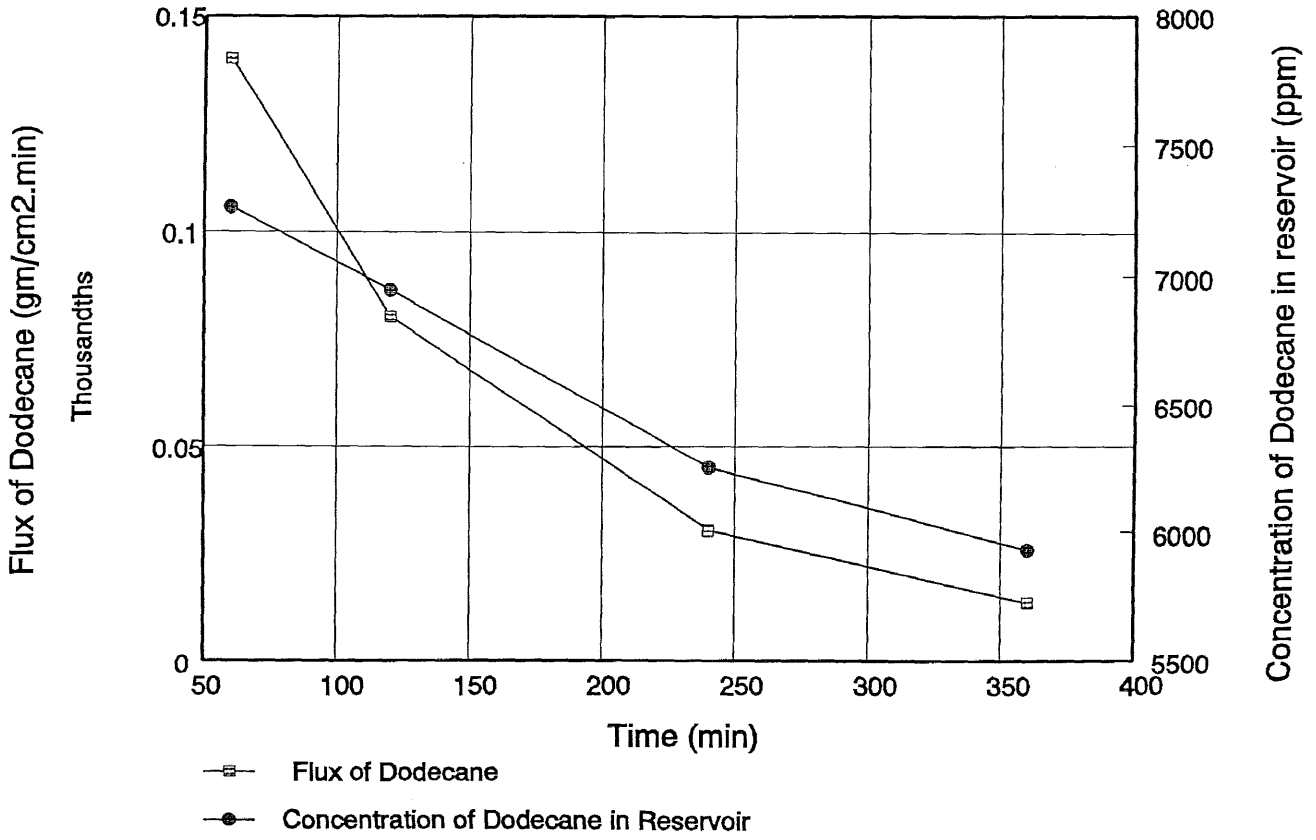

Feed pressure 7.5-{ ...decane concentration 7812 ppm; Tube-side feed

Fig ...tion

magnitude, compared to the flux from a s
without any surfactant. Figure 4.22 sho
between these two set of experiments. This
increased stability of the emulsion in pr
surfactants on the pore surface will als p
resistance to dodecane permeation. Magdich and
had observed dodecane flux of 0.249 m /min
gm/min-cm^2) under the following conditions:

concentration of dodecane:	5%
SDS concentration:	500 mg/lit
pressure:	10 psi
flow rate:	300 ml/min.
membrane:	uncoated Celgar module.

They also observed a similar adverse effect
in presence of SDS. There was no permeat
this run in presence of SDS, which was the
and Semmens (1988) faced during a similar

Table 4.12 Experimental data for flow and pressure dodecane permeation

initial feed conc. (ppm)	run time (min)	oil flux (g/cm^2-min)	flow rate (ml/min)	feed pressure (psi)
7812*	360	8.0e -5	17.25	7.5
9574*	360	5.6e -5	9.0	8.0
8001*	420	4.7e -5	17.5	8.0
7494*	360	3.5e -5	10.0	8.0
7812**	360	8.0e -5	17.25	7.5
9503**	360	1.58e -4	18.5	15.0
7635***	360	1.5e -6	18.0	8.0

* experiments to determine flow effect
** experiments to determine pressure effect
*** experiment with 0.5% SDS

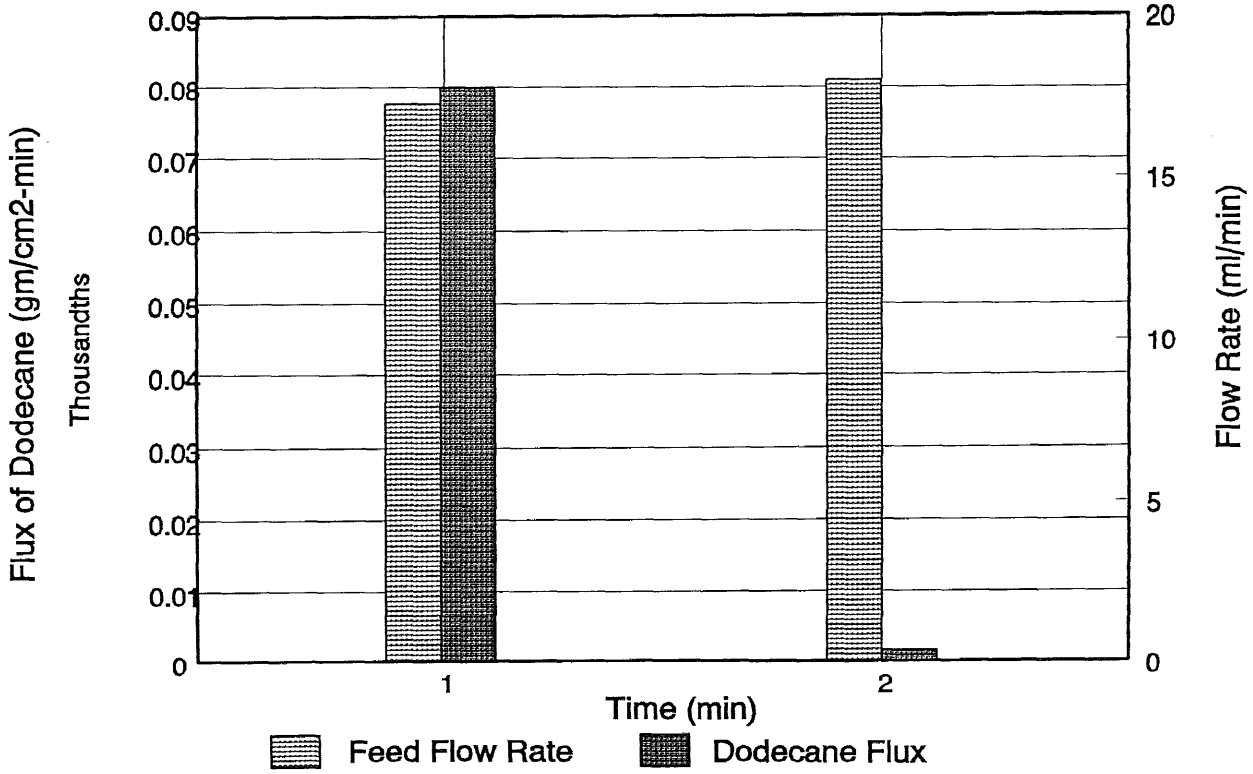

1: Pressure 7.5 psi; Initial dodecane conc. 7812 ppm; No surfactant; Feed in tube
2: Pressure 8 psi; Initial dodecane conc. 7635 ppm; 0 SDS; Feed in tube

:2 Comparison of dodecane flux with o ıt

CHAPTER 5

CONCLUSIONS

The following conclusions were drawn from the study of removal of TCE from a surfactant-flushed wastewater by pervaporation and removal of dodecane from an emulsion by permeation.

1. TCE was successfully removed at different concentrations and flow rates with or without surfactant, by pervaporation using hydrophobic hollow fiber membranes having an ultrathin plasma polymerized silicone coating on the outer surface.
2. When SDS was present, the availability of the porous hydrophobic substrate improved the performance of the membrane module for TCE removal. This was evident from a decrease in the removal of TCE when fed from the shell side of the module, in which case the VOC was exposed to the silicone coating.
3. Presence of surfactant adversely affected the performance of the pervaporation process in terms of TCE removal.
4. The flux of TCE increased linearly with an increase in TCE concentration in systems with or without surfactant.
5. TCE flux was found to be an increasing function of Reynolds number in systems with or without surfactant indicating a substantial effect of the boundary layer on the performance of the module.

6. Increase in feed temperature improved the removal rate of TCE, but it also increased the water flux in systems with surfactant.

7. Overall mass transfer coefficient in systems with or without surfactant was found to be an increasing function of Reynolds number.

8. Overall mass transfer coefficient was higher in a surfactant-free system compared to a system containing surfactant. This indicated some additional resistances in presence of a surfactant.

9. The performance of Dowfax 8390 system was better compared to a SDS system in terms of percent removal of TCE.

10. Performance of the pervaporation precess was unaffected by the presence of a high molecular weight polymer, xanthan gum.

11. From preliminary dodecane permeation experiments, it was observed that dodecane could be removed from an oil-in water emulsion using a membrane module having hydrophobic hollow fibers with a plasma polymerized silicone coating on the outside surface.

12. The oil flux obtained from the experiments where feed was in the tube side was found to be substantially higher than those where feed was in the shell side.

13. The oil permeation process was facilitated by an increase in the feed pressure and the feed Reynolds number.

14. The presence of SDS adversely affected the oil flux.

APPENDIX A

A.1 Calculation of Flux

A.1.1 Calculation of TCE Flux

The flux of TCE, J, is proportional to the feed solution flow rate Q, the solute concentration difference ΔC, and the mass transfer area A_m. They are related by the equation

$$flux\left(\frac{mol}{cm^2\text{-}sec}\right)=Q\left(\frac{ml}{\min}\right)*\left(\frac{\min}{60sec}\right)*\Delta C\left(\frac{g}{10^6 cm^3}\right)*\frac{1}{M_w}\left(\frac{mol}{g}\right)*\frac{1}{A_m}\left(\frac{1}{cm^2}\right)$$

$$J=C_1*\frac{\Delta C}{A_m}*Q \qquad \textbf{(A.1.1)}$$

where,

J = Solute flux (mol/cm^2.sec),

C_1 = Unit adjustment constant,

ΔC = Difference in concentration between the feed and the retentate (ppm),

Q = Feed flow rate (ml/min.),

M_w = Molecular weight (g/mol), and

A_m = Mass transfer area (cm^2).

Calculation of mass transfer area:

Mass transfer area of a pervaporation module (based on the outside diameter of the Celgard fibers) is given by

$$A_m=2\Pi r_o*L*N \qquad \textbf{(A.1.2)}$$

where,

r_o = Outer radius of fiber,

L = Effective length of the module,

N = Number of hollow fibers in a module.

Table A.1 Mass transfer area of pervaporation modules

	Single module (module # 1 & 2)	Twins-module (module # 1 & 2)	Trio-module (module # 1, 2 & 3)
mass transfer area (cm^2)	140.1	280.2	474.9

A.1.2 Calculation of Water Flux

The flux of water, J_w, was calculated from the volume of water collected in the condensate in the permeate side using the following relation:

$$J_w = \frac{V_w}{M_w * A_m * t} \qquad \textbf{(A.1.3)}$$

Where,

V_w = Volume of water collected in the permeate (ml),

M_w = Molecular weight of water (g/mol),

A_m = Mass transfer area of the membrane module (cm^2), and

t = Duration of experiments (min).

The following are the flux expressions:

$$TCE\ Flux\left(\frac{mol}{cm^2\text{-sec}}\right) = 1.268 * 10^{-10} * \frac{Q * \Delta C}{A_m} \qquad \textbf{(A.1.4)}$$

$$Water\ Flux\left(\frac{mol}{cm^2\text{-sec}}\right) = 9.259 * 10^{-4} * \frac{V_w}{t * A_m} \qquad \textbf{(A.1.5)}$$

A sample calculation for TCE and water fluxes is shown for a

run at a flow rate of 2.4 ml/min with 0.3% SDS. (refer to Table 4.5, Chapter 4).

ΔC = 1043-44 = 999 ppm

Q = 2.4 ml/min.

A_m = 280.2 cm^2

t = 390 min.

V_w = 1.1 ml

TCE flux = $1.268*10^{-10}*2.4*999/280.2$ (mol/cm^2-sec)

= $1.084*10^{-9}$ (mol/cm^2-sec)

= $1.084*10^{-9}*131.39*60$ (gm/cm^2-min.)

= $8.6*10^{-6}$ (gm/cm^2-min.)

water flux = $9.259*10^{-4}*1.1/(390*280.2)$ (mol/cm^2-sec)

= $9.32*10^{-9}$ (mol/cm^2-sec)

= $9.32*10^{-9}*18*60$ (gm/cm^2-min.)

= $1.0*10^{-5}$ (gm/cm^2-min.)

A.2 Calculation of Mass Transfer Coefficient

A.2.1 Boundary Layer Mass Transfer Coefficient

The boundary layer mass transfer coefficient is calculated from the following Leveque correlation:

$$Sh=1.62*Gr^{1/3} \qquad \textbf{(A.2.1)}$$

where, Sh and Gr represent the dimensionless groups, Sherwood and Graetz number respectively. Sherwood number is represented by the following dimensionless group:

$$Sh=\frac{k_b d_i}{D} \qquad \textbf{(A.2.2)}$$

where,

k_b = boundary layer mass transfer coefficient (cm/sec),

d_i = inner fiber diameter (cm),

D = diffusivity of TCE (cm^2/sec.).

Graetz number is defined as:

$$Gr=\frac{d_i^2 v}{DL} \qquad \textbf{(A.2.3)}$$

where,

d_i = inner diameter of the fiber (cm),

v = linear velocity of liquid in the fiber (cm/sec.),

D = diffusivity of TCE (cm^2/sec.),

L = effective length of the module (cm).

The parameters d_i, L, and v as defined above were obtained from the experimental data and the membrane module. The value of diffusivity of TCE in water was taken to be 9.0*10e -10 m^2/sec. (Liu et al. 1996). The mass transfer coefficient, k_b, was calculated based on equation A.2.1.

A.2.2 Overall Mass Transfer Coefficient

The overall mass transfer coefficient for TCE was calculated based on the following relations:

$$J=Flux\left(\frac{mole}{cm^2\text{-sec}}\right)=C_2*K_{ov}\left(\frac{cm}{\text{sec}}\right)*\Delta C'\,(ppm)$$

$$K_{ov}=\frac{J}{C_2*\Delta C'} \qquad \textbf{(A.2.4)}$$

where,

C_2 = unit adjustment constant,

K_{ov} = mass transfer coefficient (cm/sec)

ΔC^1 = logarithmic mean average concentration (ppm).

Concentration unit change from ppm to gmol/ml

$$C_2 * \Delta C^1 \left(\frac{mol}{ml}\right) = \frac{\Delta C^1}{10^6} \left(\frac{g}{ml}\right) * \frac{1}{M_w} \left(\frac{mol}{g}\right) \qquad \textbf{(A.2.5)}$$

For TCE, $C_2=7.61 \times 10^{-9}$.

The logarithmic mean average concentration is defined as :

$$\Delta C^1 = \frac{(C_{inlet} - C^s_{inlet}) - (C_{outlet} - C^s_{outlet})}{\ln \frac{(C_{inlet} - C^s_{inlet})}{(C_{outlet} - C^s_{outlet})}} \qquad \textbf{(A.2.6)}$$

where,

C_{inlet} = Inlet feed concentration of TCE (ppm)

C_{outlet} = outlet feed concentration of TCE (ppm)

C^s_{inlet} = permeate side concentration of TCE at inlet(ppm)

C^s_{outlet} = permeate side concentration of TCE at outlet (ppm).

Here it was assumed that $C^s_{inlet} = C^s_{outlet} \simeq 0$.

A sample calculation for the overall mass transfer coefficient (K_{ov}) is shown here. The same experimental run used in the sample calculation for TCE and water flux mentioned earlier is considered here also for calculation of K_{ov} (refer to Table 4.5, Chapter 4).

ΔC^1 = (1043 - 44)/(ln{1043/44}) = 315.5 ppm

J = $1.084 * 10^{-9}$ (mol/cm^2-sec)

C_2 = 7.61×10^{-9}

Putting all these values in equation A.2.4, K_{ov} is found to be $4.5*10^{-4}$ cm/sec (refer to Table 4.5, Chapter 4).

Table A.2 Regression data for k_m for 1% SDS system

$1/K_{ov}d_o$	$1/k_bd_i$	regression results
88886	50589	intercept = 45632 slope = 0.9 k_m (cm/sec) = 7.55e -4 (refer to Table 4.4 and Figure 4.9)
87315	39707	
72407	34734	

Table A.3 Regression data for k_m for 0.3% SDS system

$1/K_{ov}d_o$	$1/k_bd_i$	regression results
76303	50813	intercept = 34484 slope = 0.88 k_m (cm/sec) = 1.05e -3 (refer to Table 4.5 and Figure 4.11)
43432	41666	
40251	32051	
34235	27777	

Table A.4 Regression data for k_m for surfactant-free system

$1/K_{ov}d_o$	$1/k_bd_i$	regression results
39544	49138	intercept = 11488 slope = 0.6 k_m (cm/sec) = 3.00e -3 (refer to Table 4.9 and Figure 4.18)
35453	39700	
31344	31079	
26464	27272	
25330	23250	
22742	20743	

REFERENCES

1. L. M. Abriola, K. D. Pennell, G. A. Pope, T. J. Dekker and D. J. Luning-Prak, " Impact of Surfactant Flushing on the Solubilization and Mobilization of Dense Nonaqueous-Phase Liquids," *ACS Symposium Series* 594, pp. 10-23, 1995.

2. R. Ball and S. Wolf, "Design Considerations for Soil Cleanup by Soil Vapor Extraction," *Environmental Progress*, vol. 9, pp. 187-190, Aug. 1990.

3. R. C. Binning, R. J. Lee, J. F. Jennings and E. C. Martin, "Separation of liquid mixture by permeation," *Industrial Engineering Chemistry*, vol. 53, pp. 45-50, 1961.

4. H. L. Fleming and C. S. Slater, "Theory of pervaporation," in *Membrane Handbook*, edited by W. S. Winston Ho and K. K. Sirkar, pp 117-122, Van Nostrand Reinhold, New York, NY, 1992.

5. J. C. Fountain, A. Klimek, M. G. Beirkirch and T. M. Middleton, "Surfactant Flushing; a new technology for solubilizing Dense Nonaqueous-Phase Liquids," *Journal of Hazardous Material*, pp. 295-311, 1991.

6. J. C. Fountain, C. Waddell-Sheets, A. Lagowski, C. Taylor, D. Frazier and M. Byrne, " Enhanced Removal of Dense Nonaqueous-Phase Liquids Using Surfactants," *ACS Symposium Series* 594, pp. 177-190, 1995.

7. Kirk-Othmer, *Encyclopedia of Chemical Technology*, vol. 3, John Wiley & Sons, 3rd ed., New York, NY, 1983.

8. Kirk-Othmer, *Encyclopedia of Chemical Technology*, vol. 23, John Wiley & Sons, 3rd ed., New York, NY, 1983.

9. K. M. Lipe, M. A. Hasegawa, David A. Sabatini and J. H. Harwell, " Micellar Enhanced Ultrafiltration and Air Stripping for Surfactant-Contaminated Separation and Surfactant Reuse," *Ground Water Monitoring and Remediation*, Jan. 1995.

10. C. Lipski and P. Cote´, "The use of Pervaporation for the Removal of Organic Contaminants From Water," *Environmental Progress*, vol. 9, pp. 254-262, Nov. 1990.

11. M. G. Liu, J. M. Dickson and P. Cote´, "Simulation of a pervaporation system on the industrial scale for water treatment, part I: extended resistance-in-series model," *Journal of Membrane Science*, vol. 111, pp. 227-241, 1996.

12. P. Magdich and M. Semmens "The removal of oil from oil-water mixture using selective oil filtration", Report submitted to Hazardous Waste Engineering Research Laboratory, US EPA Pollution Prevention, Document No. 709-009, Cincinnati, OH, 1988.

13. M. Markelov and J. P. Guzowski. Jr., "Matrix independent headspace gas chromatographic analysis. The full evaporation technique," *Analytica Chimica Acta*, vol. 276, pp. 235-245, 1993.

14. K. Ogino and M. Abe, *Surface and Colloid Science*, vol. 15, Plenum Press, New York, NY, 1993.

15. K. D. Pennell, L. M. Abriola and W. J. Weber, Jr., "Surfactant-Enhanced Solubilization of Residual Dodecane in Soil Columns," *Environ. Sci. Technol.*, vol. 27, pp. 2332-2340, 1993.

16. R. Prasad and K. K. Sirkar, "Dispersion free solvent extraction with microporous hollow fiber modules," *AIChE Journal*, vol. 2, pp. 177-188, 1988.

17. W. C Preston, "Some correlating principles of detergent action," Journal of Physical Colloid Chemistry, vol. 52, pp 84, 1948.

18. K. Psaume, P. Aptel, Y. Aurelle, J. C. Mora and J. L. Bersillon, "Pervaporation: Importance of Concentration Polarization in the Extraction of Trace Organics from Water," *Journal of Membrane Science*, vol. 36, pp. 373-384, 1988.

19. M. J. Rosen, *Surfactants and Interfacial phenomena*, John Wiley & Sons, second ed., New York, NY, 1989.

20. D. A. Sabatini, R. C. Knox and J. H. Harwell, "Emerging Technologies in Surfactant-Enhanced Subsurface Remediation," *ACS Symposium Series* 594, pp. 1-8, 1995.

21. B. Shiau, D. A. Sabatini and J. H. Harwell, "Solubilization and Microemulsion of Chlorinated Solvents Using Direct Food Additive (Edible) Surfactants," *Ground Water*, vol. 32, pp. 561-570, July-Aug. 1994.

22. B. Shiau, J. D. Rouse, D. A. Sabatini and J. H. Harwell, "Surfactant Selection for Optimizing Surfactant-Enhanced Subsurface Remediation," *ACS Symposium Series* 594, pp. 65-79, 1995.

23. C. Tanford, *The Hydrophobic Effect*, Wiley, second ed., New York, NY, 1980.

24. N. P. Tirmizi, B. Raghuraman and J. Wiencek, "Demulsification of Water/Oil/Solid Emulsions Using Hollow Fiber and Tubular Membrane modules," Final Report submitted to Hazardous Substance Management Research Center, Newark, NJ, 1995.

25. N. P. Tirmizi, B. Raghuraman and J. Wiencek, "Demulsification of Water/Oil/Solid Emulsions by Hollow Fiber Membranes," *AIChE Journal*, vol.42, pp. 1263-1276, May 1996.

26. H. Uchiyama, S. D. Christian, E. E. Tucker and J. F. Scamehorn, "Solubilization of Trichloroethylene by Polyelectrolyte/Surfactant Complexes," *AIChE Journal*, vol. 40, pp. 1969-1975, Dec. 1994.

27. C. C. West and J. H. Harwell, "Surfactants and Subsurface Remediation," *Environmental Science & Technology*, vol. 26, pp. 2324-2330, 1992.

28. S. R. Wickramasinghe, M. J. Semmens and E. L. Cussler, "Mass transfer in various hollow fiber geometries," *Journal of Membrane Science*, vol. 69, pp. 235-250, 1992.

29. J. G. Wijmans, A. L. Athayde, R. Daniels, J. H. Ly, H. D. Kamaruddin and I. Pinnau, "The role of boundary layers in the removal of volatile organic compounds from water by pervaporation," *Journal of Membrane Science*, vol 109, pp. 135-146, 1996.

30. J. G. Wijmans, J. Kaschemeket, J. E. Davidson and R. W Baker, "Treatment of Organic-Contaminated Wastewater Streams by Pervaporation," *Environmental Progress*, vol. 9, pp. 262-268, Nov. 1990.

31. J. L. Wilson and S. H. Conrad, *Proceedings of NWWA Conference on Petroleum Hydrocarbons and Organic Chemicals in Ground Water*, National Well Water Association, Dublin, OH, 1984.

32. W. S. Winston Ho and K. K. Sirkar, *Membrane Handbook*, Van Nostrand Reinhold, New York, NY, 1992.

33. D. Yang, S. Majumdar, S. Kovenklioglu and K. K. Sirkar, "Hollow fiber contained liquid membrane pervaporation system for the removal of toxic volatile organics from wastewater," *Journal of Membrane Science*, vol. 103, pp. 195-210, 1995.

35. C. L. Zhu, C. W. Yuang, J. R. Fried and D. B. Greenberg, "Pervaporation Membranes-A Novel Separation Technique for Trace Organics," *Environmental Progress*, vol. 2, pp. 132-143, May 1983.